

https://dspace.org/

Development of diffusion carbide coatings

Fazluddin, Shahed Bhagga

1993

http://hdl.handle.net/10539/23012

Fazluddin, Shahed Bhagga (1993) Development of diffusion carbide coatings, University of the Witwatersrand, Johannesburg,<http://hdl.handle.net/10539/23012>

Downloaded from a DSpace repository. https://dspace.org/

DEVELOPMENT OF DIFFUSION CARBIDE COATINGS

Shahed Bhagga Fazluddin

A thesis submitted to the Faculty of Engineering, University of the Witwatersrand, Johannesburg, in fulfilment of the requirements for the degree of Master of Science in Engineering

Johannesburg, 1993

DECLARATION

I declare that this thesis is my own, unaided work. It is being submitted for the Degree of Master of Science in Engineering in the University of the Witwatersrand, Johannesburg. It has not been submitted for any degree or examination in any other University.

S B Kazmiddin

(Signature of Candidate)

22nd day of March 1993

DECLARATION

I declare that this thesis is my own, unaided work. It is being submitted for the Degree of Master of Science in Engineering in the University of the Witwatersrand, Johannesburg. It has not been submitted for any degree or examination in any other University.

(Signature of Candidate)

22nd day of March 1993

ABSTRACT

The formation of VC, NbC, and Cr-carbide coatings on steels immersed in molten borax baths containing carbide-forming constituents has been known for some time. A study was made of the formation of carbide coating on steel specimens treated in molten borax containing ferro-vanadium and V_2O_5 as bath additives. The prevalence of oxidizing or reducing conditions in the bath was found to play a decisive role in the formation of the VC layer. The influence of treatment factors such as time, temperature, and bath composition on the thickness of the coating was investigated. A detailed investigation into the behaviour of baths containing V_2O_5 and Al was carried out in this regard. Microstructural examination of coated specimens was performed using optical and electron microscopy. Microhardness tests, X-ray diffraction(XRD) and energy dispersive spectroscopy(EDS) analyses were carried out in order to characterise the layers produced.

The corrosion behaviour of the vanadium carbide coating was evaluated by accelerated electrochemical means. Samples of mild steel and EN9(0.5% C) steel were treated for various lengths of time in order to obtain coatings of various thicknesses. The corrosion resistance of the carbide coating was found to be superior to that of the untreated base alloys.

Five different tool steel materials were also treated. Microscopy examination and hardness testing of the VC coated tool steels was performed in order to assess the effects of treatment by this process on the base material. The austenitizing temperature and the nature of the carbides in the matrix of the tool steels was found to play an important role in this respect.

"We verily sent Our messengers with clear proofs, and revealed with them the Scripture and the Balance, that mankind may observe right measure; and He revealed **iron**, wherein is mighty power and (many) uses for mankind, and that Allah may know him who helpeth Him and His messengers, though unseen. Lo! Allah is Strong, Almighty."

The Holy Koran
Chapter LVII : "Iron"
Verse XXV

ACKNOWLEDGMENTS

Sincere thanks are due to: my supervisor Dr. A. Koursaris for his patience, guidance and understanding in this work, and, for introducing me to his lovely family.

Chris Ringas of the CSIR and Ken Cowie of Metal Technology Engineering for their assistance in this project.

The CSIR for their financial assistance.
Highveld Steel and Vanadium for the donation of materials.

My friends : Lourens Wessels, Shadrack Moqabolane, Anthony Fleischmann, Andre van Bennekom, Tracy Boniface, Bashir Essy and Tahir Patel for their support, encouragement and technical assistance.

Jean Bezuidenhout, Johnson Ndengenza, Graham Armstrong, and John Morfitt of the Metallurgy workshop and Zaid Isaacs of the CSIR for their technical assistance and humour.
Jurgen Gnoinski of the CSIR for his help on the corrosion tests.

The secretarial staff of the Metallurgy Department for their assistance : Gill van der Heever, Irene Badenhorst, Karen Dow, and, Barbara Benade.

My family : Mother Hawa, Father Ismail, Uncle Farouk, and Aunty Zubeida for their support without which it would not have been possible to complete this work.

CONTENTS **Page**

DECLARATION.....i
ABSTRACT.....ii
DEDICATION.....iii
ACKNOWLEDGEMENTS.....iv
CONTENTS.....v
LIST OF FIGURES.....ix
LIST OF TABLES.....xiii

1. INTRODUCTION 1

2. LITERATURE REVIEW 3

2.1 Wear mechanisms and Wear of Materials 3
2.1.1 Prevention of Wear 5

2.2 Overview of Surface Engineering Processes 8
2.2.1 Diffusion Coatings 8
2.2.2 Vapour Deposition Processes 19
2.2.3 Thermal Spraying Processes 23

2.3 Physical and Mechanical Properties of Coated Materials 26
2.3.1 Hardness of Coated materials 26
2.3.2 Influence of Residual Stresses 30

2.4 Physical Chemistry and Metallurgy of Melts 35
2.4.1 Types of Melts 35
2.4.2 Reactions between ionic and network-forming oxides 37
2.4.3 Applications of Borax 42

2.5 The TD Process 44
2.5.1 Background 44
2.5.2 Processing Technique 44

2.5.3 Growth Mechanism and Formation of Carbide Layers 47
2.5.4 Properties of carbide layers and coated materials 55
2.5.5 Applications of the TD process 64

3. EXPERIMENTAL PROCEDURES 66

3.1. Preparation of Experimental Materials.....66
3.1.1. Measurement of Coating Thickness.....68

3.2. Exploratory Tests.....69

3.3. Analysis of VC Coated Specimens.....72
3.3.1. Microscopy of VC Coated Specimens.....72
3.3.2. Determination of Coating Hardness.....72
3.3.3. Determination of Coating Composition.....73
3.4. A Detailed Study of Baths containing V_2O_5 and Aluminium.....75
3.4.1. Effect of Temperature on Coating Thickness.....77
3.4.2. Influence of Substrate Carbon Content on Coating Thickness.....77
3.4.3. Effect of V_2O_5 Content on Bath Activity...77
..
3.4.10. Analysis of Baths containing 10% V_2O_5 and 5% Aluminium.....83

3.5. Corrosion Testing of VC Coated Samples.....83
3.5.1. Microscopy of Corrosion Samples.....87

3.6. Treatment of Tool Steels.....87
3.6.1. Microscopy of VC Coated Toolsteels.....90

4. RESULTS.....91

4.1. Exploratory Tests.....91
4.2. Analyses of VC Coated Specimens.....94

4.3.1. Microstructure of VC Coated Specimens.....94
4.3.2. Determination of Coating Hardness.....97
4.3.3. Determination of Coating Composition.....103

4.4. A Detailed Study of Baths containing V_2O_5 and Aluminium.....108
4.4.1. Effect of Temperature on Coating Thickness.....108
4.4.2. Influence of Substrate Carbon Content on Coating Thickness.....108
4.4.3. Effect of V_2O_5 Content on Bath Activity..108
..
4.4.10. Analyses of Baths containing 10% V_2O_5 and 5% Aluminium.....121

4.5. Corrosion Test Results of VC Coated Specimens...123
4.5.1. Appearance of Corrosion Surfaces.....134

4.6. Treatment of Tool Steels.....138
4.6.1. Microstructure of VC Coated Tool Steels..145

4.7. Problem Areas and Solutions.....149
4.7.1. Method of Immersion of Samples.....149
4.7.2. Cleaning of Treated Samples.....151
4.7.3. Cleaning of Steel Pots used for Baths....151
..
4.7.8. Moisture in Borax.....164

5. DISCUSSION.....165

5.1. Choosing between FeV and V_2O_5 in the bath.....165

5.2. Exploratory Tests.....165

5.3. Analyses of VC Coated Specimens.....169
5.3.1. Microstructure of VC Coated Specimens....169
5.3.2. Hardness of VC Coatings.....170
5.3.3. Composition of Carbide Coatings.....171

5.4. A Detailed Study of Baths containing V_2O_5 and Aluminium.....172
5.4.1. Effect of Temperature and Substrate Carbon Content on Coating Thickness.....172
5.4.2. Effects of Bath Composition.....172
5.4.3. Influence of Particle Size of V_2O_5 on Bath Activity.....174
..
5.4.7. Analyses of Baths containing 10% V_2O_5 and 5% Aluminium.....177

5.5. Corrosion Testing of VC Coated Specimens.....179

5.6. Treatment of Tool Steels.....181
5.6.1. Microstructure of VC Coated Tool Steels..183

5.7. Problem Areas and Solutions.....185
5.7.1. Method of Immersion of Samples.....185
5.7.2. Cleaning of Treated Samples.....185
5.7.3. Cleaning of Steel Pots used for Baths....185
..
5.7.6. Staining of Coated Samples.....188

6. CONCLUSIONS.....190

7. FUTURE WORK.....191

8. REFERENCES.....193

A. APPENDICES.....201

A.1. XRD Data list of VC Coated Sample.....202
A.2. XRD Data List of Bath Sample.....203
A.3. Microstructure of Tool Steels.....205

LIST OF FIGURES

Figure		Page
2.2.1.	Microstructure of Boride layer[100X]	17
2.2.2.	Variation of boride layer thickness with time	17
2.2.3.	Reactions involved in CVD processes	21
2.2.4.	Oxyfuel gas-wire spraying	24
2.3.1.	Basic(a) and auxiliary(b) diagrams of residual stresses	33
2.4.1.	2-D representation of an oxide M2O3 in (a)crystalline (b)glassy form	38
2.4.2.	Reaction between sodium oxide and silica tetrahedra	40
2.4.3.	2-D representation of the structure of soda-silica glass	40
2.4.4.	The effect of sodium oxide addition on the viscosities of its mixtures with P2O5, B2O3 and SiO2	41
2.4.5.	Activation energies for electrical conduction of some binary borates	43
2.5.1.	Salt Bath furnace for carbide coating	46
2.5.2.	Outline of the TD process	46
2.5.3.	Relationship between the free energy of formation of oxides of elements contained in the bath and kinds of layers formed(1000 C)	48
2.5.4.	Growth model of carbide layer	48
2.5.5.	The time taken to establish saturation in borax/ferro-niobium baths	53
2.5.6.	Effect of treating time and temperature on the thickness of NbC layers	53
2.5.7.	Effect of carbon content on the rate of layer	

formation 56
2.5.8. Effect of carbide type on the rate of layer formation 56
2.5.9. Variation in hardness with carbide species 59
2.5.10. Comparison of wear resistance of VC coated samples in sliding test against textile fiber 63
2.5.11. The effect of substrate hardness on wear loss in sand crushing tests 63
2.5.12. The effect of carbide species on wear depth in compression test 64

3.1. Position of hardness indentations in coated specimens 74
3.2. Method of immersion of sample rods 82
3.3. Method of sectioning of coated EN9 steel rods 82
3.4. Method of mounting of corrosion samples 85

4.1. Growth of VC layer on 0.5% C steel treated in a 10% FeV bath for 3, 6, 9, and 12h at 950°C 93
4.2. Comparison of the activities of baths containing FeV and V_2O_5 93
4.3. Appearance of VC coated 0.5% C steel 95
4.4. Microstructure of VC coating on 0.2% C steel 95
4.5. Microstructure of VC coated 0.5% C steel showing ferrite grains beneath carbide layer 96
4.6. Microstructure of (a)0.5% C(400X) and (b)0.2%C (400X) steel towards the core of treated samples 96
4.7. Appearance of carbide layer on 0.5% carbon steel before etching in nital 98
4.8. Morphology of carbide layer on coated steel surface 98
4.9. Microstructure of hardened 0.5% C steel after coating at 950°C 99

4.10. Appearance of microhardness indentations made at varying loads on carbide coating 99
4.11. Variation in hardness with load 101

4.12. Hardness profiles on VC coated 0.5% carbon steel samples (Load = 10gf) 101
4.13. Variation in "composite" hardness with load of VC coated 0.5% C steel 0.2% C steel 104
4.14. Typical EDS spectrum of VC Coating 104
4.15. Typical diffractogram of VC coated sample 107
4.16. Effect of temperature on coating thickness produced in a bath of 10% V_2O_5 plus 5% Al 109
4.17. Comparison of carbide layer growth on 0.2% and 0.5%C steels treated at 950°C for 3, 6, and 9h 109
4.18. Effect of %V_2O_5 on the thickness of coatings produced at 950°C and 3, 6, or 9h of treatment 110
4.19. Effect of %Al on bath activity at 950°C for 3, 6, 9h of treatment 111

4.20. Change in bath activity with bath composition at 950°C (V_2O_5:Al = 2:1) 112
4.21. Effect of particle size on bath activity at 950°C for 3, 6, and 9h of treatment 113
4.22. Change in bath activity over 25h and 50h periods at 950°C 113
4.23. Variation in coating thickness with distance above the bath bottom for rods treated in baths aged for 8h and 16h 115
4.24. Comparison of coating thicknesses at distances of 30mm, 50mm, and 70mm above the bottom of baths aged for 8h and 16h 116
4.25. Comparison of coating thicknesses produced on 0.5% C steels treated in three 10% V_2O_5 and 5% Al baths aged for 2h, 8h, and 16h 117
4.26. Appearance of sample rods after cleaning 119
4.27. Appearance of aluminium attached to treated rod 119
4.28. Nature of carbide layer on (a) Diamond polished (b) Ground (c) Sand Blasted Surfaces (400X) 120
4.29. Typical diffractogram of bath sample 121

4.30. Typical potentiodynamic curves for mild steel samples. 124

4.31. Typical potentiodynamic curves for EN9 steel samples 125
4.32. Typical cyclic polarization curves for mild steel samples 130
4.33. Typical cyclic polarization curves for EN9 steel samples 131
4.34. Comparison of corrosion rates of coated and uncoated substrate 135
4.35. Nature of (a)Lacquer/sample interface and (b) General surface corrosion of coated steel sample after potentiodynamic test 135
4.36. Nature of (a)Lacquer/sample interface and (b) General surface corrosion of coated steel sample after pitting test 136
4.37. Extensive corrosion of uncoated steel substrate: (a) Lacquer/sample interface (b) General surface corrosion 137
4.38. Coating thickness produced on tool steels treated for 3h and 6h at 950°C 141
4.39. Variation in coating thickness with substrate carbon content for 3h and 6h treatment times at 950°C 141

4.40. Comparison of average coating thicknesses produced on annealed and heat treated substrate treated for 3h at 950°C 142
4.41. Microstructure of VC coated tool steels : (a) D2[400X] (b) D3[1000X] (c) H13[400X] (d) H21[1000X] (e) M2[400X] 146
4.42. Appearance of VC coating (a)round corner[200X] (b)inside a hole[200X] (c)on D2 tool steel[1000X] 147
4.43. Oxidation of steel sample 150
4.44. Immersion of samples using a frame 150
4.45. Appearance of treated samples (a) before and (b) after cleaning 152
4.46. Appearance of "two phase" layer 153

4.47. Typical EDS spectrum of light area using spot analyses 154
4.48. Typical EDS spectrum of darker area using spot analyses 154
4.49. Patchy appearance of spalled sample[10X] 157

4.50. Spalling of carbide layer 157
4.51. Cross-sectional view of spalling carbide layer typifying varying extent to which spalling occurred 158
4.52. Cross-sectional view of spalled carbide layer 158
4.53. Close-up view of spalled area displaying apparent brittle fracture surface 159

4.54. Appearance of quench cracked specimen[8X] 160
4.55. Extension of quench crack though carbide layer 160
4.56. "Stained" area of coated sample 162
4.57. Morphology of carbide layer in "stained" area 162
4.58. Typical EDS spectrum of "stained" area 163
4.59. Detailed view of morphology of "stained" area 163

LIST OF TABLES

Table **Page**

2.5.1. The solubility of carbide forming elements in borax 50
2.5.2. Variation of layer thickness of VC on a 0.4%C steel with the age of the bath 55
2.5.3. Effect of carbide coating on toughness 60
2.5.4. Comparison of corrosion resistance of coated specimens in various aqueous media 61
2.5.5. Typical life improvements achieved by TD processing of tools and dies 65

3.1. Chemical Analysis of Ferro-Vanadium 67
3.2. Chemical Analysis of Vanadium Pentoxide 67
3.3. Conditions used for Exploratory Tests 70
3.4. Process Parameters Studied 76
3.5. Treatment Conditions of Corrosion Samples 84
3.6. Hardening and Tempering Conditions used for the Tool Steels 90

4.1. Results of Exploratory Tests 92
4.2. Results of Hardness Tests on VC Layers 100
4.3. Samples used for measuring "Composite" Hardness of VC Coated Surfaces 102
4.4. Results of Quantitative EDS analyses on samples treated in baths containing V_2O_5 and Al 105
4.5. XRD Data of VC Coated Specimens 105
4.6. XRD Data of Bath Sample 122
4.7. Measured and Estimated Coating Thicknesses of Corrosion Samples 123
4.8. List of Potentiodynamic Test Data 127
4.9. Average Potentiodynamic Test Data 128

4.10. List of Pitting Test Data 133
4.11. Average Results from Pitting Tests 134
4.12. Composition of Tool steels 139
4.13. Hardness of As-Received Tool Steels 139
4.14. Hardness of Hardened and Tempered Tool Steels 140
4.15. Core hardness of oil-quenched or air-cooled VC Coated Samples 143
4.16. Hardness of VC Coatings on Tool steels 144
4.17. Quantitative EDS of "Two phase" Layer from Surface to Substrate 155

1. INTRODUCTION

The performance of machine tools such as dies, punches, jigs, etc. is essential to the efficiency of mass production. Cost and product quality are also significantly influenced by the performance of these and other machine components. The increasing demands being made on equipment performance has placed even more emphasis on the need for materials which can fulfil the requirements of modern industry. The development of surface treatment processes and their applications, over the past few decades, has been viewed as a means of meeting these demands. Post processing of cheap machined materials by surface coating has proven to be an effective substitute to expensive tool materials in terms of both quality and cost.

The more conventional coating processes such as plating, carburising and nitriding have been inadequate in meeting the increasing demands on performance. This stems mainly from the relatively low wear resistance and seizure resistance of coatings produced by these processes. Even the more advanced metal spraying technique has been fairly ineffective in eliminating spalling of coated components. It is essentially for these reasons that the need for more competent coating processes has increased.

Considerable success in terms of wear resistance, and seizure and spalling resistance has been achieved with more recently developed coating techniques. Amongst the most significant of these techniques, is the CVD (Chemical Vapour Deposition) process, used mainly for the application of carbide coatings, eg. TiN or TiC (Titanium carbide) coatings. This process produces coatings with excellent wear and seizure resistance, as well as reducing component failure by spalling.

Another process, called the TD(Toyota Diffusion) process, has also generated carbide coatings with wear and seizure resistance equivalent to that of CVD, at the same time reducing spalling significantly. However, unlike the CVD process, the TD process is much simpler to perform. It simply involves dipping of the material to be treated into a molten salt bath, between 800°C and 1000°C, under ambient atmosphere for a period of time. The bath comprises mainly borax and carbide forming compounds. Unlike with other methods, no protective atmosphere or complicated equipment for waste treatment is required with the TD process. In addition the process is applicable to almost any kind of carbon-containing substrate material, eg. steels and cemented carbides. The most common types of carbide coatings deposited by this process are VC, NbC, and Cr-carbide.

In this work, molten borax baths containing both ferro-vanadium and V_2O_5 as carbide forming additives were studied. Bath conditions such as temperature, time, and, bath composition were investigated. Several substrate materials were treated and the VC coated substrates were characterised in terms of microstructure, hardness, and, composition. Corrosion tests were also carried out on VC coated carbon steel substrates. Finally, problem areas encountered are also presented and possible solutions to these problems are proposed. The following section provides a concise literature review which it is hoped will provide the reader with an insight into the research carried out and the results obtained, as well as, the discussion of these results.

2. LITERATURE REVIEW

2.1. Wear Mechanisms and Wear of Materials

The quality of metal components is largely influenced by their surface condition and surface deterioration during service. Engineering component life is almost always limited by surface deterioration or wear. There are numerous definitions of wear each based on the same underlying concept. To quote a few, wear may be regarded as

"The unintentional deterioration of material resulting from use or environment ,

or,

"The progressive loss of material from the operating surface of a body occurring as a result of relative motion of the surface with respect to another body"[2].

Increasing demands on performance from machine components and on minimising material losses, downtimes, cost, etc., in recent years, has led to a phenomenal expansion in the field of surface engineering. Reducing wear in components is of immense significance as the supply of raw materials is continually diminishing.

Wear involves the displacement and detachment of particles from a metal surface. This arises essentially from two principal modes of contact, namely adhesive wear or abrasive wear. Adhesive wear involves contact between two metals while abrasive wear involves contact between a metal and an abrasive material which may be metallic or non-

metallic. An industrial survey on wear has shown that the two modes of wear listed above account respectively for 50 and 15% of all wear situations making them the predominant wear processes[3].

Wear is often considered to be a surface phenomenon, however, it is also true that it is a systems phenomenon as the behaviour of the wearing surface is affected to a greater or lesser extent by other conditions in a system. Usually, wear also involves a combination of the adhesive and abrasive mechanisms[4]. The variety of conditions from system to system complicate the wear phenomenon even further. A list of variables which make wear such a complex process with regard to both system and surface is given below.

(i) Temperature;
(ii) Environment;
(iii) Type of loading;
(iv) Hardness and surface finish;
(v) Lubricant;
(vi) Composition and compatibility of mating parts;
(vii) Relative speeds of mating parts;
(viii) Presence of foreign particles.

These factors contribute either negatively or positively, or, transform the wear mode into a special form of the principal wear modes. For example, hardness and strength decrease with increasing temperature. The likelihood of plastic deformation increases at higher temperatures thereby increasing surface damage. Hot hardness is often required in materials used at elevated temperature and under wear applications.

In a corrosive environment, there is a tendency for reaction products to form on one or both surfaces in a wear

couple. These products arise from surface reactions taking place due to the environment in which the wear couple is situated. Oxides mostly form in dry air at elevated temperatures. In moist air, both oxides and hydroxides are formed. Sulphates, nitrates and chlorides are common in industrial atmospheres. Usually, reaction products have poor adhesion to the metal surface. Mechanical rubbing removes layers of reaction product, thereby exposing bare metal. Thus, wear rate is increased and the corrosive medium appears more aggressive than it is under static conditions.

2.1.1. Prevention of Wear

Wear prevention is generally achieved by a variety of methods, materials, or combinations of both. Selection of a method or material in this regard is usually preceded by a thorough analysis of service conditions. Control of operating parameters, eg. loads or sliding speeds, is a means of reducing wear within a system. The use of lubricants and coolants also plays an important role. Davison[5] estimated that without the use of lubricating oil, the number of men required to drag an Egyptian statue of about 60 tons would be 516, in contrast to the actual number of men used, ie. 172. Selection of suitable hardness, toughness, and other material properties can also help minimise wear. One of the most effective variables for reducing wear is hardness and this deserves greater attention.

Hardness is one of the most important properties determining the wear resistance of a material. By reducing the possibility of initial surface indentation and subsequent wear or deformation through high hardness, one can greatly increase wear resistance.

Wear rate is inversely related to hardness at times. Practical results on abrasive wear however, do not confirm this proportionality. Pure metals, because of their simple microstructure, may display such proportionality. Typical engineering alloys have much more complex structures and therefore do not follow this relationship[2]. For example, in steels, hardness and wear resistance are controlled by C-content and the structural condition of the matrix. Hard phases such as carbides, borides, nitrides and phosphides are used successfully in improving abrasion resistance. The composition, amount and morphology of these phases generally determine the degree of improvement. The use of hard carbide in a softer matrix is an effective way of combatting wear. Saltzman[6] studied the effect of TiC particle additions to a Fe-Cr-C matrix on wear resistance in wet sand abrasion tests and showed that wear decreased with increasing TiC in the matrix.

Wear of a surface tends to be reduced if the ratio of its hardness to that of the abrading body increases over the range 0.5 - 1.3[2]. The hardness of a worn surface is a factor often overlooked when considering hardness in relation to wear. Hardness of unworn components serves merely as a good indicator. Most metallic surfaces work harden during wear. Thus, the hardness of a worn surface will be influenced by the structure and composition of the material. In the case of coated components, the hardness of both the coating and substrate material play a part.

Generally, coated materials used in wear resistant applications tend to have improved properties over the uncoated material. Wear tests done by Venkatesh[7] using TiC coated WC base material, as well as, TiC coated TiC base material, showed that in both cases wear resistance was improved over that of the uncoated material. The thickness of coatings has a definite influence on their wear

resistance. However, it is coating hardness which is the more influential factor. Habig[8] performed adhesive and abrasive sliding wear tests on the same steel substrate coated by five different processes.

(i) Diffusion/Thermochemical;
(ii) CVD (Chemical Vapour Deposition);
(iii) PVD (Physical Vapour Deposition);
(iv) Plasma Spraying;
(v) Electrodeposition.

Results from these tests showed that the diffusion coatings, in this case FeN /FeB /Fe_2B /Cr_7C_3 and VC, had higher wear resistance than the other coatings although, the thicknesses of these diffusion coatings were amongst the smallest. It therefore appears that the hardness of surface coatings applied to components is most effective in reducing wear in these components.

2.2. Overview of Surface Engineering Processes

2.2.1. Diffusion Coatings

Wear resistance, corrosion resistance and high temperature resistance can be imparted to metals by relatively thin diffusion layers. The thickness of these layers can vary from a few micrometres to several hundred micrometers. It should be noted that many of these so called diffusion "coatings" do not constitute a physically distinct layer from the substrate, as is the case with sprayed, vapour deposited or electroplated coatings. Instead, these "coatings" represent a thin surface layer of the diffusion treated component, whose structure has been modified to a certain depth by the diffusion of certain elements into the component surface.

2.2.1.1. Carburising

Carburising is one of the earliest and cheapest methods of diffusion treatment in which the surface layers of steels are enriched in carbon. The general purposes of carburising are to increase surface hardness while maintaining core ductility, wear resistance and fatigue strength. Case thicknesses vary between 0.1-0.3mm for large and 0.5-2.0mm for small and medium-sized components. Typical temperatures range between 900-950°C, but this increases for alloy steels. Treatment times vary with case depth requirements and a treatment at 920-930°C for one hour produces a layer of 0.1-0.12mm depth. Carbon diffusion into the steel surface is achieved in various ways[9].

(i) Pack carburising;
(ii) Gas carburising;

(iii) Melt carburising - Here, a melt containing 78-85% Na_2CO_3, 10-15% NaCl, and 6-8% SiO_2(typically), is used as the carburising medium. Advantages of this method are that heating is more uniform with lower temperatures being required. Component distortion is low and automation is possible. A major drawback however, is the fact that the bath requires correction quite often(about every 3 hours).

Usually, carburised layers consist of three regions. An outer region of hypereutectoid pearlite and secondary Fe_3C. A middle region of eutectoid pearlite only, and an inner region of hypoeutectoid pearlite and ferrite. Surface carbon contents vary between 0.8 and 1.1%, decreasing obviously towards the interior. A two phase layer of globular carbides on the surface and austenite beneath this, is produced in alloy steels containing Cr, V, Mn, W, and Mo. The presence of these carbides raises the surface carbon content to 1.8-2.0%.

The most important properties improved by carburising are surface hardness, wear resistance and fatigue strength. Surface hardness of 60-65 HRC is not uncommon. The hardness distribution in the diffusion layer - typical of all carburised articles - depends on the carburising time, heating rate, and quenching and annealing temperatures. Wear resistance is improved via carburizing provided the diffusion layer consists of fine martensite, little globular carbide, and small amounts of residual austenite. Optimum carbon contents, in this respect, have been found to lie in the range 0.8-1.0%.

2.2.1.2. Nitriding

The very rapid diffusivity of nitrogen in iron is exploited

in nitriding. The valuable properties obtained from nitrided layers are high hardness(1300 HV), high seizure and wear resistance, considerable hot hardness at 500-600°C, and improved corrosion resistance. Among the drawbacks are the process times and the drop in corrosion and heat resistance of treated components. The attraction in nitriding lies in its wide industrial application and the variety of materials which can be treated. Examples of the areas of application are cutting tools, aircraft parts, and machinery in the car and oil industries. Examples of materials treated are Cr, Al, and low-alloy steels, austenitic and stainless steels, as well as heat resistant steels. There are three common methods of nitriding[9].

(i) Gas nitriding;
(ii) Glow-Discharge nitriding;

(iii) Melt nitriding - The types of melts used for nitriding vary with the manner in which nitrogen is introduced into the component. Fused salt baths used for "salt" nitriding have a high cyanide content and operate at 540-590°C. With neutral salts, ammonia gas is blown into the melt. Where aqueous ammonia solutions are employed, heating is achieved through high frequency current and components become enveloped in an ammonia-rich gas layer.

The structure of nitrided layers can be quite complex, complexity varying with treatment time, temperature, and type of steel. Since nitrides dissolve carbon, complex carbonitrides usually form, eg. $Fe_2(C,N)$ and $Fe_4(C,N)$. Steels containing nitride-forming elements - Cr, Mo, Mn, W, Ti - tend to form very small inclusions of their nitrides along grain boundaries within the diffusion layer. The high hardness of nitrided layers is attributed to the finely dispersed nitride particles at the surface. However, experimental confirmation of this hardness has not been clearly established. For instance, a study on the influence

of nitriding times on hardness distribution showed that time has almost no influence on surface hardness. Longer times simply increase layer depths[9]. Nitrides of alloy steels are harder and also have greater thermal stability than carbon steels.

2.2.1.3. Chromizing

The attractive properties of chromized articles stems from their high surface hardness and good wear, corrosion, and heat resistance. Practical examples of chromizing applications are numerous, covering a wide industrial scale. Chromizing of dies for pressing of glass articles increases their wear resistance 17 fold. The life of hack-saw blades is increased by a factor of 15 using this process. Corrosion and SCC(Stress Corrosion Cracking) resistance of steels are also increased in this way[9]. A brief discussion of the different chromizing processes is given below.

Solid phase chromizing involves deposition(usually electrolytic) of chromium onto the metal surface followed by heating. Chromizing in vapours(the earliest method) entails vaporization of chromium and its absorption onto the metal surface. This method has been developed to include treatment of components in vacuum. In bath chromizing, components are treated in fused salt baths containing chromium or ferro-chrome. These baths usually contain sodium chloride, calcium chloride, barium chloride, and sometimes chromium chloride. In some cases, chromizing is performed in baths containing molten lithium impregnated with metallic chromium. An inert gas is passed over the melt in order to prevent oxidation of the molten salt.

Most attention today is focused on gas chromizing as this technique yields thick high quality cases and can be controlled easily. Contact chromizing is carried out in various powder mixtures in a reducing or inert atmosphere. Powder mixtures typically contain chromium-bearing substances(chrome, ferro-chrome, chromium oxide, etc.), substances which prevent sticking of particles to the metal surface(aluminium oxide, refractory clays, corundum, etc.), and substances which act as activators(usually ammonium chloride).

Some of the variations of contact gas chromizing processes deserve greater attention because of the similarities of these processes with the salt bath process under study here. In one method, chromizing is performed in a mixture of chromium oxide and carbon powder or barium carbonate to activate reduction of the oxide to metallic chromium. This method makes it possible to overcome the difficulties of chromizing in chromium or ferro-chrome mixtures such as, melting of the mixture, sticking of the mixture to articles, and necessity of grinding the ferro-chrome which has become attached to articles. Another method involves chromizing in contact with a special alloy, which consists of ferro-chrome and of chemical elements necessary for transporting the chromium to the surface of the article. Gas chromizing in sealed containers is used in the machinery industry. The seal consists of a low melting point(700-800°C) sodium- or borosilicate glass through which the evolved gases escape at the beginning of the process[9]. Paste chromizing is intermediate between the melt and gas methods where articles are covered with a paste consisting of water mixed with ferro-chrome, binder(bentonite), and NH_4Cl. Upon heating, the metal surface becomes impregnated with chromium.

During gas chromizing in HCl and H_2, Cr atoms diffuse into

the steel surface which is austenitic at the chromizing temperature. A $(Cr,Fe)_{23}C_6$ carbide layer forms via reactive diffusion. A polymorphic gamma-alpha transformation occurs with further Cr-enrichment of the austenite. Higher carbon content accelerates formation of the above carbide and also leads to $(Cr,Fe)_7C_3$ formation. Carbide zone depth increases with increased time (2-20 hours) and temperature (900-1100°C) of contact chromizing. Chromized layers are characterised by an intermediate zone between the surface carbide zone and the decarburized zone. Both the intermediate and decarburized zones increase with chromizing time, but the depth of these zones approaches a constant value after about 6-8 hours because of carbon diffusion from the core to the surface. In cases where powder mixtures containing aluminium oxide (as inert addition) are used, articles are impregnated with Al as well, in amounts of 3-6% in steel. Such infiltration hampers the diffusion process and is detrimental to layer structure and properties.

2.2.1.4. Boronizing

Boronizing of steel is carried out on carbon steels, ferritic and austenitic alloy steels, nickel and nickel alloys, as well as other materials. The primary application of boronized components is in that requiring wear resistance, eg. bushings, dies, nozzles, and protective shells in pumps. Boronizing also imparts corrosion resistance in steel, and reduces friction in dies, cams, jigs, blades, and bearings. Savings achieved via this process are due not to a low treatment cost, but rather, to the longer life of treated articles and to the fact that inexpensive materials can be used. Boronizing has extended from the initial method where treatment is done in powder mixtures, to other methods outlined below[9,10].

Boronizing in powder mixtures - Powders of amorphous boron, ferro-boron, iron-boron-aluminium alloys, or boron carbide, are used in this process. Since the process is simple, it can be used in every plant. Components are placed in a container and covered on all sides with the boronizing powder. The container is then closed, sealed with heat resistant clay and heated for several hours at 950-1100°C. To prevent caking and sticking of powder to articles, the boronizing medium should contain inert substances like aluminium oxide or chamotte. Also, to accelerate the process, ammonium chloride, borax and other compounds are added. Boronizing in powder mixtures of amorphous boron and NH_4Cl for 4 hours at 900°C produces a 70µm case. In the case of boron carbide powders, addition of NH_4Cl increases case thickness by 15-20%. In a study using a mixture containing 84% boron carbide and 16% borax, steel specimens treated for 6 hours at 950°C developed cases 150µm thick. The use of induction heating is thought to accelerate the boronizing process.

Electrolytic boronizing - This method is based on the electrolytic treatment of articles in molten baths containing borax or other boron-bearing materials. Anodes are made of graphite, or, of carbon rods impregnated with borax. The process is usually carried out at 900°C. To increase crucible life they are also boronized. In order to reduce costs and to activate baths, boronizing has been carried out in a melt containing 40% borax and 60% boric acid(anhydride). Electrolysis for 4 hours at 950oC in such baths produced 320µm thick layers on 0.5%C steel. The addition of NaCl to baths results in more uniform layers, while addition of NaF increases the process rate.

Molten bath boronizing - Baths used here contain borax and sodium or barium chloride with the addition of boron carbide. The simplicity of this method allows it to be used in any plant. Extensive investigation into this process has been carried out. A bath containing 60% borax and 40% boron

carbide was found to be the optimum. Using this bath, five hours treatment of Armco iron at 1000°C produced a 300μm thick layer. Baths containing borates, ie. $Na_2B_4O_7$ or $K_2B_4O_7$, and up to 12% elemental boron may also be used. Such baths operate at 815-1175°C and the use of elemental boron accelerates the process. Another bath composition contains a metal whose free energy of oxidation is higher than that of boron, eg. Ca, Mg, Be, Ce, Li, Al, or Ti, and which reduces borates to elementary boron. Ultrasonic waves have been found to intensify boronizing while additions of phosphates, PbO or Bi_2O_3 reduce process temperature.

Gas boronizing - Since gaseous media have a higher activity, gas boronizing is more efficient resulting in faster diffusion. Typical gaseous boron compounds used are B_2H_6, BCl_3, BBr_3, etc. Temperatures range between 700-950°C.

By comparison, electrolytic boronizing produces thicker cases in a relatively short time. Molten bath boronizing is slower with the equipment needed being much simpler. However, bath depletion takes place rapidly. Gas boronizing is most promising, but the high toxicity of the gases limits industrial application. Boronizing in powders is slower than the above methods, but the simplicity of equipment and high quality of cases produced makes it favourable. Recently developed boronizing methods with little practical use as yet, include coating from B-containing slurries followed by diffusion, and, boronizing in B_2O_3 - Al mixtures.

Boronized steels generally contain a surface layer of iron borides, beneath which exists a carbon-rich zone and an alpha-solid solution. Excess carbon in the carbon-rich zone comes from the surface layer. Boronized surfaces comprise two layers, namely an upper FeB layer with a Fe_2B layer beneath this. The borides in these layers are acicular and

orientated perpendicularly to the surface, as shown in **Figure.2.2.1.**

The duration of boronizing influences the depth of the boride layer, and the extent of the zones beneath this layer. The thickness of the boride layer decreases with increasing carbon content. Growth of the boride layer is governed by a parabolic law, as indicated by **Figure.2.2.2,** which shows the boride layer growth with time for steel boronized in a powder mixture. The duration of boronizing also influences the extent of FeB and Fe_2B in the layer, with longer times increasing the amount of the FeB phase. Higher carbon contents result in a decrease in the amount of the FeB phase and an increase in the amount of the Fe_2B phase.

Hardening and high temperature annealing of boronized steel is considered to have no influence on the microhardness of the borides, due to their high temperature stability. The dimensions of steels are altered with boronizing with the dimensions of low carbon steels are increased. The influence of boronizing on the mechanical properties of steels is not uniform since the relatively thin and brittle case cannot have a major effect on the tensile strength or the yield strength of the substrate material. Thus, boronizing increases the UTS and yield strength of steel slightly. Ductility as well, is little affected. Boronized cases adhere strongly to the substrate mainly because of their acicular structure. Adhesion strengths of these cases are similar to that of carburised layers.

2.2.1.5. Vanadizing

The impregnation of the surface of steel components with



Figure.2.2.1. Microstructure of boride layer[10]. [100X].

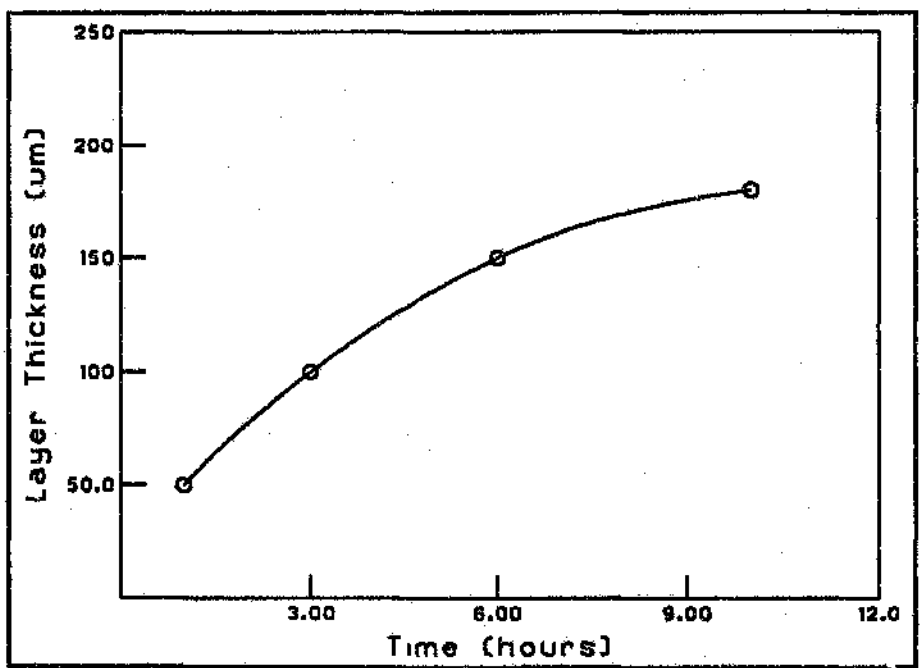


Figure.2.2.2. Variation of boride layer thickness with time[9].

vanadium is a technique which is relatively unexploited in industry. As might be expected, little information regarding this process is available. A number of methods have been developed whereby vanadium is diffused into steel. Vanadizing in powders is typically carried out in mixtures containing ferro-vanadium, aluminium oxide, and ammonium chloride. Gas impregnation of vanadium usually involves HCl and H_2 mixtures in the presence of vanadium or ferro-vanadium. Other gas mixtures are sometimes used, eg. VCl_4 and H_2[9].

Coarse columnar crystals of a solid solution of vanadium in alpha-iron are formed on the surface of vanadized iron or low-carbon steels. These crystals may contain up to 50% vanadium. In the case of substrate materials with higher carbon contents, vanadium carbide layers are formed on the surface. Vanadium content decreases sharply towards the interior of vanadized components. As in the case of chromizing, the kinetics of vanadium carbide layer formation are based on the diffusion of vanadium atoms into the steel and of carbon atoms from the core to the surface. The thickest carbide layers are formed in steels containing 0.5-0.65%C, all process conditions being equal. A zone of alpha-solid solution exists beneath the carbide layer, and a decarburized zone below this.

Adhesion strengths and uniformity of these layers is good. Typical microhardness values of the carbide zone lie in the range 1850-2000 kg/mm^2. However, layers formed are quite thin(0.010 - 0.020 mm) depending on method and process conditions. Nonetheless, vanadized steels have high wear resistance. The thickness of the diffusion layer, which influences the mechanical properties of vanadized steel, depends on the diffusion rate of vanadium which in the case of Armco iron may be represented by the equation,

$$D = 0.17 \exp[-\frac{47700}{RT}]$$

An investigation into the properties of vanadized medium-carbon(0.5%C) steel, using different powder mixtures produced the following results. Vanadizing in a powder mixture of 60% ferro-vanadium, 33% aluminum oxide, and 7% ammonium chloride for 6 and 16 hours at 1100°C produced carbide zones 0.012(12μm) and 0.02(20μm) respectively. Using a modified mixture of 60% V, 35% Al_2O_3, and 5% NH_4Cl, and vanadizing for 6 hours at 1000°C, produced a diffusion layer 6-12 microns thick. The abrasive wear resistance of metal treated in the modified mixture was improved. In addition, the corrosion resistance in water, NaCl, and sulphuric acid increased, but was reduced in alkaline solutions[9].

2.2.2. Vapour Deposition Processes

Vapour deposition processes produce coatings on substrate materials by one of two methods. PVD(Physical Vapour Deposition) techniques involve condensation from the vapour phase, while CVD(Chemical Vapour Deposition) methods involve reaction from the vapour phase. PVD is confined almost wholly to making relatively thin films(10μm to 100μm) whereas CVD produces both thin films and layers in excess of 1mm. At present however, there is an extensive overlap in CVD and PVD processes with hybrid techniques continually emerging. The main reason for this is the extensive development taking place in these areas in order to meet industrial demands. Therefore, hard and fast distinctions with respect to individual vapour deposition process are becoming increasingly difficult to make. The underlying principles of the various processes nonetheless remains the same.

All vapour deposition processes are characterised by the fact that components are treated in a chamber, which is either a vacuum chamber, or one designed to withstand the high temperature and corrosive gases which are used in CVD. Although the size of objects to be coated is limited in this respect, this limitation is attributable more to capital expenditure rather than process fundamentals. This is confirmed by the coating of aircraft components, with aluminium, in 2m by 3m chambers. A further confirmation of this is the solar coating of architectural glass in plants of up to 60m long. Another characteristic feature of vapour deposition is the batch basis on which components are treated. Exceptions to this are the barrel-coating of large numbers of small objects, and, the vacuum evaporation of Al onto paper/plastic sheet which is a continuous process.

Coating vapours used in PVD processes can be generated by evaporation from a molten source, or, ejection of atoms from a solid source undergoing bombardment by ions. If the vapour is left as a stream of neutral atoms in vacuum the process is referred to as vacuum evaporation. In the case of ion plating and sputter coating, the vapour is mixed with an ionised gas(typically 0.1%) and is then deposited on an earthed/biased substrate. A highly ionised vapour stream forms a plasma which is attracted to a biased substrate in the arc plasma evaporation process. At the extreme end, a 100% ionised beam can be focused and accelerated to energies high enough to penetrate the substrate. This last process is commonly known as ion implantation. Ion bombardment of the source allows a wider range of materials to be deposited, as well as, the production of thin optical and electronic films.

CVD covers a broad range of processes, all of which use gaseous reagents undergoing chemical reactions near or on the heated surface which is to be coated. **Figure.2.2.3**

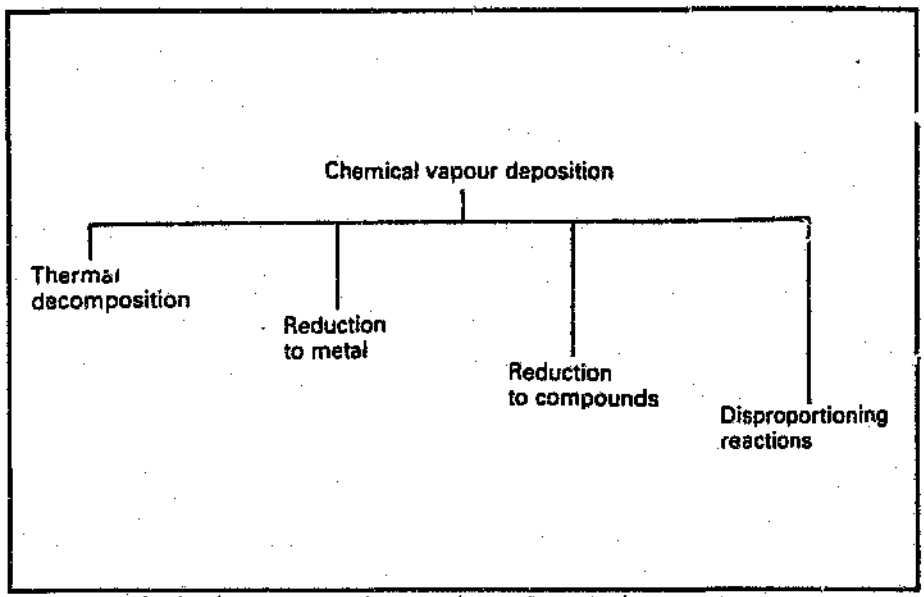


Figure.2.2.3. Reactions involved in CVD process[4].

displays the different reaction types involved in CVD processes. Generally, three stages are involved in these processes.

(i) Production of the volatile carrier compound, eg. nickel carbonyl ;
(ii) Transportation of the reagent gas - without decomposition - to the deposition site ;
(iii) Chemical reaction to produce coating on substrate.

These stages may be distinct in both time and space, or, they may all occur simultaneously. An example of the latter is the quartz-iodide lamp where the tungsten filament is continually re-coated by its own evaporated vapour. Although these characteristics limit the CVD technique in many ways, CVD is particularly useful for depositing materials which are difficult to deposit by other means to the required thickness. CVD is probably

unique for its ability to make pyrolytic carbon and pyrolytic boron nitride.

Substrate cleanliness requirements are less stringent in CVD than with PVD, mainly because of the high temperatures used and the general nature of the reactions involved. Throwing power is excellent since gases are used around atmospheric pressure. Thus all exposed surfaces are coated to a high degree of uniformity. Coating roughness, especially with thick coatings(10μm-1mm), is usually greater than that of the underlying substrate.

As with PVD, ionisation of the reactive species by the introduction of a glow discharge enhances the capabilities of conventional CVD processes. Plasma activated CVD(PACVD) makes use of DC and RF plasmas for enhancing deposition characteristics. The application of PACVD in the manufacture of diamond films is currently of considerable interest in wear resistant applications. Such films are deposited from a mixture of hydrogen and organic gases containing methyl radicals at growth rates of about 10μm/hour. Russian workers have been reported to be producing coatings in excess of 1mm thickness. Diamond films also have huge potential application in the semiconductor field. In this respect, CVD is probably the only technique that can be used to deposit diamond films to thicknesses above a few micrometers.

The techniques described above all involve complex equipment and operational control, and high capital expenditure. Other limitations of these techniques, are the low deposition rates which are achieved. For example with sputter ion plating, coating rates cannot exceed 0.1μm/hour.

2.2.3. Thermal Spraying Processes

In thermal spraying processes, consumable coating material is fed into a high temperature spray gun. The coating material is heated to a molten state within the gun, at which point it is projected in particulate form towards the workpiece. These hot particles form inter-locking splats when they collide with the workpiece (**Figure.2.2.4**). In this way, a coating of desired thickness is built up over the substrate. Generally, thermal spraying offers great flexibility because spraying can be done in air. In addition, virtually all material compositions may be deposited provided there is a stable liquid phase.

Metals, ceramics, carbides, or plastics, or combinations of these, may be deposited. As such, the strength of bond between coating and substrate varies over a wide range, depending on both the material and spray process used. The density of sprayed coatings varies with coating material and the temperature at which it strikes the workpiece, and, the impact energy of the molten particles. Coating adhesion depends on the same factors with the surface condition of the substrate having significant influence. For adequate adhesion properties, surfaces must be clean and suitably roughened. Adhesion strengths of thermally sprayed coatings vary from relatively low values to those approaching welded bond strengths. High strengths are obtained in the processes involving high temperature diffusion between coating particles and substrate.

Thermal spraying processes fall into two categories, namely the low energy and high energy processes. The former processes are often referred to as metallising and are used extensively for spraying metals such as zinc and aluminium for corrosion resistance (**Figure.2.2.4**). Metallising usually

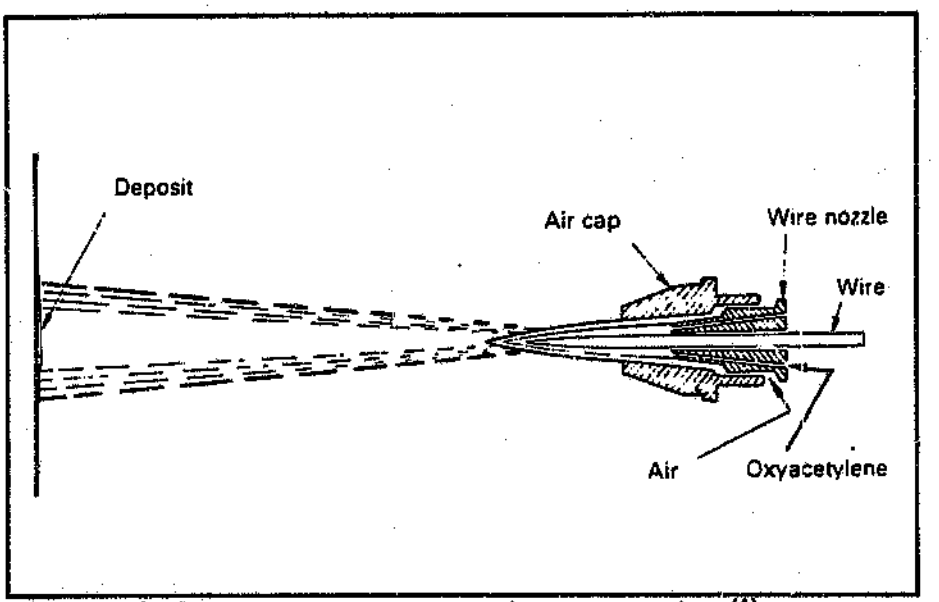


Figure.2.2.4. Oxyfuel gas wire spraying[4].

finds application where components to be coated are large and the magnitude of thermal and mechanical shock, as well as abrasive wear is small. One of the distinctive features of coatings produced by low energy processes is the relatively higher porosity present than that found in higher energy processes. The effects of porosity may be positive or negative. The positive aspect stems from the fact that it decreases residual stresses and acts as a reservoir for lubricant in bearing applications. On the negative side, corrosion could penetrate the coating through these pores. Examples of low energy spraying processes are arc or flame spraying.

Higher energy processes such as plasma, D-gun and high velocity combustion spraying provide coatings of higher density, reduced porosity, and improved adhesion strength. Moreover, these processes are suitable for materials with higher melting points, thereby extending the application of sprayed coatings to include resistance to thermal and mechanical shock, and wear resistance. Another important

distinction between the two groups of spray processes, is cost and portability. Metallising processes generally involve lower capital cost and greater flexibility, while the high temperature methods involve higher capital expenditure and tend to be used in fixed installations.

Graded coatings are useful in reducing spalling due to the different expansion characteristics between substrate metal, eg. steels, and coating, eg. ceramic. Typically, a layer with 70-80% metal component is applied first, then a layer with 20-30% metal, and finally a layer of ceramic. In doing so, the respective wear resistance and thermal conductivity of ceramic and metal are combined.

Thermal spray processes are line of sight processes. Therefore, surfaces to be coated must be accessible to spray guns chosen for a particular process. Small recesses and holes pose a problem. Furthermore, there is inadequate ventilation for gas and overspray in such areas. It is important to note that overspraying constitutes a health and safety risk.

2.3. Physical and Mechanical Properties of Coated Materials

2.3.1. Hardness of Coated materials

The hardness of a material can be defined as its resistance to permanent deformation[11]. Hardness of bulk material can quite easily be determined using macrohardness testing. In other cases, for instance those of distinct microstructural features or thin coatings, microhardness testing becomes necessary. However, there are a number of limitations associated with both macro- and microhardness testing.

One of the general problems with hardness tests is the variation in hardness obtained with loads used. In order to reduce the probable error when carrying out hardness tests on a material, it is proposed that the largest possible load be used to obtain a large indentation which can be measured accurately. With large indentations the percentage error, for a specified accuracy of the testing machine, is reduced[11]. However, the shortcoming to this approach is that the probable error on hardness testing also varies with the size of the indentation made. The likely error for a given indentation size increases as the load used to obtain that indentation increases. Additional limitations arise when the microhardness of microstructural features, e.g. grains or inclusions, or thin surface layers and coatings have to be assessed.

Assessing the microhardness of coated materials directly, by measuring indentations on the coating is a complex task involving a number of complications. Conventional microhardness machines employ indenters which press too deeply into coated samples, ie. the indentation is in close

proximity to the coating-substrate interface, or, it extends beneath this interface. As a consequence of this, hardness values recorded for surface layers are influenced by the hardness of substrate materials. This effect is more pronounced in implanted layers where the layer depth is of the order of 1 μm, whereas the indenter depth lies in the range 1-2 μm[12]. The maximum depth of indentations is usually not greater than one seventh the length of the diagonal.

In recent years, the increasing use of wear resistant or protective coatings has created a need for proper characterisation of coatings and their properties. Among the important properties requiring characterisation is hardness. Characterisation of thin film(1-10μm) hardness is difficult since such films require indentation depths between 0.1-1 μm to give what is referred to as "true" film hardness. By "true" film hardness it is meant a hardness independent of and not influenced by the substrate material[12].

To achieve film-substrate independency with respect to hardness, the film thickness should necessarily be ten times the indentation depth. This apparently accounts for subsurface damage beneath an indentation by eliminating the influence of the substrate-coating interface proximity. In doing so, the effects of substrate hardness on coating hardness is eliminated. In practice, indentation depths of 0.1-1μm are beyond the capability of most commercial microhardness apparatus. Various methods have been devised to determine the hardness of thin coatings. One method used quite successfully involves the use of an ultra-low load microhardness testing machine, thereby achieving indentation depths in the range stated above.

Other efforts towards characterisation of thin coating hardness have centred on modelling of hardness behaviour based on a number of theories. For instance, some researchers quote hardness values for thin films that have been obtained from specially produced thick films(often still less than 10μm thick), using the minimum load that produces a measurable impression. Interestingly enough, such values tend to be higher than those listed for the bulk material in literature. One of the main reasons for this is the fact that hardness is not a material constant but varies with load[13].

Alternative methods to measuring thin film hardness by small indentations aim at accounting for the contributions to measured hardness from both the film and the substrate. This would appear to be a more appropriate technique since the hardness of a coated material is a composite value, reflecting the contributions to hardness by both the coating and substrate. Several attempts have been made to model this composite hardness behaviour of coated materials based on empirical or semi-empirical approaches.

One model proposed[14] combines substrate hardness **Hs**, and film hardness **Hf**, to give a "composite" hardness **Hc** using the equaton,

$$H_c = H_s + \alpha.(H_f - H_s)$$

where,

Hc = composite hardness ;
Hf = film hardness ;
Hs = substrate hardness;
α = empirical factor independent of material.

Alpha varies smoothly with the ratio of the diagonal length of the indentation to the coating thickness to some extent. It is essentially a weighting factor determining to what extent the coating influences composite hardness. For relatively thick, hard coatings(5-10μm) on less hard substrate, it was found that coating hardness could be established when indentation depths were less than one tenth the coating thickness.

A more recent model proposed by Jonsonn and Hogmark[15] requires the hardness of coated and pure substrate, as well as the coating thickness. This model allows one to obtain the characteristic microhardness of a coating using a conventional microhardness tester. Layer hardness in this case is calculated according to the relation,

$$H_f = H_s + \left[\frac{H_c - H_s}{(2.G.(t/D)) - G^2.(t/D)^2}\right]$$

where all variables are as in the above equation, and, G is a geometric factor.Hc and Hs are calculated from the Vicker's hardness formula,

$$H = \frac{1854.4\ P}{d^2}$$

where,

P = load in g;
d = average length of diagonals in μm.

The application of this model in measuring the microhardness of nitrogen implanted layers on steel was carried out by Bredell and Malherbe[14]. Their results showed that there is a critical dependence of hardness on

film thickness. Thus, the more non-uniform a coating, the greater the variation in hardness one could expect. A peculiarity about this model is that it fails when indentation depths are less than the film thickness.

As can be discerned from the above discussion, measuring the hardness of thin coatings is not a straightforward procedure. Varying results are obtained using different models. Variations also arise due to other factors like non-uniformity of coating thickness over relatively large distance on substrate materials, compelling one to quote an average hardness value. Moreover, the scarcity of reliable hardness data for thin films makes it difficult to judge how accurate or reliable a particular model is. The main criterion of any method is that it generate reproducible data which can be used to rank the hardness of different materials. To achieve this with coated materials, the correct load and indentation size have to be chosen for a given coating thickness.

2.3.2. Influence of Residual Stresses

Residual stresses induced by coatings have a considerable influence on substrate materials. To appreciate the effects of residual stress induced by coatings, it is necessary to understand these stresses in general. Apart from residual stresses due to overlay or diffusion coatings, such stresses can also be generated by processes like rolling, shot peening, induction hardening and so on. In these cases, compressive residual stresses are introduced in the surface of the material. Tensile stresses in the bulk material can balance the effect of these compressive residual stresses. Residual stresses compensated for in this way without the application of an external load are referred to as residual stresses of the "first kind"[9].

Transformations, not only at the metal surface, but in the bulk material also induce residual stresses. Changes in the specific volumes of neighbouring regions within a material can give rise to these stresses. Such volume changes may be due to[1],

(i) Differences in plastic deformation ;
(ii) Structural changes ;
(iii) Concentration changes ;
(iv) Chemical transformations ;
(v) Thermal transformations.

of the metal in these regions. Work hardening is a common example where volume changes in a surface layer induce residual stresses. Residual stresses caused by non-uniform heating are referred to as "thermoplastic" stresses. Diffusion processes also give rise to residual stresses[9].

The stability of residual stresses within a particular material at room temperature has a significant influence on the strength and endurance of the material. Residual stress stability in this case would depend on time, stress-intensity, the properties of the metal and the way in which the stresses were induced. For instance, it has been found that prolonged ageing of steel at room temperature reduces residual stresses by 5-8%[9]. Compressive residual stresses raise the endurance limit of steels in air, this behaviour being attributed to the fact that compressive residual stresses concentrate in the vicinity of notches. Tensile residual stresses have an opposite effect in that they increase the notch sensitivity of steels. There are some exceptions to the above findings. Certain physical and mechanical changes in the surface layers of materials can increase fatigue strength even in the presence of tensile residual stresses. An interesting example of this is found in decarburized surface layers. Loss of carbon produces tensile residual stresses, but the low notch sensitivity of

ferrite in the surface layers can increase the fatigue strength[16].

Numerous effects are induced by residual stresses in materials. When assessing the influence of these stresses in steels, the sign and magnitude of these stresses at the surface of the material, as well as, their distribution and gradient in the bulk of the metal must be known. With regard to coated materials, analysis of stresses in coated steels, and alloys, has shown that residual stress diagrams, which describe the sign and distribution of stresses in these materials, can be plotted[9]. Generally, all diagrams of this type can be divided into six main types and two auxiliary types. The distinction between the different types is based on the location of the maximum residual compressive or tensile stress in the coated material. **Figures.2.3.1.(a) and (b)** illustrate the eight types of residual stress diagrams encountered. Each diagram can be described as follows, with an example given for each case.

Type I - Compressive residual stresses with a maximum intensity at the surface, eg. work-hardened and induction heated components. Also found in processes where there is uniform or step-wise decrease in concentration of a diffusing element from surface to interior.

Type II - Compressive residual stresses with maximum intensity at the surface. This maximum can be transformed into a tensile stress with maximum intensity at a metal-coating boundary. In the case of diffusion coatings, where the boundary is arbitrary, a boundary must be chosen. This arises in diffusion layers comprising several regions of differing structures and physical or mechanical properties, eg. in steels impregnated with strong carbide-forming elements or steels with an austenitic region beneath the diffusion layer.

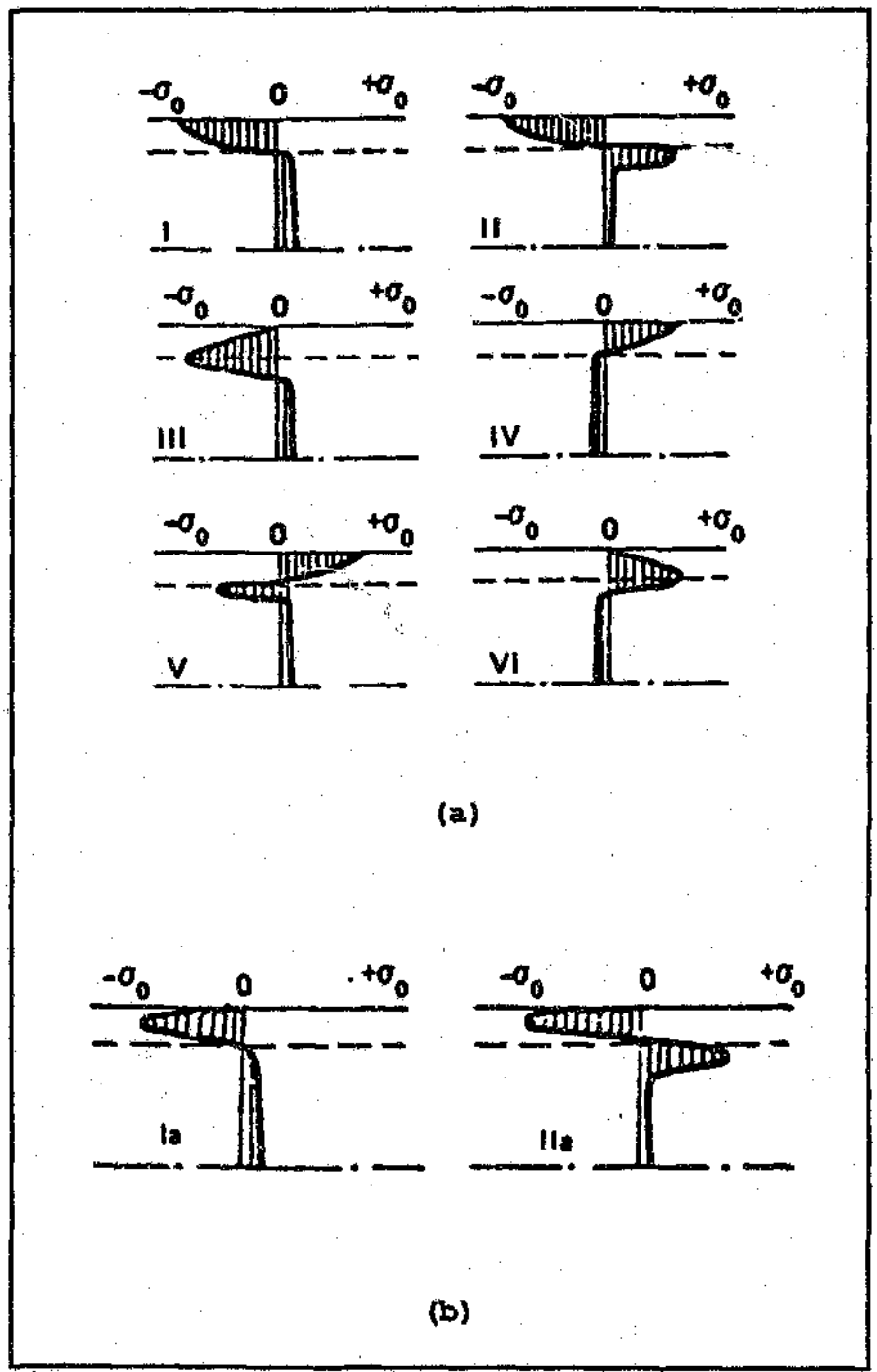


Figure.2.3.1. Basic(a) and Auxiliary(b) diagrams of the distribution of axial residual stresses[9].

Type III - Compressive stresses with a maximum intensity at the metal coating boundary. This is found in articles with electrodeposited diffusion coatings, where the coating material is first electrodeposited and then heated to promote thermal diffusion. Heating of articles with composite coatings leads to diffusion of coating material into the substrate beneath the metal/coating boundary. This forms a diffusion layer with a specific volume different to that of either substrate or coating and leads to compressive stresses of this type.

Type IV - Residual tensile stresses with maximum intensity at the surface, eg. electroplating and decarburized surface layers.

Type V - Residual tensile stress with a maximum at the surface, which can be transformed into compressive stresses with a maximum at the metal-coating boundary, eg. electrodeposited diffusion/composite coatings.

Type VI - Residual tensile with a maximum at the metal diffusion layer boundary, eg. steels with a decarburized case containing an austenitic layer.

Auxiliary types - These are variations of the above types, the difference being that the maximum intensities are not situated at the surface or metal-coating/diffusion layer boundary, but rather at a depth smaller than the coating/diffusion layer thickness. This occurs as a result of residual stress relaxation processes, causing a shift in the maximum intensity.

A number of variables therefore influence the distribution of residual stresses in surface treated components. The classification given here covers most of those encountered in practice. Exceptions occur in cases where the stress distributions are more complex as in the case of laminated materials or composite diffusion coatings.

2.4. Physical Chemistry and Metallurgy of Melts

In this section, attention was paid to the physicochemical aspects of melts and glasses, especially with regard to melts similar to borax. Knowledge of the chemistry and thermodynamics of the borax melt, as well as melts in general, would be useful in understanding the nature of the TD process.

2.4.1. Types of Melts

Variations in the nature and properties of melts are due mainly to the differences in the components making up the melt. These differences are highlighted below[17,18].

(i) Ionic Halides - As implied by the name, these melts are made up of salts comprising a metal and non-metal (halide), eg. NaCl, KCl, NaI. Generally, melts of this kind have relatively high conductance. This stems from the strong ionic character of the constituents.

(ii) Non-Ionic Halides - Examples of such melts are $BeCl_2$ and $ZnCl_2$. These melts may be distinguished from the previous type by the very low conductance they have. However, increasing the temperature of these melts greatly increases their conductance. This is chiefly due to the dissociation of melt constituents into anions and cations at high temperatures.

(iii) Sulphides - Sulphide melts consist of compounds such as FeS, Cu_2S, Ni_3S_2, etc. Conduction in sulphide melts is mainly electronic, by contrast to ionic-halide melts, resulting in relatively high specific conductance. In the case of FeS and Cu_2S, the conductance increases as the concentration of sulphur increases.

(iv) Stable polyatomic anion melts - These are melts containing polyatomic anions like NO^{3-}, NO^{2-}, CO_3^{2-} and SO_4^{2-}. Typical melts of this type are those containing nitrates, nitrites, sulphates and carbonates. The polyatomic anions listed above, are preserved on melting, ie. they are stable.

(v) Oxides - Oxide melts fall broadly into two groups, namely ionic and covalent. The most important oxides of the latter group are those in which oxygen is bonded to form 3-D networks of the kind found in melts of B_2O_3, SiO_2, GeO_2 and P_2O_5. Melts of these oxides have very high viscosities and very low specific conductance.

Ionic oxide melts on the other hand, have very high conductances, even higher than those of ionic-halide melts. Oxides falling into this category are Cr_2O_3, TiO_2, V_2O_5, Bi_2O_3, FeO and MnO. The high conductance of these melts arises primarily from two conduction mechanisms[17]. One mechanism involves electronic conduction arising from normal semi-conduction, where conducting electrons are not localised, ie. they move between ions of different type. The second mechanism involves the movement of localised electrons between ions of varying charge within the melt. These ions are all of the same type, hence the reference to "localised" electrons. These melts usually contain ions of more than one valency, eg. Cr^{2+}/Cr^{3+} or Fe^{2+}/Fe^{3+}. With these melts, very little change in conductance occurs with melting. The process of fusion has little effect on electron movement, but enormous influence on ion movement.

In spite of the complexity of electrical conduction in liquid oxides, it is convenient when considering structure and reaction mechanisms, to regard them as consisting primarily of metal and oxygen ions. The structure of liquid oxides differ from the corresponding solid with respect to coordination numbers, nearest neighbour distances and so on. With some oxides, complex ions may exist alongside the

simple oxygen and metal ions[19].

(vi) Network-forming oxides - Oxides which form glasses when melted and cooled are called glass-forming or network-forming oxides, because of their ability to build up continuous 3-D random networks. Silicate(SiO_2), phosphate (P_2O_5) and **borate**(B_2O_3) melts, which form part of the covalent group of oxide melts described above, are remarkable for their tendency to supercool and form solid glasses, unlike other melts which crystallise on cooling. Glasses are supercooled liquids which do not have sharp melting points, but soften gradually and eventually become fluid due to the continuous fall in viscosity with rising temperature[18]. Oxides of this nature give rise to highly viscous melts with very low electrical conductances. The low conductances confirm that bonding is covalent, and the high viscosities that the 3-D covalent network is retained on fusion.

XRD(X-Ray diffraction) studies on liquid B_2O_3 have shown that the basic building units are BO_3-triangles which share corners with each other. The difference between the regular crystalline lattice and that of glasses is illustrated in **Figure.2.4.1**, where the oxide M_2O_3 represents B_2O_3. In both cases (a) and (b), the structural unit is the $MO_3(BO_3)$-triangle, however, with the glass structure long-range order is absent. Instead, glasses possess short-range order with their networks being non-periodic. This is essentially the reason why glasses unlike regular crystals do not give sharp, well-defined X-Ray spectra[17].

2.4.2. Reactions between ionic and network-forming oxides

It is important in the light of this project to understand the physicochemical reactions which occur when an ionic oxide like Na_2O is added to a glass-or network-forming

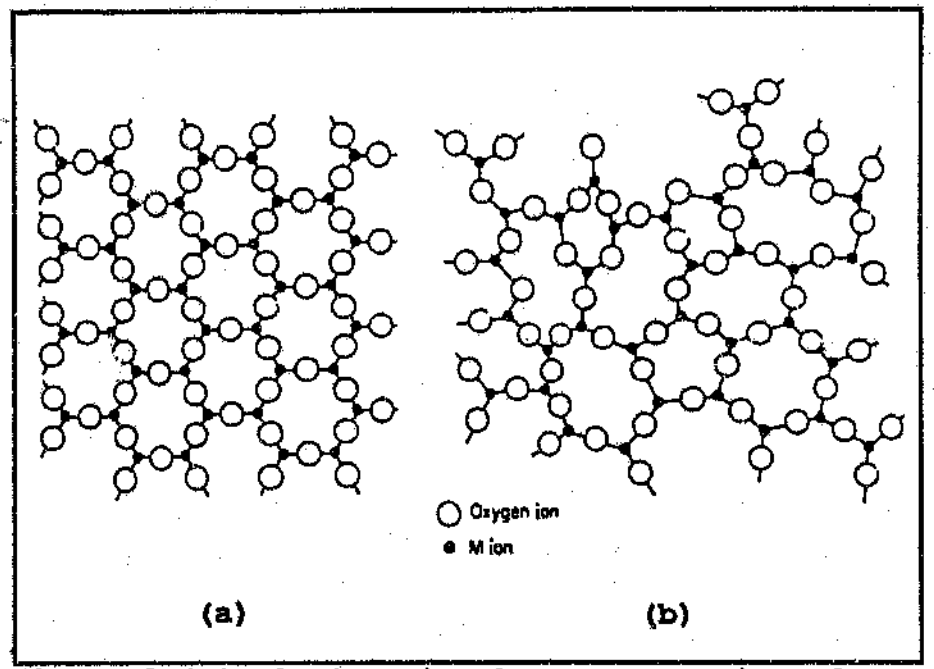


Figure.2.4.1. 2-Dimensional representation of an oxide M_2O_3 in (a) Crystalline form and (b) Glassy form[17].

oxide like B_2O_3, since these two oxides make up the borax ($Na_2B_4O_7$ or $Na_2O.2B_2O_3$) melt.

Ionic oxides added to glass-forming oxides can be separated into two groups according to the functions they perform within the glass structure[17]. These two groups are known as intermediate oxides or network-modifying oxides. The former group of oxides is capable of taking part in the glass network, eg. aluminium oxide. The latter group, eg. Na_2O, more relevant in this case, are incapable of building up a continuous network structure and as such their effect on the glass network is usually to weaken it.

The changes which occur when Na_2O is added to B_2O_3 are well represented by those which take place when Na_2O is added to silica glass. This is so because SiO_2 and B_2O_3 are oxides of

the same type. Addition of Na_2O to SiO_2 causes structural changes to the network as shown in **Figure.2.4.2**, where the oxygen bridges between SiO_4-groups are broken down. There are now two non-bridging oxygen atoms between SiO_4-groups, one of which has been contributed by Na_2O. Thus Na_2O produces gaps in the continuous network structure, with Na^+ ions being accommodated in holes or interstices within the random network structure as indicated by **Figure.2.4.2**[20].

The first crystalline structures which can be formed when ionic-oxides are added to silica have the general formula $M_2O.2SiO_2 (=Na_2O.2B_2O_3)$. These structures are stable only when the cations are large and univalent, eg. Na^+ or K^+. When divalent cations are added, eg. $Ca^{2+}(CaO)$ or $Mg^{2+}(MgO)$, one cation is present for each pair of non-bridging oxygen ions. In this case, where the cations are univalent, two cations are present for each pair of non-bridging oxygen atoms. This is shown in **Figure.2.4.3**.

Higher proportions of Na_2O cause progressive breakdown of the silica or borate network, resulting in different structures. Reaction between Na_2O and B_2O_3 gives rise to a branched structure. XRD studies indicate that B_2O_3 has a coordination number of 3.1 at room temperature. Addition of Na_2O increases the coordination number until at 0.33 mole fraction it becomes 3.9. This implies that the boron atom changes form from triangular to tetrahedral. This transformation from three to four is thought to be mainly responsible for the anomalous behaviour of borates with respect to viscosity and temperature. **Figure.2.4.4** displays this behaviour of borates.

Unlike silica and phosphate mixed with Na_2O, the viscosity of $Na_2O.B_2O_3$ increases initially and then decreases to a mole fraction of 0.33 Na_2O. Thereafter it decreases again.

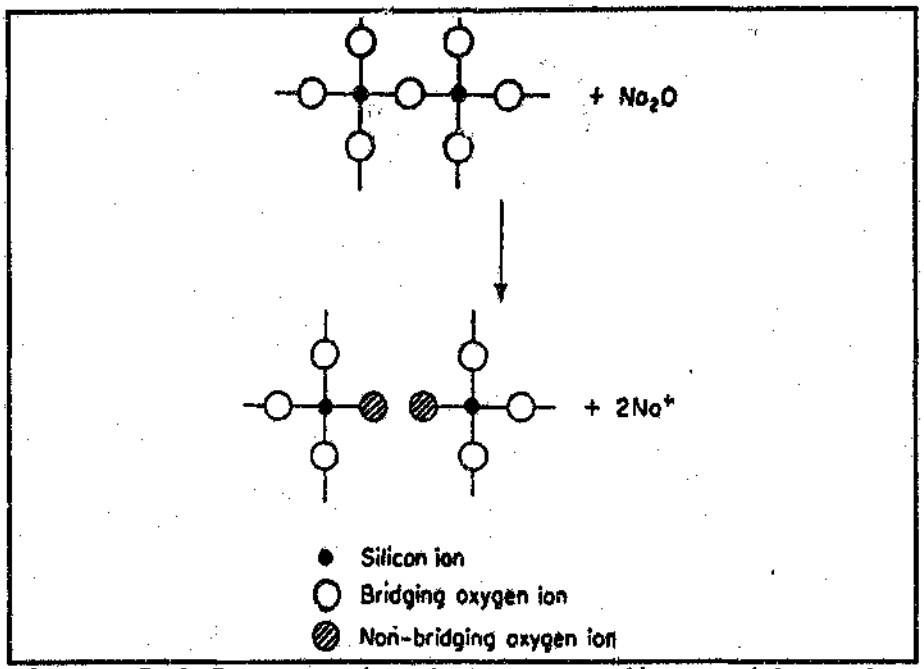


Figure.2.4.2. Reaction between sodium oxide and silica tetrahedra[17].

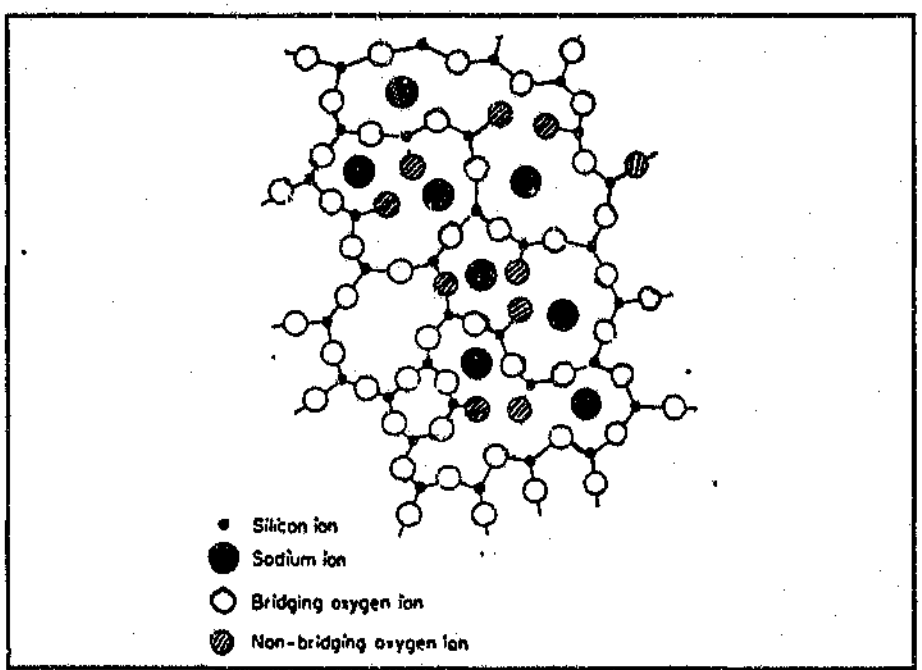


Figure.2.4.3. 2-Dimensional representation of the structure of soda-silica glass[17].

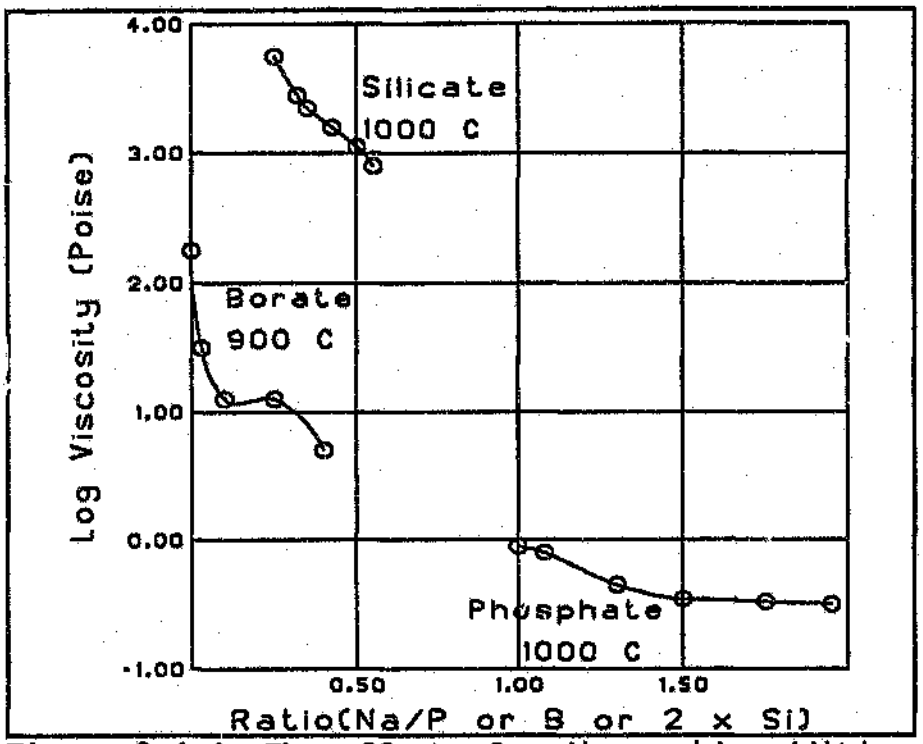


Figure.2.4.4. The effect of sodium oxide addition on the viscosities of its mixtures with P_2O_5, B_2O_3, and SiO_2[21].

This is attributed to the progressive weakening of the structure due to breakdown of B-O-B links, allowing easier expansion of the borate structure.There is nonetheless an overall decrease in viscosity with increasing Na_2O percentage. The relation between viscosity and temperature for glasses is important in a number of ways. For instance, a low viscosity favours rapid rise of gas bubbles through the melt, thereby rendering the melt fairly free of gas[17]. The addition of Na_2O to B_2O_3 is significant in this respect since it decreases the viscosity of the melt as shown in **Figure.2.4.4.**

Another important property of the melts described here is their conductance. The conductance of silicate melts is always raised by addition of metal oxides and the

conduction mechanism is primarily ionic. Similar effects are found in molten phosphates and borates and a transport number of unity has been reported for cations in glassy $Na_2O.B_2O_3$ at 300°C. **Figure.2.4.5** shows the decrease in activation energy for electrical conduction([Ek]p) with increasing MO percentage for borates. It can be seen that at 50% Na_2O, there is a fair increase in conductance with a corresponding decrease in [Ek]p[17].

2.4.3. Applications of Borax

A knowledge of the uses of borax salt would shed some light on the way it functions in the salt bath. Boric oxide(B_2O_3) is often used as a fluxing agent for decomposing and dissolving analytical samples. When the decomposition of samples which are to be analyzed by conventional methods is slow, or in some cases non-existent, fluxes such as B_2C_1 are employed[22]. This is typically the case where refractory materials have to be analyzed.

Fluxes decompose most substances by virtue of the high temperature at which they are used(300-1000°C) and the high concentration of reagent(flux) which is brought into contact with the sample. This is usually ten times the sample weight[23]. The high concentration of flux is required for successful fusion of the sample. Fusion involves intimate mixing of the flux and sample, preferably in the crucible to be used for melting, and then heating the mixture gradually to the required temperature. Fusion times range from few minutes to several hours. There are certain disadvantages associated with the large amount of flux used. Firstly, the high temperatures used enhance the danger of volatilisation losses. There is also the possibility of significant contamination which may be introduced by the large amounts of flux used.

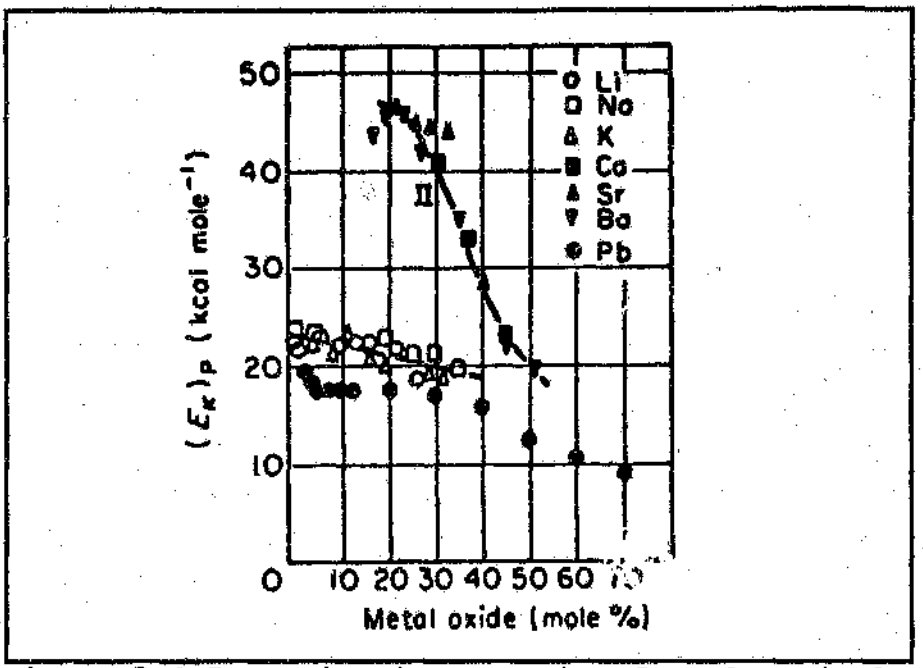


Figura.2.4.5. Activation energies for electrical conduction of some binary borates[17].

Lastly, some attack by the flux on the crucible material also results. Boric oxide is an acidic flux which gives rise to high viscosity melts with very low electrical conductance. Addition of Na_2O to B_2O_3 renders the melt more basic, decreases its viscosity and increases conductance. As such, borates form part of the basic group of fluxes[24].

2.5. The TD Process

2.5.1. Background

It was stated initially that studies of a similar nature to that carried out in this project were implemented in Japan in the early seventies. Over the last two decades, these studies have culminated into what is today known as the Toyota Diffusion(**TD**) process. In 1968, research was initiated in Japan into the development of hard, wear resistant boride coatings. These coatings were produced by diffusing boron into the metal surface, the metal component being immersed in a salt bath[25].

Salt baths used in the initial boriding studies contained borax and various additives, operating at temperatures between 800-1000°C. Subsequently, it was found that carbide coatings formed over metal surfaces containing carbon, when the borax baths comprised additives such as V, Cr, and Nb. The decision was made to develop these coatings, and factors governing treatment technology, such as coating reproducibility, bath deterioration and treatment conditions. It was believed that development of these coatings would be much more fruitful than those obtained from boriding, as the latter process did not ensure toughness[25].

2.5.2. Processing Technique

One of the outstanding features of the TD process is its simplicity, especially when compared to other carbide coating processes like CVD. Materials to be treated are simply placed in a heat resistant pot containing borax and

carbide forming additives which in turn is placed in a salt bath furnace, as shown by **Figure.2.5.1.**

Operating temperatures are quite high and range between 800-1250°C, with treatment times between 3-12 hours. The percentage of ferro-alloy added to the bath is typically about 10%. Higher additions have an adverse effect on bath fluidity and homogeneity, whereas smaller amounts affect reaction rates and bath saturation[26]. **Figure.2.5.2** outlines the steps involved in processing components by this process. These are as follows :-

(1) Component degreasing - Ensures coating uniformity and good adhesion properties ;
(2) Component preheating - Done in an ordinary heat treatment furnace to prevent cracking and distortion due to rapid heating in bath ;
(3) Immersion - Layer thickness varies with bath temperature, time and substrate composition ;
(4) Hardening - Quenching in air, oil or salt to harden components if required, since bath temperatures are close to those required for hardening steels ;
(5) Tempering - Included if treated parts are rapidly quenched ;
(6) Cleaning - Of attached salt, which is easily accomplished by boiling in hot water ;
(7) Dimensional control - To check if parts, are distorted, cracked or require further finishing.

Some noteworthy features of the TD process, which can be overriding if selecting a particular carbide coating process, are listed below.

(i) Simple equipment and easy operation;
(ii) Variable and selective(by masking) coatings;
(iii) Non-line of sight with uniform coatings;
(iv) No air pollution or complex waste disposal;
(v) Low cost with long bath, and pot lives.

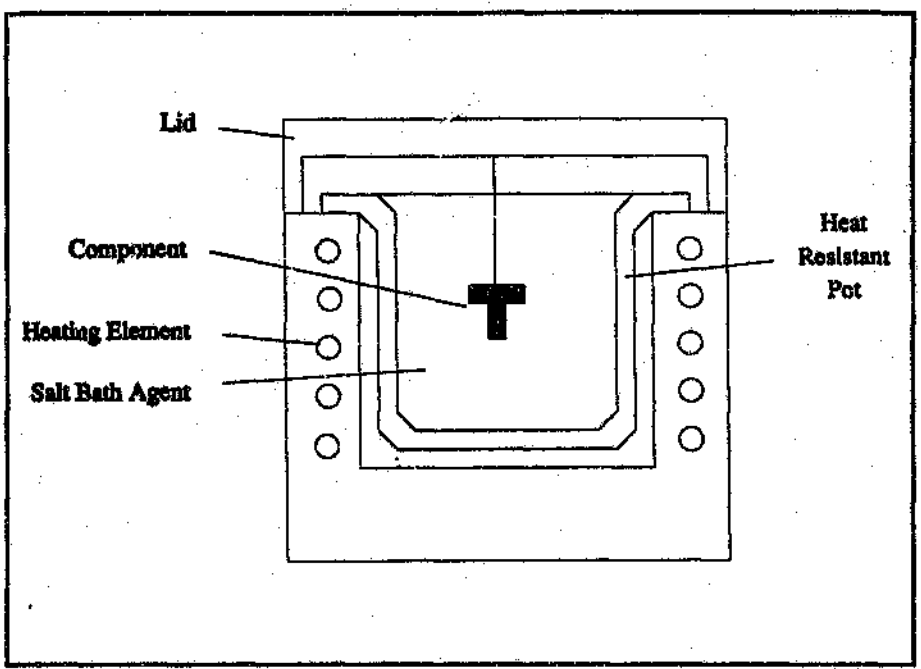


Figure.2.5.1. Salt bath furnace for carbide coating[27].

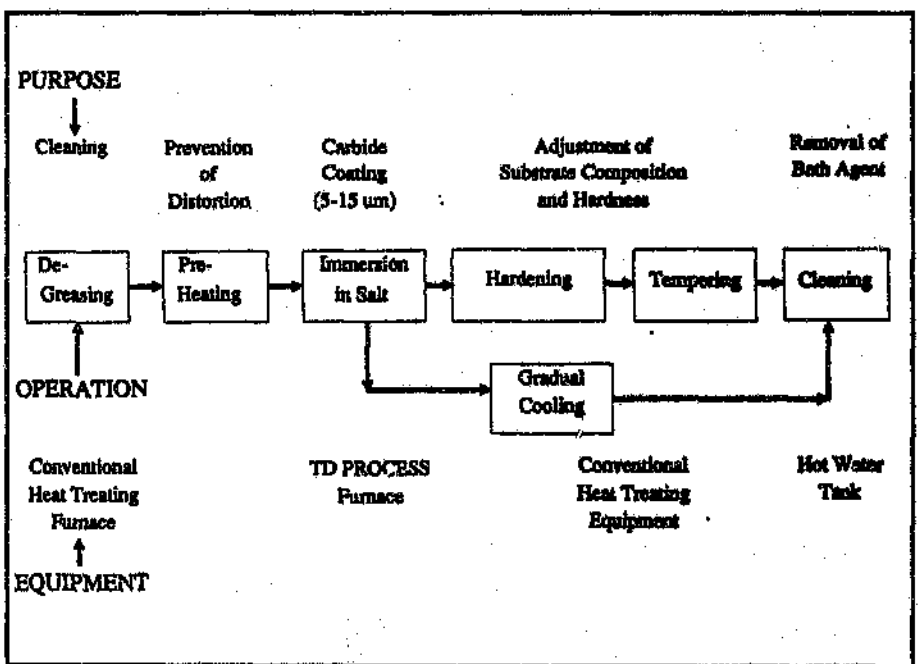


Figure.2.5.2. Outline of the TD Process[27].

2.5.3. Growth Mechanism and the Formation of Carbide Layers

Arai[25] states that the reactions between the various additives and borax in the bath could generally be explained in terms of the free energy of oxide formation and the free energy of carbide formation of the various bath constituents. This is indicated by **Figure.2.5.3.** Elements having free energies of oxide formation more negative than B_2O_3, eg. Al or Mg, reduce B_2O_3 in the bath, resulting in the diffusion of active boron into the steel to form boride layers comprising Fe_2B and FeB. Formation of such boride layers is apparently unaffected by the free energy of carbide formation.

Elements with free energies of oxide formation less negative than that of B_2O_3, and free energies of carbide formation more negative than that of Fe, eg. V, Cr, and Nb, combine with carbon in the steel to form a layer of VC, Cr_7C_3 or $Cr_{23}C_6$, and NbC respectively, as these elements do not reduce B_2O_3. Finally, elements with more positive free energies of oxide and carbide formation do not reduce B_2O_3 or form any carbide, eg. Co. Interestingly enough, it was found that under certain conditions these elements diffused into the steel to form alloy layers of Fe-Ni or Fe-Co.

A model proposed by Arai[28] representing the growth of carbide layers by this process is illustrated in **Figure.2.5.4.** Initially, the carbide forming element dissolved in the molten borax combines with carbon at the steel surface to form a very thin carbide layer. Thereafter, carbon in the substrate diffuses through this initial layer and reacts with carbide forming elements at the surface of the layer, leading to further growth. Virtually none of the substrate elements are found in the

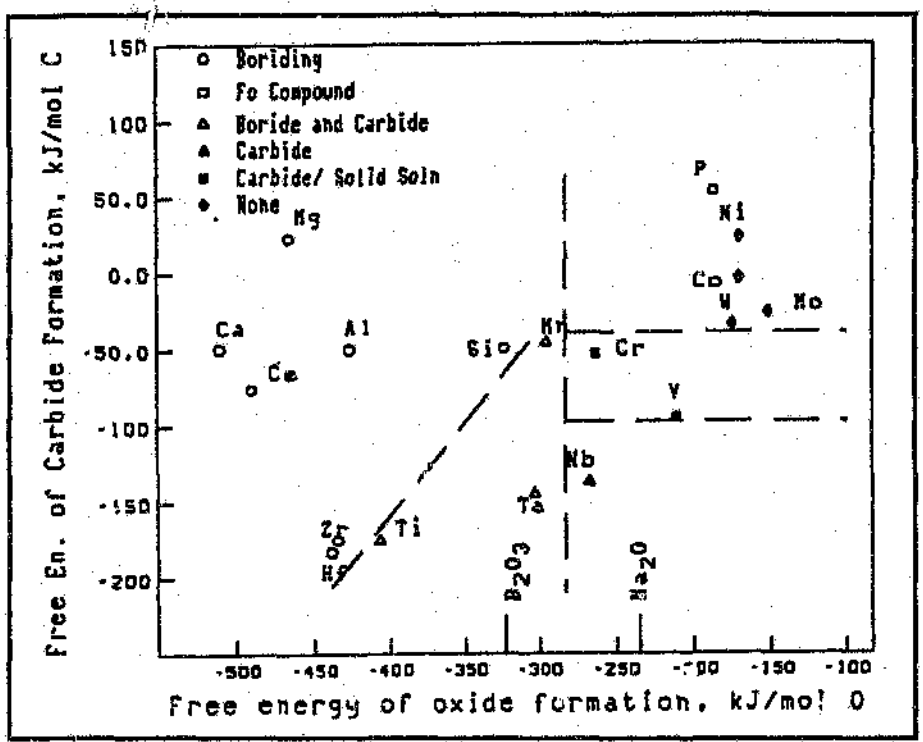


Figure.2.5.3. Relationship between free energy of formation of oxides of elements contained in the bath and kinds of layers formed(1000°C) [25].

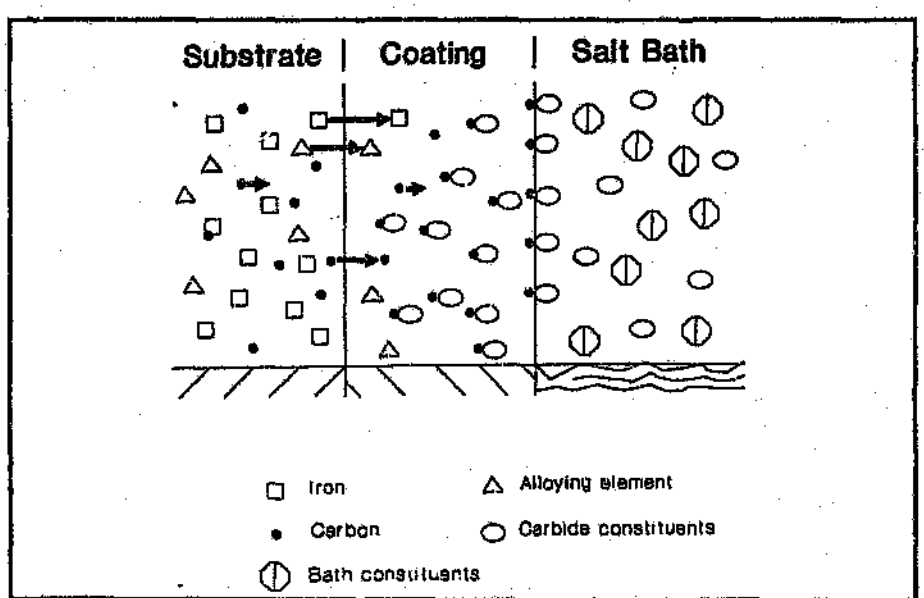


Figure.2.5.4. Growth model of carbide layer on steel surface [25].

carbide layer, as they have a low speed of diffusion in the layer. By contrast, the carbide forming elements diffuse into the base metal to a small extent[25].

It appears however that the mechanism of carbide formation is more complex than implied by this discussion. Child et al.[26] found the state of oxidation of the reactive species, ie. carbide forming element, to be critical to the formation of layers. They speculated as to whether the layer formation occurred by reaction at the bath-substrate interface between the solid ferro-alloy and the carbon in the substrate, with possible side reactions in the molten borax. It was found that the carbide forming element, eg. V, oxidised rapidly under certain conditions. No VC layers formed on steels treated in small stainless steel crucibles containing about 1kg borax with 10% ferro-vanadium(-100 mesh), when the bath was heated under strongly oxidising conditions.

It was also found that carbide coatings could be obtained in such baths if about 8% ferro-aluminium was added[26]. The addition of ferro-aluminium rendered the bath active. This suggested that oxidising conditions could occur in borax baths especially if such baths are small. The result of oxidation is a dark glassy slag of vanadium oxide and borax. Child et al.[26] also found that VC layers formed satisfactorily on steels immersed in 2kg borax baths, when a blanket of argon was maintained over the melt. Incidentally, the borax glass appeared to be green in colour in this case. It is interesting to note from this viewpoint that currently, the largest operating furnace of this type in Japan is 700mm in diameter and 1500mm in depth. Much of the early work performed by Arai[25] used small graphite crucibles and presumably avoided oxidation. Oxidation may occur at the salt/air interface, especially if the bath is stirred. During melt-down of fused borax

powder there may be oxidation by entrapped air, since borax contains about 4% moisture.

It was stated previously that Child et al.[26] found the state of oxidation of the reactive species to be critical. Optical and X-ray dispersive analysis carried out by them, on samples taken from baths at different temperatures, established the temperature/solubility data listed in **Table.2.5.1.** The borax glass contained about 2% V in solution.

Table.2.5.1. The solubility of carbide forming elements in borax[26].

Temperature(C)	V%	Nb%	Cr%
900	1.4	-	1.4
950	1.8	3.5	3.6
1000	2.4	-	-
1050	2.8	3.9	4.5

Qualitative chemical analysis revealed that baths were active when vanadium was present in the tri-valent state, ie. as V_2O_3. This finding was confirmed by XRD analysis of residues extracted from baths. Child et al.[26] state that this result is consistent with the data on the standard free energy of formation of the two oxides of vanadium. The lower oxide V_2O_3, has a value of -456.1 kJ/mol V compared to -518.8 kJ/mol V for V_2O_5. Based on these results, Child et al.[26] concluded that ferro-alloys do not dissolve as metals in fused borax, but are first oxidised.

Similar studies[26] using ESR(electron spin resonance) on

samples from active Nb-containing baths ruled out Nb_2O_5 as the reactive oxide. The results of these studies also suggest a lower oxide as the reactive species. This is again consistent with free energy data, with Nb_2O_3 having a value of -564.8 kJ/mol Nb compared to -669.4 kJ/mol Nb for Nb_2O_5. As indicated in **Table.2.5.1**, the solubility of the carbide forming elements in the borax melt is low. Achieving maximum concentration (saturation) takes time, and the rate of dissolution is affected by the following variables.

(1) Amount of ferro-alloy added ;
(2) Size of powder used ;
(3) Bath temperature ;
(4) Agitation ;
(5) Prevailing bath conditions - oxidising/reducing.

Another crucial factor determining how active the bath will be, is the concentration of the active oxide. In this regard, the graph shown in **Figure.2.5.5** was established. This shows the time taken for 2kg Fe-Nb baths to reach saturation at different temperatures and concentrations. It can be seen that the time taken for saturation is about 24 hours. However, a 5% Fe-Nb bath with a 68% Nb content is insufficient to saturate the bath after the same period.

Child et al.[26] also found from XRD studies on undissolved particles of ferro-alloy that the iron content of these particles increased while the reactive element, eg. V, decreases. Accordingly, they state that dissolution of reactive element occurs via a selective leaching mechanism. They also found the iron contents of FeV baths to be as low as 0.04%, implying that little iron is dissolved in the bath.

Arai et al.[28] found that the thickness of layers formed on

different steels immersed in baths containing ferro-vanadium, varied with dipping time according to the equation,

$$d^2 = K.t$$

where,

d = layer thickness;
t = time in hours;
K = rate constant.

The rate of layer formation varies with temperature, type of carbide produced, and, substrate composition (particularly carbon). Arai et al.[28] also determined the rate constants K, from the equation above. K varied with temperature T(Kelvin) according to the equation,

$$K = K_o.\exp(-\frac{Q}{R.T})$$

where, Ko = constant;
Q = activation energy;
T = temperature;
R = gas constant.

For VC coatings, it was found that Q varied from 185 - 211 kJ/mol, while for NbC coatings, this value was between 126 - 180 kJ/mol. Q was considered to be the activation energy for carbon diffusion in the carbide.

The rate of layer formation is affected by temperature in the manner shown by **Figure.2.5.6.** However, this suggests a linear relationship between thickness and time. By contrast, some of the graphs presented by Arai[29] show a parabolic relationship. The former relation suggests that

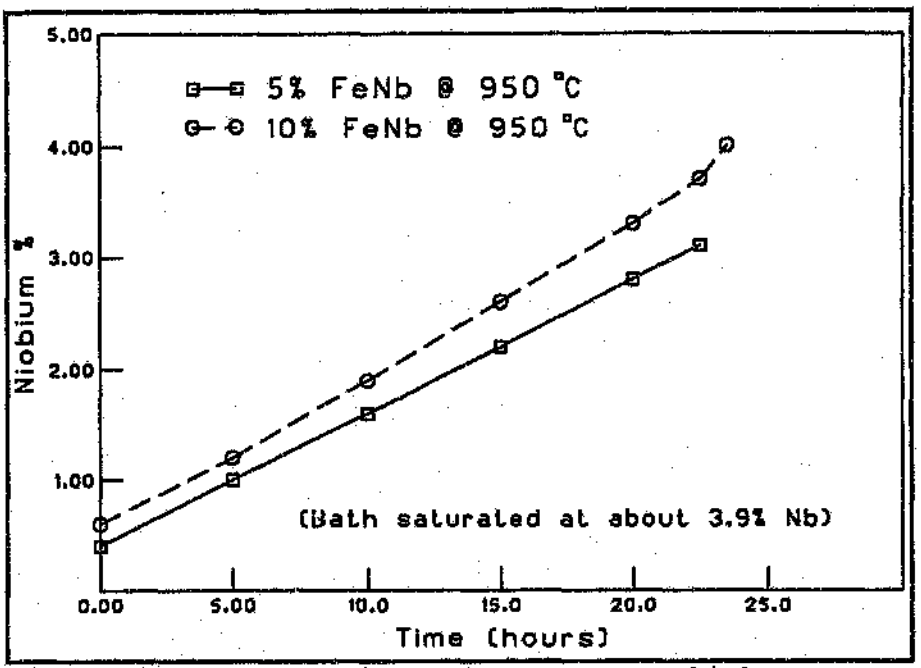


Figure.2.5.5. The time taken to establish saturation in borax/ferro-niobium baths[26].

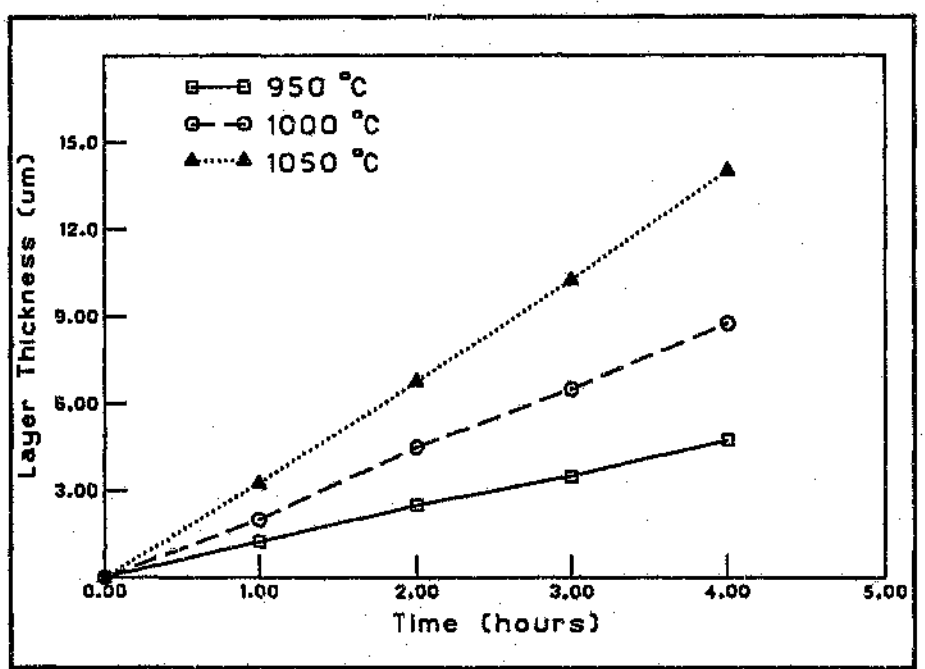


Figure.2.5.6. Effect of treating temperature and time on thickness of NbC layer[30].

layer formation is controlled by reaction rate in the bath, whereas the latter relationship implies a diffusion rate controlled process. Both Arai and Child et al.[26] conclude that an ideally conditioned bath will be diffusion rate controlled. If the bath is not ideally conditioned, meaning that if a sufficient amount of reactive oxide is not maintained in the bath so as to provide the bath/layer interface with a constant supply of the reactive species, it then becomes reaction rate controlled. The reason for this is that the bath would become depleted in reactive oxide, and the growth of the layer will be limited by the rate of reaction in the bath. The deterioration of baths with age, when no addition of ferro-alloy is made, is shown in **Table.2.5.2**, which indicates that an insufficient supply of reactive species to the bath would limit layer formation in the manner described above.

According to Child et al.[26], repeated agitation is essential if full advantage is to be taken of the ferro-alloy in the bath. They also suggest that make-up additions be made at regular intervals, with agitation to promote controlled oxidation, because layer formation is often reaction rate controlled as described above. They conclude that the layer depth produced is a function of the degree of oxidation of the bath.

The effect of carbon content on the rate of layer formation is well illustrated in **Figure.2.5.7**. As expected, the rate increased with increasing carbon content. Also the effect of the type of carbide on layer formation rate is shown by **Figure.2.5.8**. It appears from this that Cr has a slightly higher rate of formation than the other carbide types.

Table.2.5.2. Variation of layer thickness of VC on a 0.4% C steel in a 10% FeV containing bath for a 4 hour treatment, with the age of the bath[26].

Bath Age(Hours)	Layer Thickness(μm)
8	13.4
12	12.9
16	10.8
24	9.4
28	5.2
32	No layer

2.5.4. Properties of carbide layers and coated materials

Carbide layers formed by the TD process are claimed to be pore-free and dense. Furthermore, the high processing temperatures employed encourages mutual diffusion of atoms between the layer and steel substrate, providing such large bond strengths, that the layer does not exfoliate in severe service conditions, eg. cold forging. Layers formed consist of carbide only, free from any binder phase[25].
In addition, these layers scarcely decrease the toughness of the substrate material. Coated materials are characterised by an excellent combination of surface properties inherent in carbides and high strength and toughness inherent in the substrate material. However, the residual stresses between substrate and coating may be high because of the large differences in physical and thermal properties between carbide and substrate[32].

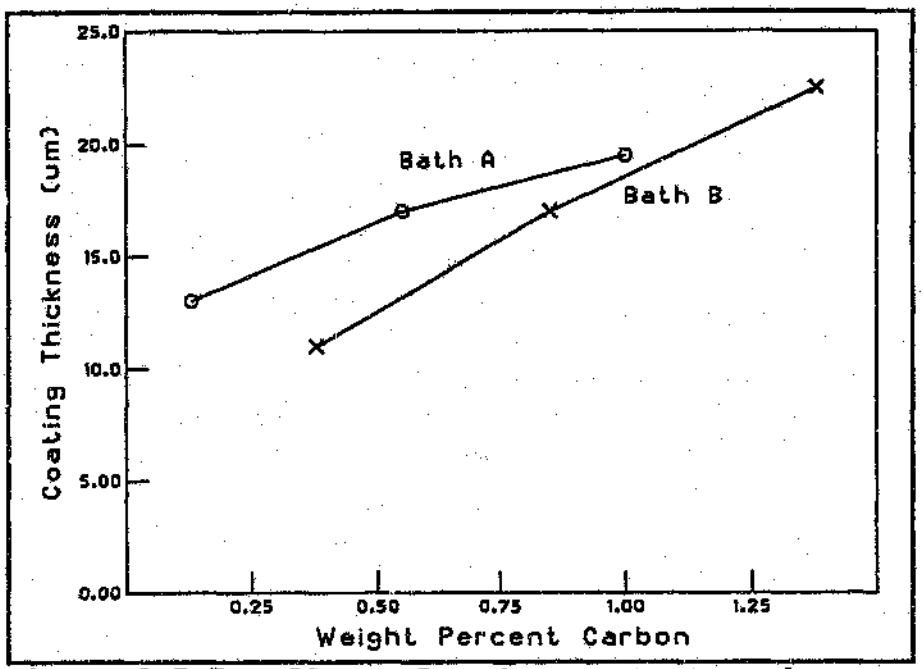


Figure.2.5.7. Effect of carbon content on layer formation rate(4 hours treatment at 1000°C) [26].

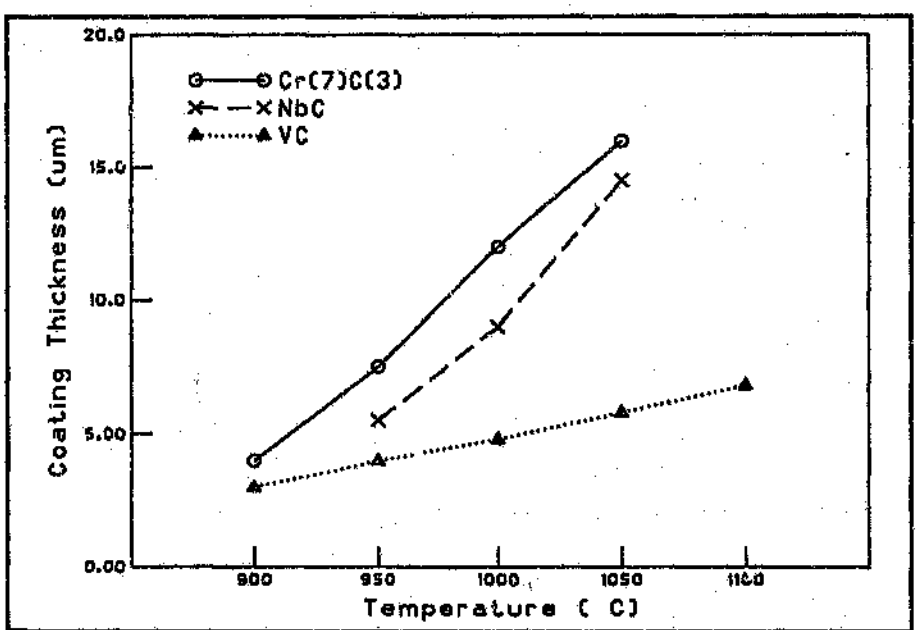


Figure.2.5.8. Effect of carbide type on layer formation rate(4 hours treatment at 1000°C) [26].

Due to the inherent brittleness of carbides, too thick coatings are likely to cause spalling and embrittlement problems. Also, increasing layer thickness did not affect toughness to a great extent, although it did decrease the critical-strain at which microcracks were induced in the coating[26].

Coatings can be applied practically to all carbon containing substrate materials namely,

(1) C-containing Co or Ni alloys ;
(2) Graphite ;
(3) Carbide coatings ;
(4) Cemented carbide ;
(5) Cast iron ;
(6) Steels, stainless steels, and tool steels.

In cemented carbides, coatings are formed mainly from carbon dissolved in the binder phase, while in steels the layers form mainly from carbon in the substrate. Also interesting is the fact that dissolved carbon reacts more efficiently than carbon which exists in the base metal as carbides or graphite[25]. With tool steels, the alloy content affects carbon activity at any carbon level with the result that the rate of layer formation is affected.

In a test carried out to determine the positional relationship between the layer formed and the steel surface[28], a platinum-marker was secured to the surface of a number of steel specimens. These specimens were then treated in baths containing ferro-V, ferro-Nb or metallic chromium powder. In the case of VC and NbC, layers formed on the steel surface, with no layers forming inside the steel. However, in the bath containing Cr powder, a Cr_7C_3-layer was formed on the initial boundary surface, and a solid solution of Fe-Cr formed above this. This indicated

that mutual diffusion of Cr and Fe occurred in the boundary between Cr_7C_3 and steel.

Child et al.[26] found that VC and NbC coats were monophase, with very little iron content. It was also shown that duplex layers formed in the case of chromium carbides, comprised an outer layer of $(Fe,Cr)_7C_3$ and an inner layer of $(Fe,Cr)_{23}C_6$, with iron content increasing as the layer/substrate interface is approached. Slight diffusion of chromium into the steel, as well as intrusions of Cr-carbide were also found. In the case of Cr-plated steel, carbide coatings are formed over a Cr-carbide layer produced from the plated layer. Composite carbide coatings can be obtained by dipping into baths containing more than one carbide forming element or in different baths.

Arai et al. performed extensive tests[25,29,30,32,33] to determine the properties of coated materials. These results are discussed below. In many instances, results obtained on TD treated specimens were compared to results obtained from specimens treated by other processes, eg. CVD.

2.5.4.1. Hardness

The hardness of these layers varies according to the type of element added to the bath. VC layers are claimed to have hardness values ranging between 3000-4000HV. Moreover, these layers maintain hardness even at fairly high temperatures. **Figure.2.5.9** shows how coating hardness varies with the type of carbide, and compares the hardness of these layers with those of other coating processes. Child et al.[26] evaluated the microhardness(HV0.02) of VC layers to lie between HV2100-2700. They determined the hardness of the other carbide types to be as follows :-

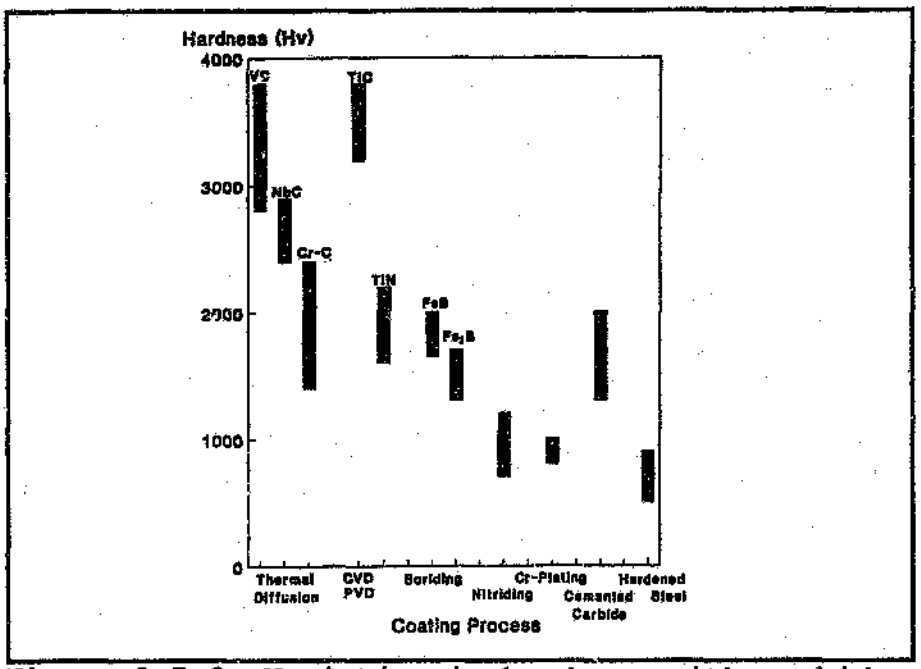


Figure.2.5.9. Variation in hardness with carbide species[32].

$Cr_{23}C_6$ = 1100-1300 HV0.02;
Cr_7C_3 = 1700-2300 HV0.02;
NbC = 1900-2500 HV0.02.

2.5.4.2. Oxidation resistance

Coated steel specimens were heated in ambient atmosphere for 40 hours and then cooled. In the range 400-500°C, no significant change in mass or appearance was noted on specimens. At 600°C, oxidation was observed on VC and NbC coated specimens. The Cr-carbide coated specimens were not noticeably oxidised even at 800°C.

2.5.4.3. Toughness

The effects of these coatings on toughness were determined using static bending and impact tests. Results from such tests are displayed in **Table.2.5.3.** Also listed in **Table.2.5.3,** are comparative results obtained on hardened

Table.2.5.3. Effect of carbide coating on toughness[30].

Test	Treatment Conditions	Substrate Hardness (HRc)	Impact Strength (J)	Rupture Load (kg)
IMPACT TEST	Hardened 1000°C,1/2h	49.7	16.4	-
	NbC Coated (6µm thick)	49.8	17.0	-
	VC Coated (6µm thick)	49.4	16.2	-
STATIC BENDING	Hardened 1000°C,1/2h	48.8	-	1030
	NbC Coated (6µm thick)	50.0	-	960

specimens. The heat treatment conditions which test specimens were subjected to, and, the substrate hardness are also indicated in the table. As can be seen from these results, coated specimens did not show a reduction in the rupture load or impact strength.

2.5.4.4. Corrosion resistance

Specimens treated by the TD process have shown excellent corrosion properties in various types of aqueous solutions (**Table.2.5.4**). It was observed, however, that the kind of substrate material had an effect on the corrosion resistance of coated specimens, especially in aqueous media. This is thought to be due to the penetration of acid through micro-pores in the coatings. It has been suggested

Table.2.5.4. Comparison of corrosion resistance of coated specimens in various aqueous media (Room temperature, 50 hours)[27].

SOLUTION	Uncoated	Coated		
	304	NbC	Cr-Carbide	VC
5% NaCl	O	O	O	O
5% NaOH	O	O	O	O
10% H_3PO_4	O	O	O	O
10% HNO_3	O	O	O	O
10% H_2SO_4	X	O	O	O
50% H_2SO_4	X	O	O	O
10% HCl	X	O	O	O
20% HCl	X	O	-	-
36% HCl	X	O	O	O

X = Severe corrosion;
O = No Corrosion;
(-) = Not tested.

that appropriate selection of substrate material or coating conditions are means of minimising pore formation, thereby increasing corrosion resistance.

2.5.4.5. Wear resistance

Tests done by Arai et al.[32] revealed that the wear resistance of coated specimens varied with variables such as carbide species or substrate hardness. A comparison of the wear resistance of VC coated specimens against the wear resistance of specimens treated by other methods, as obtained in a sliding test against textile fibre, is

provided in **Figure.2.5.10.** Tetron or cotton fiber was slid over specimens at a speed of 650m/min, with the tension in the fiber fixed at 50g. The depth of wear scars obtained for total sliding distance covered of up to 1000km was recorded. These wear tests show the superior performance of TD specimens.

The effect of substrate hardness on wear resistance of TD treated steel is evident from **Figure.2.5.11,** which shows that TD coated substrate steels with hardness as low as 39.0 HRC failed to show satisfactory wear resistance. As shown in **Figure.2.5.11,** the same substrate material treated by different methods, was subjected to a wear test in which coated specimens of this material are used to crush silica sand, with engine oil being used most probably as lubricant. The VC coated specimen with a substrate hardness of 39.0 HRC showed the poorest wear characteristics. Second to this was the hardened specimen. Those specimens with substrate hardness above 39.0 HRC displayed little weight loss. This effect of low substrate hardness is thought to be due to the inability of the substrate to support the hard surface layer.

The type of carbide also has significant influence on the wear resistance of coated specimens. The influence of carbide species on wear resistance is illustrated in **Figure.2.5.12.** Specimens of D2 steel were treated by a number of processes as indicated and used in compression tests on 1010 steel strip. A compression ration of 0.5(1.8mm to 0.9mm reduction) was used at a rate of 161 shots/minute. No lubricant was used and the wear depth of test specimens was evaluated after a set number of shots had been completed. As indicated by **Figure.2.5.12,** VC coated specimens showed the lowest wear depth for a particular number of shots.

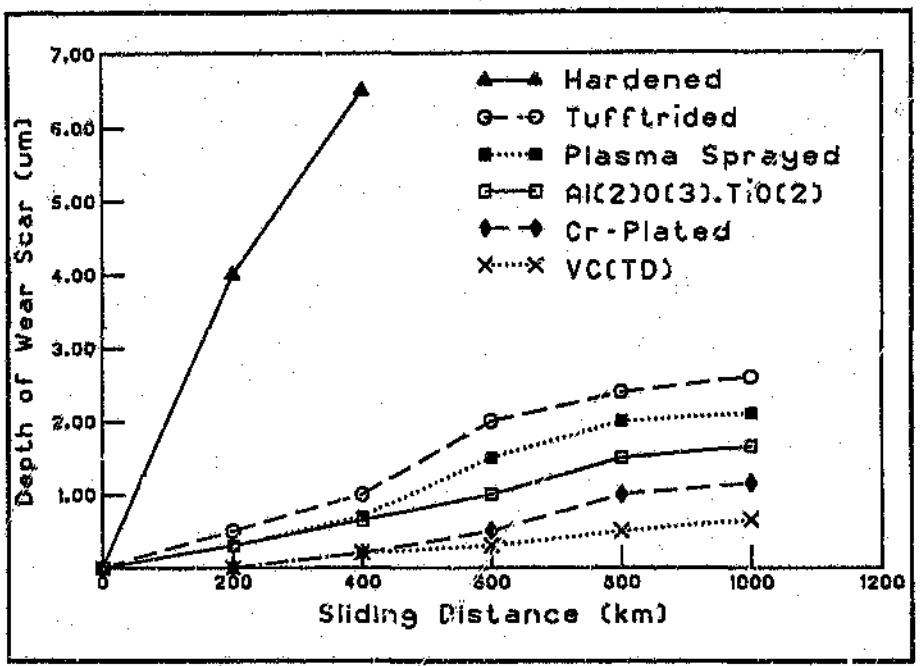


Figure.2.5.10. Comparison of wear resistance of VC coatings in sliding wear test against textile fiber[27].

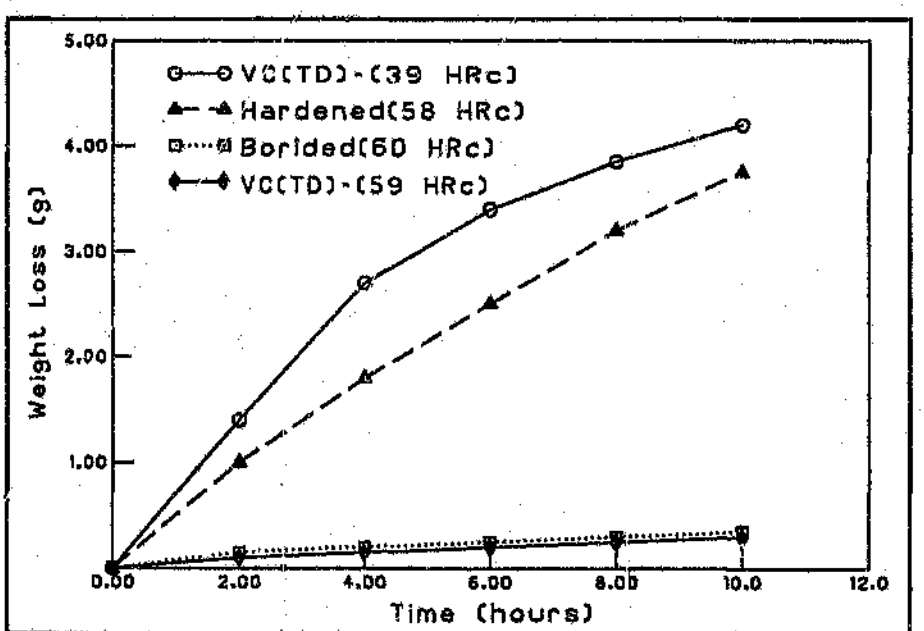


Figure.2.5.11. The effect of substrate hardness on wear loss in sand crushing tests[32].

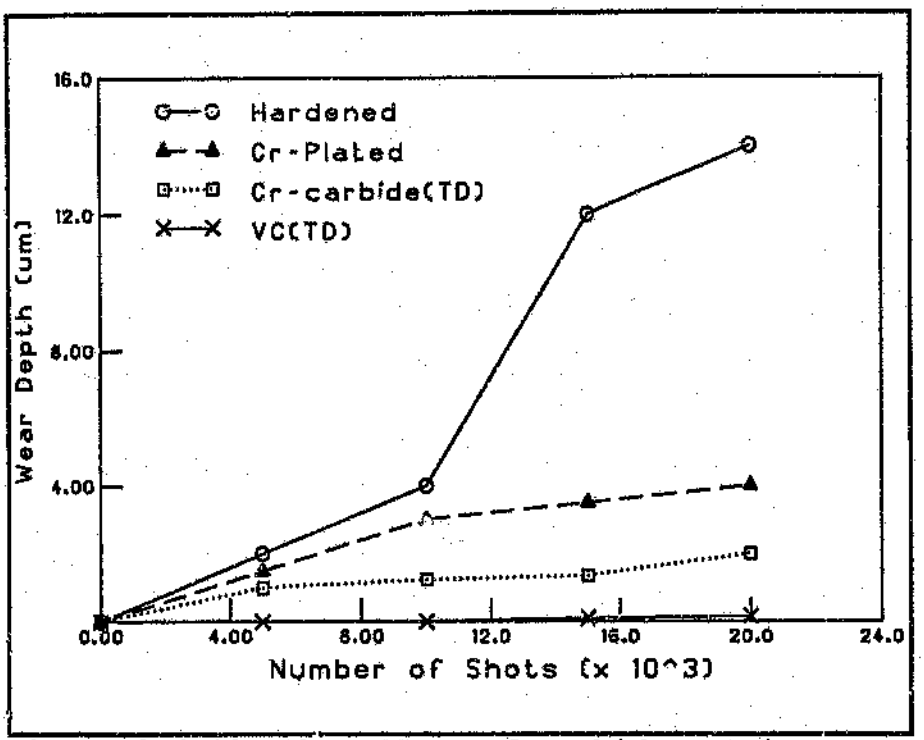


Figure.2.5.12. The effect of carbide species on wear depth in compression tests[32].

2.5.5. Applications of the TD process

The applications of this process are numerous and those described here serve merely to give an idea of the range of applications, and, the improvements in component performance which can be achieved through it. A list of applications of the TD process with regard to tools and dies, and the corresponding cost saving and component life increases which can be obtained, is provided in **Table.2.5.5.** Component life was increased in almost all the applications listed here, implying that significant savings can be made using the TD process. The corresponding "life increase to cost increase" ratio should also be noted.

Table.2.5.5. Typical life improvements achieved by TD processing of tools and dies[31].

COMPONENT	Life increase Factor	Life increase / Cost increase
Piercing Punch	5 - 10	2 - 8
Cold Forging Punch	5 - 10	2.6 - 5.2
Aluminium Die-Casting Dies	2 - 10	-
Hot Forging Die	2 - 5	-
Extrusion Die	2 - 15	-
Plastic Moulding Die	5 - 10	-

From the information presented here it appears that the potential of coatings produced by the TD process for various applications - especially those requiring wear resistance - is good.

3. EXPERIMENTAL PROCEDURES

3.1. Preparation of Experimental Materials

Initial experimental work aimed at producing VC coatings owing to the greater potential of this coating. It was necessary at this stage to perform a series of exploratory tests. Before such tests could be executed, however, a number of procedures had to be established. These procedures are outlined below.

The carbide-forming compounds, ie. ferro-vanadium(FeV) and vanadium pentoxide(V_2O_5), were reduced to -500µm to render them more reactive in the bath. The FeV was received in the form of chunks, and the V_2O_5 in the form of flakes. Both vanadium-containing additives were reduced to powder by crushing and pulverizing. The FeV was much harder than the V_2O_5 and therefore more difficult to crush and pulverise. Chemical analyses of the FeV and V_2O_5 powders are provided in **Table.3.1** and **Table.3.2** respectively. The vanadium-content of the FeV was high (80.5%) with a low level of Si and Al impurities. The V_2O_5 content of the pentoxide was high(99.7%) with a low level of impurities. No moisture was detected in the pentoxide. To obtain comparable results, both V-containing compounds were utilised in the -500 µm size range only. According to Child et al.[26], particle size influences the rate of dissolution of the carbide-forming compound in the bath. As far as the borax is concerned, the anhydrous form of this salt was selected to ensure that the moisture content of the salt was low.

Aluminium used in the tests was in the form of pieces of strip which were cut from pure Al(99,9% Al) sheet. Steel specimens used in these tests were cut from rod(diameter

Table.3.1. Chemical Analysis of Ferro-Vanadium.

ELEMENT	PERCENTAGE
V	80.5
Fe	13.8
Si	1.0
Al	1.6
C*	0.12
TOTAL	97.02

* = As determined from carbon analysis;

Table.3.2. Chemical Analysis of Vanadium Pentoxide.

COMPONENT	PERCENTAGE
V_2O_5	99.70
Fe	0.04
Na_2O	0.18
SiO_2	0.01
S	0.003
P	0.003
Moisture	-
C*	0.015
TOTAL	99.941

* = As determined from carbon analysis;

= 16mm). Mild steel(0.2% C) and EN9 steel(0.5% C) were treated. Pieces of average length 15mm were cut from these rods, and holes(diameter = 3.5mm) drilled through the centre of each piece for the purpose of suspending the specimens in the bath. The two end surfaces of these cylindrical specimens were surface ground and this surface finish was given to most samples prior to coating. Scale on the cylindrical surface of the specimens was removed by turning.

A heat resistant pot of 310 stainless steel was used to contain the molten salt. The high corrosion and oxidation resistance of this material made it suitable for the purpose at hand. The dimensions of this pot were as follows,

Internal diameter = 100 mm;
Wall thickness = 10 mm;
Depth of pot = 200 mm.

These dimensions allowed for a maximum bath size of 1.5 kg of borax in granular form. Upon melting, the salt contracted by about 30% by volume. Induction heating and resistance heating were available for heating and melting the salt. Induction heating was used initially and a few tests were carried out using this mode of heating. However, resistance heating was finally resorted to due to practical problems with the induction furnace.

3.1.1. Measurement of Coating Thickness

Coating thicknesses were measured by use of the optical system of a microhardness testing machine. Using this facility, 10 or 15 readings were taken and an average thickness established. The thickness values quoted in this work are the average values.

3.2. Exploratory Tests

As mentioned earlier, a number of exploratory tests were performed to gain some insight into the conditions under which coatings could be produced. The conditions of these exploratory tests in terms of temperature , time, and, bath composition, etc., are listed in **Table.3.3**. As can be seen, the treatment temperatures chosen were intermediate to those listed in the literature(850-1150°C). Substrate materials were mild steel and EN9 steel. Mild steel was used in most of the tests. Treatment times were selected so as to obtain data on the growth of the VC layer with time. It must be stated that the use of the term "bath activity" refers to the thickness of coating produced on a given substrate material in a given time period and at a specific temperature. Thus, a bath producing a thicker VC coating was regarded as having a higher "activity".

Overall, the purpose of these tests was to :-

1) Determine if VC coatings could be produced on steel specimens treated under conditions similar to those specified in the literature ;

2) Gain some insight into the factors affecting bath activity and coating conditions ;

3) Use **coated** specimens obtained from these tests to characterise the nature of the coatings in terms of microstructure, hardness, and, composition;

4) Perform a detailed study of the process based on the results of these exploratory tests.

Table.3.3. Conditions used for Exploratory Tests.

TEST No.	BATH COMPOSITION (% of borax mass)	BORAX MASS (kg)	TEMP. (°C)	%C IN BASE MATERIAL	TIME (h)	MODE of HEATING (I/R)#
1.	20% FeV	1.0	950	0.5	7	R
2.	10% FeV	1.0	950	0.5	3 6 9 12	I
3.	20% V_2O_5	1.5	1000	0.2	12 24	R
4.	20% V_2O_5 + 5% Al	1.5	1000	0.2	*5 10 15 20	R
5.	10% V_2O_5 + 5% Al	1.5	1000	0.2	*6 18 34 54	R
6.	10% FeV + 5% Al	1.5	1000	0.2	*6 18 34	R

: I=Induction heating; R=Resistance heating;

* : Time indicates bath life;

Test numbers 1, 2, and 3, aimed at determining if VC layers could be produced on specimens which were simply immersed in baths with compositions as listed in **Table.3.3**. For this reason, these baths contained only borax mixed with carbide -forming compounds, ie. FeV and V_2O_5. According to Child et al.[26], VC layers cannot be produced in baths containing only V_2O_5 as the bath additive. In tests 3, 4, and 5 aluminium was added to the bath. The importance of Al was realized from the results of previous experiments and this will be discussed in greater detail in Sections 4 and 5. Treatment times marked with an asterisk(*) indicate the life or age of the bath. The period between two successive times indicates for how long the specimen was immersed in the bath. For example, in test No.4, four specimens were treated for 5 hours each. The times indicated in **Table.3.3** however, are the accumulated times. Thus, the age of the bath, after the fourth specimen in test No.4 was removed, was 20 hours. Similarly in test No.5, specimens were treated for 6, 12, 16, and 20 hours with the age of the bath being 54 hours at the end of the test.

Test No.4 is a continuation of test No.3, where the effect of 5% Al addition on the activity of a bath containing only 20% V_2O_5 was studied. Test numbers 5 and 6 compare the activities of baths containing 10% V_2O_5(plus 5% Al) and 10% FeV(plus 5% Al) respectively. Of interest here was the change in activity of the two baths over a time period(34 hours), and, the rate of layer growth obtained using either carbide-forming compound.

A significant amount of information was obtained from the results of these exploratory tests. These results are provided in Section.4 and discussed in Section.5.

3.3. Analysis of VC Coated Specimens

Specimens treated in the exploratory tests were used to characterise the VC layers in terms of microstructure, hardness, and composition.

3.3.1. Microscopy of VC Coated Specimens

The appearance of the carbide layer was investigated in cross-section as well as directly on coated samples. To obtain a cross-sectional view of the VC layer, the coated cylindrical steel specimens were sectioned longitudinally. These longitudinal sections were mounted in lucite or bakelite. The harder bakelite was found to be more effective in preserving the edges of specimens and hence the coating during grinding and polishing. Mounted samples were given a final polish using 1μm diamond paste and etched in 2% Nital. Specimens were examined by optical and electron microscopy in both the polished and etched conditions.

3.3.2. Determination of Coating Hardness

As stated in Section.2.3.2, evaluating the hardness of thin coatings is not simple, since hardness is influenced by both the substrate and the loads used. A number of methods are available for establishing the hardness of thin VC coating. One method is to perform hardness tests on the coated surface and apply the equations derived for thin coatings as discussed in Section.2.3. It appears from the literature[12,13,14], however, that this method still yields hardness values which are considerably lower than those reported for the bulk material.

An alternative method is to perform hardness tests on the carbide layer of coated specimens. For this purpose, samples with relatively thick VC layers have to be used. Indentations were made midway across the thickness of the layer(**Figure.3.1**). In this way, errors due to the limited thickness of the coating and possible edge effects were minimised. Most of the hardness tests were performed using this method. Hardness tests were also performed on the surface of VC coated specimens to establish the coating hardness. The load used in this method was low to avoid penetration of the substrate by the indenter. However, the hardness values obtained may be influenced by the properties of the substrate even when the indentation does not penetrate the coating. This is due to the proximity of the indentation to the substrate and possible plastic deformation of the substrate. On average, the thickness of the coatings varied between 3 and 15μm depending on the carbon content of the substrate. Nonetheless, some tests were carried out using this third method in order to investigate the hardness values obtained by this method.

3.3.3. Determination of Coating Composition

Two techniques were available for the purpose of establishing the chemical composition of the VC coatings, namely Energy Dispersive Spectroscopy(EDS), and X-Ray Diffraction(XRD) analyses.

3.3.3.1. EDS of Coated Specimens

The composition of the coatings was assessed by both qualitative and quantitative EDS analyses. Qualitative EDS analyses provided information regarding the major and minor elements in the coatings and approximate proportions of

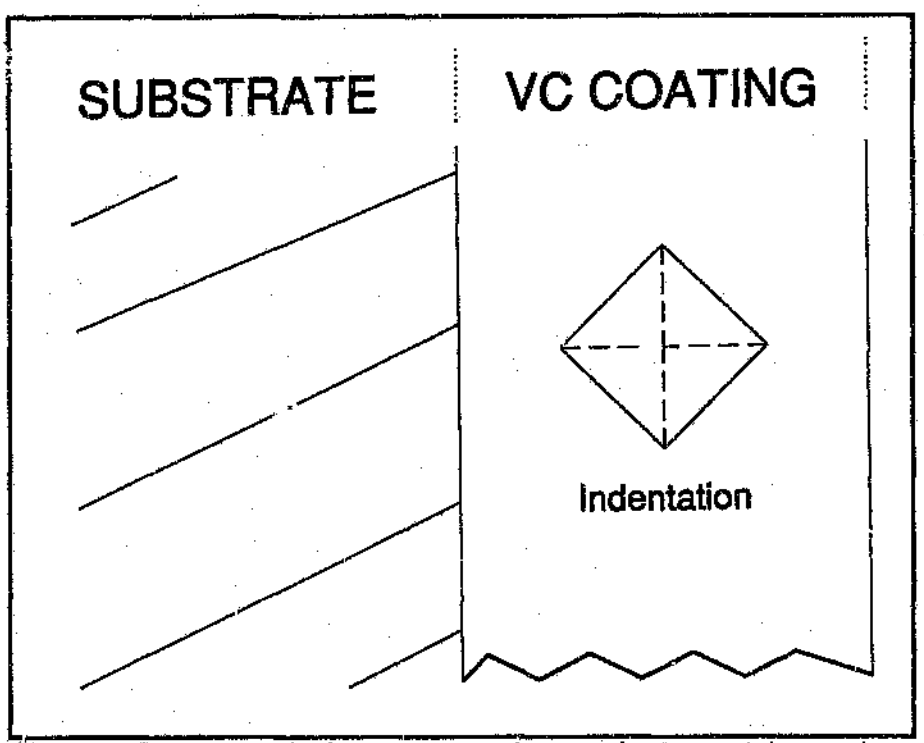


Figure.3.1. Position of hardness indentations in coated specimens.

these elements. Spot analyses provided information regarding the composition of the coating at specific points on the carbide layer and were carried out at different points across the thickness of the coating. This was done in order to establish possible variations in composition from the substrate to the surface of the coating. This technique could also provide information on the nature and extent to which substrate elements had diffused into the layer.

Quantitative EDS analyses supplied information concerning the concentration of elements in the carbide layer. Area analyses and line scans were performed in addition to spot analyses. An area analysis allows one to evaluate a relatively large area of the VC layer. A spot analysis usually provides information on the composition of a very small volume of material, typically 1μm^3. The volume of

material affected depends on instrument settings and the density of the material involved. A line scan provides an analysis in a straight line along the length of the coating. The composition obtained from a line analysis is an average one. Thus, a larger portion of the coating is analysed than in the case of spot analyses, producing a more representative analysis of the coating. The results obtained by use of these techniques are presented in Section.4.2.3.1.

3.3.3.2. XRD of Coated Specimens

Samples treated in V_2O_5- and Al-containing baths were selected for XRD. A number of XRD scans were performed on these samples using various diffractometer speeds to optimise the quality of the diffractograms obtained.

3.4. A Detailed Study of Baths containing V_2O_5 and Al

It was stated previously that a detailed study of the thermal diffusion process would be made on the basis of the results obtained from exploratory tests, as well as, the results obtained from analyses of coated specimens. The decision was therefore made to investigate baths containing only V_2O_5 and Al as additives. Apart from the fact that FeV has a fairly high iron content (80.5% V; 13.8% Fe; 0.12% C) and a higher density, which causes it to settle to the bottom of the bath faster than V_2O_5 (99.7% V_2O_5; 0.04% Fe; 0.015% C), little information regarding V_2O_5-containing baths is to be found in the literature. It is important to note at this stage that the V_2O_5 used in these tests contained 99.7% V_2O_5, which constitutes 56,03% V by mass.

A number of process variables were recognized as those which could influence both bath activity and coating conditions. These variables required investigation under a variety of conditions in order to ascertain their influence on the process. To do this, certain parameters were kept constant throughout experimentation, so that their influence could be eliminated. In so doing, a better understanding of the effect of these parameters was acquired. The process parameters which were studied are listed in **Table.3.4.**

Table.3.4. Process Parameters Studied.

	PROCESS VARIABLE	VALUE
1)	Bath Size	1.5 kg
2)	Bath Composition	10% V_2O_5 and 5% Al
3)	Treatment Temperature	950 °C
4)	Substrate Carbon Content	0.5% C
5)	Treatment Times	3, 6, 9, or 12h
6)	Particle Size of V_2O_5	-500 µm
7)	Surface Finish of Samples	Machine Ground
8)	Specimen Height above bottom of pot	20 to 30 mm

It must be stated however, that in certain tests, some of the parameters listed above were altered. For example, in the test examining the effect of temperature on bath activity, a range of temperatures were used rather than 950°C. A description of the experimental procedure used to study the effect of each parameter is given below. The objective behind each step is also outlined.

3.4.1. Effect of Temperature on Coating Thickness

To study the effect of temperature on the thickness of coating produced in a given time period, temperatures of 950, 1000, and 1050°C were employed. A standard bath composition (10% V_2O_5 and 5% Al) was used and samples were treated for 3, 6, and 9 hours.

3.4.2. Influence of Substrate Carbon Content on Coating Thickness

Using a constant bath composition as well as treatment times, steel samples with carbon contents of 0.2% and 0.5% C were treated at 950°C. In this way, the influence of substrate carbon content on the coating thickness could be determined.

3.4.3. Effect of V_2O_5 Content on Bath Activity

Three different bath compositions were prepared by varying the concentration of V_2O_5 in the bath. The concentration of V_2O_5 was 5%, 10%, or 20%, while the amount of aluminium was kept constant at 5%. The temperatures and treatment times were kept constant in all three cases. The objective here was to determine how bath activity changed as the V_2O_5 concentration changed, and, as the concentration of V_2O_5 added approached that of the Al, ie. 5%.

3.4.4. Effect of Aluminium Content on Bath Activity

In these tests, the V_2O_5 content of the bath was kept

constant at 10% and the aluminium content was 5%, 10%, or 20%. The three baths were operated at 950°C for 3, 6, or 9h. The aim was to determine the effect of aluminium content on bath activity.

3.4.5. Effect of Bath Composition on Coating Thickness Produced

The effect of bath composition on coating thickness was investigated using two different baths. One contained 20% V_2O_5 and 10% Al and the other 2% V_2O_5 and 1% Al. Samples were treated for 3, 6, or 9h at 950°C to ascertain the bath activity under these conditions. Changes in bath activity would be reflected in the coating thickness produced.

3.4.6 Influence of Particle Size of V_2O_5 on Bath Activity

The particle size of the reactants in the bath was expected to influence the activity of the bath, since the particle size seemed likely to have some effect on the kinetics of the process. This is fairly probable when one considers the greater surface area of finer particles and also, the fact that there is a tendency for larger particles to settle to the bottom of the bath faster. Three particle size ranges of V_2O_5 were prepared by crushing and pulverising the as-received V_2O_5 flakes. Four particle size ranges were then tested under the conditions outlined in **Table.3.4.** These ranges were as follows :

Range 1 - particle size < 0.5 mm
Range 2 - particle size between 0.5 mm and 4.75 mm;
Range 3 - particle size between 4.75 mm and 9.5 mm;
Range 4 - particle size > 9.5 mm(As-received V_2O_5 flakes).

3.4.7. Change in Bath Activity with Time

The variation of the activity of the bath over a fairly long period of time was investigated by holding baths at temperature for 25h and 50h and treating specimens for periods of 5 hours. For both baths, the first sample was introduced as soon as the melt reached temperature. At the end of the first 5 hour period, the first sample was removed from the melt and the second one introduced immediately thereafter. In this manner, batches of 5 and 10 specimens were treated - one at a time - over the 25 and 50 hour periods respectively. Apart from the treatment time used here, all other test conditions were as in **Table.3.4.**

It was expected that the coating thickness produced on these samples would provide an indication of the changes in bath activity with time. Such information would be important in establishing the time available before reconditioning of the bath became necessary. It was envisaged that reconditioning would be accomplished by one of two methods. Firstly, by making small additions of bath constituents to the deteriorating bath. Secondly, by mechanical stirring of the deteriorating bath. This will be discussed in greater detail in Section.5.

3.4.8 Effect of Bath Depth and Bath Age on Coating Thickness Produced

Among the variables recognised as those which may influence the activity of the bath, and therefore the coating thickness produced within a given time period, were the age of the bath and the depth at which samples are immersed during treatment. In this regard, it was envisaged that the height of a sample above the bottom of the bath might have

considerable influence on the thickness of coating produced given the fact that, the reactants tend to settle to the bottom - especially those of high density - and, that oxidation occurs at the surface of the melt. It would seem from these factors that the thickness of the coating produced on a sample could vary with the position of the sample in the bath.

In conjunction with the effect of bath depth, the age of the bath was also regarded as a variable which could alter the activity of the bath and thus the coating thickness produced in a given time period. Arai[25] mentions the deterioration of FeV-containing baths. Child et al.[26] mention the saturation of ferro-niobium containing baths, stating that a 5% Fe-Nb with a 68% Nb content is insufficient to saturate the bath in 24h. A 10% Fe-Nb bath of similar Nb content does, by contrast, saturate the bath in the same time period and at the same temperature. However, neither worker makes mention of the use of aluminium in these baths. In light of the above, it was presumed that a bath held at temperature for a specific time period, prior to the immersion of any samples, would be more active than one held at the same temperature for a shorter time period.

In order to study the effect of bath age and sample depth below the surface, eight samples 140mm long and 15mm in diameter were fabricated from EN9 steel rod. Two tests were carried out in which four samples were immersed vertically in the bath for 3, 6, 9, and 12 hours in each test. A 316 stainless steel plate (%C < 0,02) was made for holding these rods upright in the bath as shown in **Figure.3.2**. The plate was 98mm in diameter with four 16mm holes drilled at intervals of 90°. The holes were drilled at a distance of 14mm away from the edge of the plate.

A bath containing 10% V_2O_5 and 5% Al was used in both cases at 950°C. The only difference between the two tests was that the baths were aged for 8h and 16h respectively, prior to the immersion of any of the sample rods. After immersion, the samples were removed from the bath one at a time at 3h intervals. In this way, treatment times of 3, 6, 9, and 12 hours were established.

From the procedure outlined above, it can be seen that the purpose of this test was two-fold. Firstly, to examine the effect, if any, of bath depth on the thickness of coating produced along the length of these rods. Secondly, different time periods were used to determine if the age of the bath had a significant effect on its activity. Thus, any settling effects or saturation effects in the case of the two baths might be established from the coating thickness produced along the length of the sample rods.

After removal of these rods from the bath, and cleaning, they were examined macroscopically for any salient features. Each rod was then sectioned in the manner illustrated in **Figure.3.3.** The sections were mounted and prepared metallographically in order to evaluate the average coating thickness on each section. In so doing, the variation in coating thickness with bath depth could be evaluated.

3.4.9. Influence of Surface Finish on Coating Thickness Produced

A bath containing 10% V_2O_5 and 5% Al was used at 950°C to treat EN9 samples with three different surface finishes. The samples were treated for 8 hours and air-cooled after treatment. The surface finishes used were as follows.

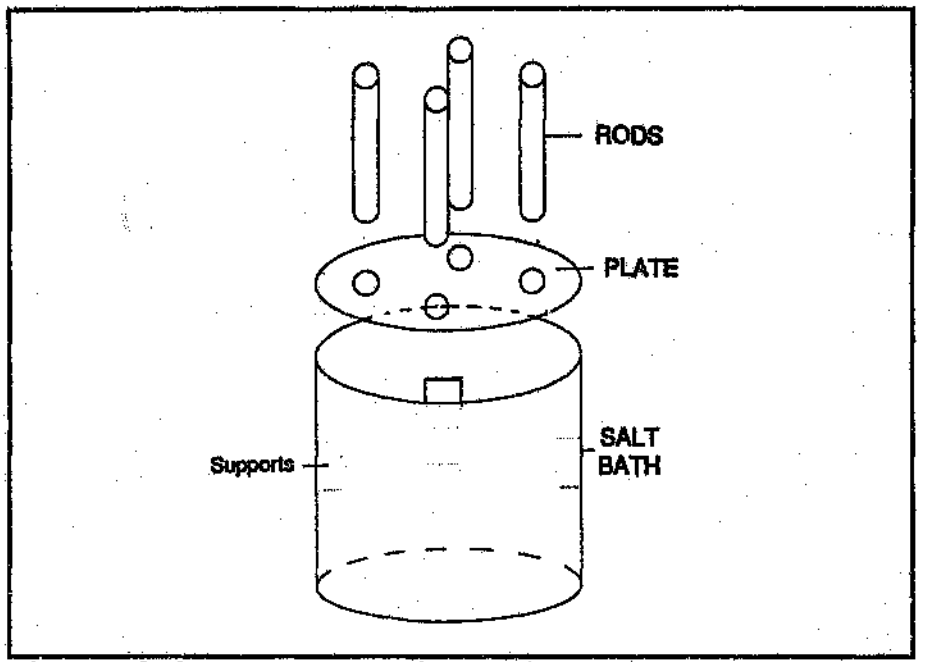


Figure.3.2. Method of immersion of sample rods.

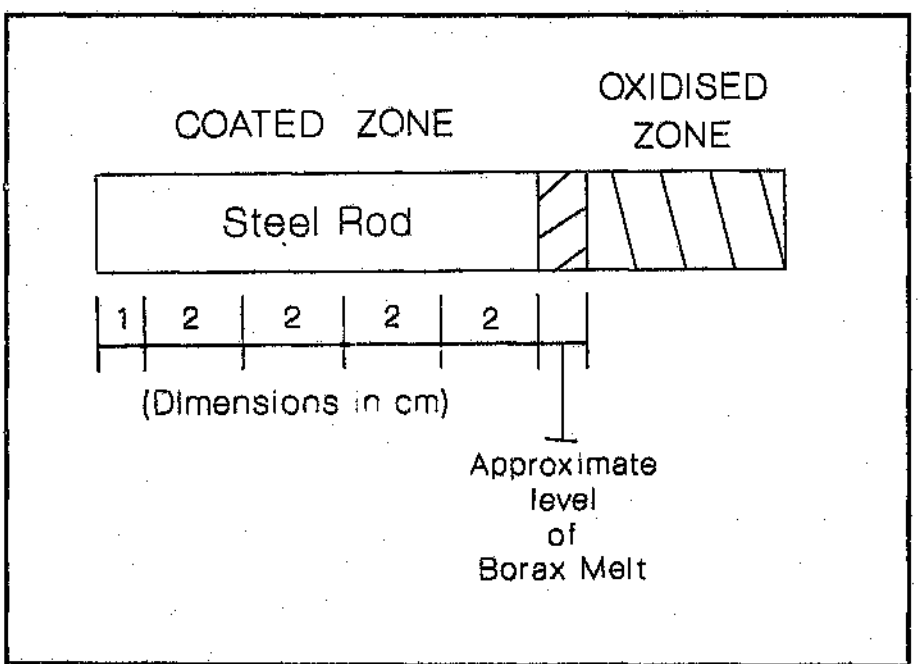


Figure.3.3. Method of sectioning of coated EN9 steel rods.

1) Diamond polished(1μm);
2) Machine ground - Standard surface finish;
3) Sand blasted(grit size = -0.5mm).

These samples were examined microscopically to assess the effect of these surface finishes on the microstructure of the coated steel substrate.

The nine variables discussed in sections 3.4.1 to 3.4.9 are considered to be the main variables which influence the outcome of a particular treatment. The results obtained from the tests outlined above are presented in Section.4.2.

3.4.10. Analysis of Baths containing 10% V_2O_5 and 5% Aluminium

Samples were taken from melts containing 10% V_2O_5 and 5% Al and analysed by XRD. These samples had to be crushed and pulverised into powder to render them more suitable for XRD analyses. A number of XRD scans were performed on the samples. The objective of this procedure was to obtain information regarding the species present in the bath which would be useful in understanding the process mechanisms.

3.5. Corrosion Testing of VC Coated Samples

A number of samples 15mm in diameter and 7mm thick were prepared specifically for the purpose of evaluating the corrosion properties of the VC coatings. A list of the substrate materials used and the treatment conditions these samples were subjected to is provided by **Table.3.5.** Dummy samples were treated with each batch of samples for the purpose of obtaining an idea of the average coating thickness obtained on the actual corrosion samples. These

Table.3.5. Treatment Conditions of Corrosion Samples.

SUBSTRATE MATERIAL	TREATMENT* TEMPERATURE (°C)	TREATMENT TIME (hours)
Mild Steel (0.2%C)	950°C	4h 6h
EN9 (0.5%C)	950°C	4h 6h

*Samples treated in a 10% V_2O_5 and 5% Al Bath.

cylindrical samples were surface ground on the ends prior to coating. Six samples of each material in the coated and uncoated condition were prepared in order to compare the corrosion behaviour of coated and uncoated substrate. The object of treating 0.2% C and 0.5% C steels for 4h and 6h was to obtain VC layers of increasing thickness. It was thought that this might affect the corrosion behaviour of coated samples.

After cleaning, one end of each of the coated cylindrical samples was ground to remove the coating from this surface. This enabled electrical wire to be soldered to the exposed metallic surface. With the uncoated samples, this procedure was not necessary. All samples were checked for electrical conduction after soldering. The coated and uncoated samples were then mounted in araldite epoxy resin as illustrated by **Figure.3.4.** To avoid spreading of the resin over the surface of coated specimens, the samples were mounted face down onto plate glass on which a layer of vacuum grease had been smeared. This prevented excessive resin blemishes on the surface of coated samples. It should be noted that it was necessary to keep the coated surfaces free of any such

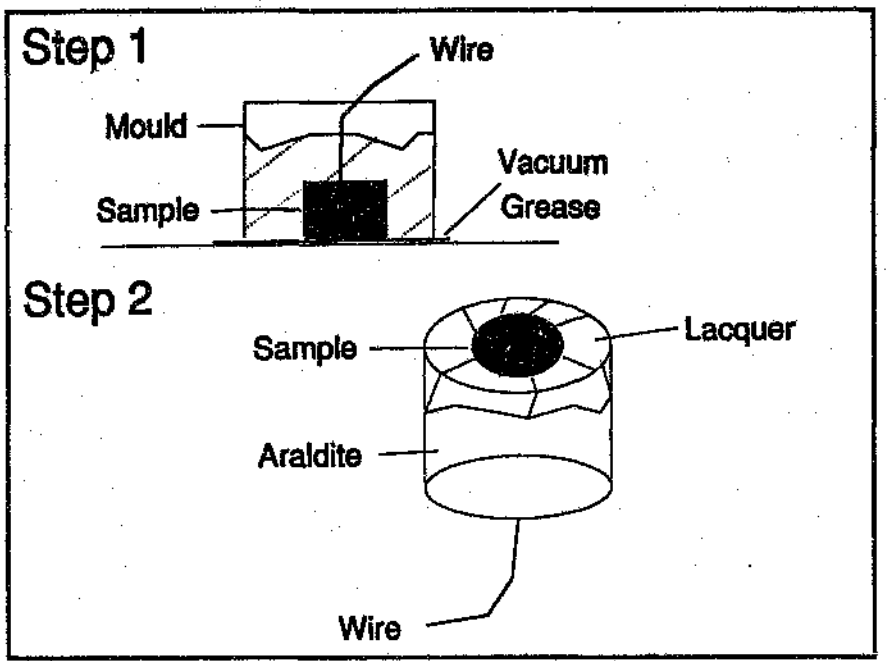


Figure.3.4. Method of mounting of corrosion samples.

deposits as the surface could not be ground afterwards.Once mounted as shown in **Figure 3.4**, a measured area(0.5 to 1.0 cm^2) of the surface of coated and uncoated specimens was exposed by marking off such an area with Stop Off No.45 lacquer. A shortcoming of this method, however, is that the interface between the lacquer and the exposed surface tends to act as a crevice.

Such crevicing does have considerable effect on the results one obtains from corrosion testing[76,77]. However, due to the nature of the VC coated specimens, the method of sample preparation outlined in ASTM standards G5-78 and G61-78, which were the standards referred to in this study, could not be adhered to. Furthermore, these standards are relevant to cast or wrought materials and not thin coatings. Therefore, it was decided to adopt the above approach simply to rank the corrosion properties of coated and uncoated substrate and for evaluating the corrosion behaviour of the VC layers.

With regard to the corrosion tests, both potentiodynamic and cyclic polarization measurements were made on coated and uncoated specimens. These measurements provided an indication of the susceptibility of a material to uniform corrosion and localised corrosion respectively. ASTM standard G5-78 was referred to as far as potentiodynamic testing was concerned. For the cyclic polarization tests - also referred to as pitting tests - the standard practice ASTM G61-78 was consulted. In both cases, the standards were adhered to as far as was possible. As mentioned above, these standards do not apply directly to thin surface coatings. However, they do allow one to achieve reproducible results. Alterations made to the standard practice were as follows,

i) Lacquering of the surface of samples to expose a measured area of the sample;

ii) The use of UHP (Ultra High Purity) nitrogen gas for purging the corrosive medium instead of an inert gas;

iii) The use of graphite auxiliary electrodes instead of the recommended platinum electrodes.

For potentiodynamic testing, a 1N H_2SO_4 solution was used at 30°C as the corrosive medium, while in the case of pitting tests a 0.6M NaCl solution was used at 25°C. These solutions were purged with N_2 gas for an hour prior to testing in order to remove oxygen. All samples were polarised at -900mV for 5 seconds prior to the start of a scan. Such "conditioning" of samples was done to ensure the removal of any oxide or passive layers which may be present on the active surface prior to testing. Three coated and three uncoated samples of either material were tested by each of the two techniques described above. The results are reported in Section.4.4.

3.5.1. Microscopy of Corrosion Samples

Corrosion samples were examined and electron microscopy after testing to determine how the VC coated samples had responded to the corrosive media. The appearance of the corroded surface of coated specimens after potentiodynamic and cyclic polarization tests was assessed. Of interest also were differences in the appearance of coated and uncoated substrate after tests.

3.6. Treatment of Tool Steels

Possibly one of the most important areas of application of VC coatings produced by the thermal diffusion process is on tool steels. It is primarily for this reason that the decision was taken to treat a variety of tool steel substrates. The thickness of VC coatings produced on such steels, many of which have carbon contents in excess of 0.5% C, was of interest. The influence of the carbide layer on the substrate material was also of interest.

The types of tool steels which were treated are listed below[1].

1) D2 and D3 - High carbon and high chromium containing steels which can be air or oil quenched;
2) H13 and H21 - Hot working steels where H1-H19 are Cr-based and H20-H39 are W-based steels which can be air quenched;
3) M2 - A Mo-based high speed steel which can be oil quenched.

These steels were in the annealed condition. As a first step, samples of the as-received material were cut from the bulk material and analyzed using spectrometric analyses. Samples were also prepared for microstructural examination. Qualitative EDS analyses were also performed on these samples and the hardness of the steels was determined using a 10kg load.

In the first treatment done on these tool steels, two samples of each of the as-received materials were prepared for coating by grinding the surface. Because the samples varied in shape and size, each sample was ground on the flat ends. For example, cylindrical samples were ground on the two ends.

The two samples of each material were treated in a 10% V_2O_5 plus 5% Al bath at 950°C for 3h and 6h respectively, the aim being to obtain coatings of different thicknesses and examine the growth of the VC coating with treatment time for the different steels. The samples treated for 3h were air cooled after removal from the bath, while the samples treated for 6h were oil quenched. As indicated earlier, some of these tool steels harden in air while others can be oil quenched. Hardness tests were performed on these samples using a 10kg load to determine to what extent the tool steels had hardened, since the treatment temperature of 950°C was below the austenitizing temperature of all these steels except for the D3 tool steel(925-1020°C). It should be noted that these hardness tests were done on the polished surface of the coated specimens where there was no VC coating and thus the values obtained represent that of the substrate material after treatment.

It was stated above that the as-received materials were in the annealed condition. As such, it was expected that most of the carbon in the steels would be in the form of carbides and that the matrix of the steels would be

ferritic. This was expected to retard the growth of the carbide coating because layer growth requires diffusion of carbon through the matrix towards the specimen surface. In addition, the diffusion of carbon out of the carbides in the steel would take some time, depending especially on the treatment temperature used, since the carbides in the matrix of the steel are stable to fairly high temperatures (1100-1300°C)[78]. At temperatures below the austenitizing temperatures of these steels this effect was expected to be more significant.

In order to assess the extent, if any, of this effect on the thickness of coating produced in a given time period and at a specific temperature, two samples of each of the tool steels were hardened and tempered. The hardening and tempering conditions used are shown in **Table.3.6.** By hardening the steels, the matrix would be transformed to martensite. As such, the carbon content of the matrix would be higher than that of the annealed material which was ferritic, since the solubility of carbon in ferrite is virtually zero. In this respect, the hardened samples may form thicker coatings than the annealed specimens under similar treatment conditions. From each pair of hardened and tempered samples, one sample was used for microscopic examination and hardness testing to compare its hardness and microstructure with that of the as-received material. The other sample was treated together with a sample of the as-received material in a 10% V_2O_5 and 5% Al bath at 950°C for 3 hours. For reasons which will be discussed in Section.4.6, the H13 sample was not treated. The samples were all oil quenched after removal from the bath.

After cleaning, the coating thickness on these specimens was evaluated to assess if hardening had played a significant role on the coating thicknesses produced. Hardness tests(HV10) were also done on these samples to

Table.3.6. Hardening and Tempering Conditions used for the Tool Steels.

MATERIAL	CONDITIONS OF PREHEAT		HARDENING TEMP. & TIME		QUENCHING CONDITIONS		
	Temp. (°C)	Time (min)	Temp. (°C)	Time (min)	Quench Medium	Temp (°C)	Time (min)
D2	540	30	1020	20	gas	540	60
D3	540	30	1020	20	gas	540	60
H13	540	30	1050	20	gas	540	60
H21	600	30	1050	20	gas	540	60
M2	600	30	1050	20	gas	540	60

determine the extent to which the substrate materials had hardened. Hardness tests were carried out on the coating in section to compare the hardness of the coating formed on tool steels with that formed on plain carbon steel EN9. As before, the thickest coatings were chosen in order to obtain indentations of measurable size.

3.6.1. Microscopy of VC Coated Tool Steels

VC coated tool steel samples were mounted in Epomat epoxy resin, which is much harder than lucite or bakelite, and prepared metallographically for microscopic examination. The microstructure of the coated substrates was examined to acquire some understanding of the effect of substrate microstructure on the formation of the VC layer.

4. RESULTS

4.1. Exploratory Tests

The results obtained from the exploratory tests are provided in **Table.4.1** which lists the coating thickness (μm) against the treatment time (hours) and the process conditions used for each test. From **Table.4.1** it can be seen that VC coatings can be produced in baths containing only FeV (Tests No.1 and No.2), whereas no coatings were formed in baths containing V_2O_5 only (Test No.3).

Graphs showing the variation in coating thickness with time were plotted using the results listed in **Table.4.1**. The graph in **Figure.4.1** is a plot of the results from Test No.2 showing the growth of the VC layer with time on 0.5% C steel samples treated at 950°C for 3, 6, 9, and 12 hours in a 10% FeV bath. It can be seen that a coating thickness of 10μm, which is regarded as being adequate for practical purposes[25], formed within the first six hours. The growth of the carbide layer with time, in this case, appears to follow a parabolic relationship.

Figure.4.2 compares the activities of the baths used in Tests No.5 and No.6. The two baths respectively contained 10% FeV and 10% V_2O_5 and were used to treat 0.2% C steel samples at 1000°C for 6h, 12h, and 16h successively. It should be noted that a 5% (by mass of borax) addition of aluminium was made to both baths. The activity of the two baths was found to be similar for treatment times of 5h. The activity of the FeV-containing bath appeared to become higher towards the middle of the treatment time. Towards the end of the test period, the activities of the two types of bath were practically identical.

Table.4.1. Results of Exploratory Tests.

TEST No.	BATH COMPOSITION (% of borax mass)	BORAX MASS (kg)	TEMP. (°C)	% CARBON (wt%)	t (h)	COATING THICKNESS (μm)
1.	20% FeV	1.0	950	0.5	7	10.0
2.	10% FeV	1.0	950	0.5	3	8.9
					6	11.8
					9	12.8
					12	13.5
3.	20% V_2O_5	1.5	1000	0.2	12	-
					24	-
4.	20% V_2O_5 + 5% Al	1.5	1000	0.2	*5	-
					10	2.4
					15	4.3
					20	4.6
5.	10% V_2O_5 + 5% Al	1.5	1000	0.2	*6	3.4
					18	6.2
					34	7.1
6.	10% FeV + 5% Al	1.5	1000	0.2	*6	3.2
					18	4.5
					34	7.3

* : Time indicates bath age for these tests.

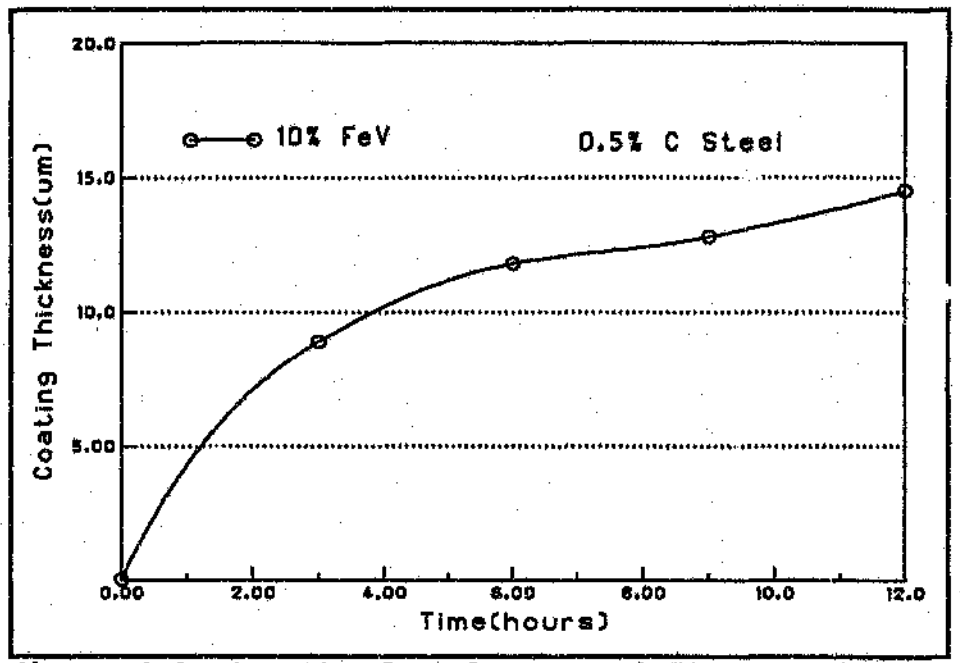


Figure.4.1. Growth of VC layer on 0.5% C steel treated in a 10% FeV bath for 3, 6, 9, and 12 hours at 950°C.

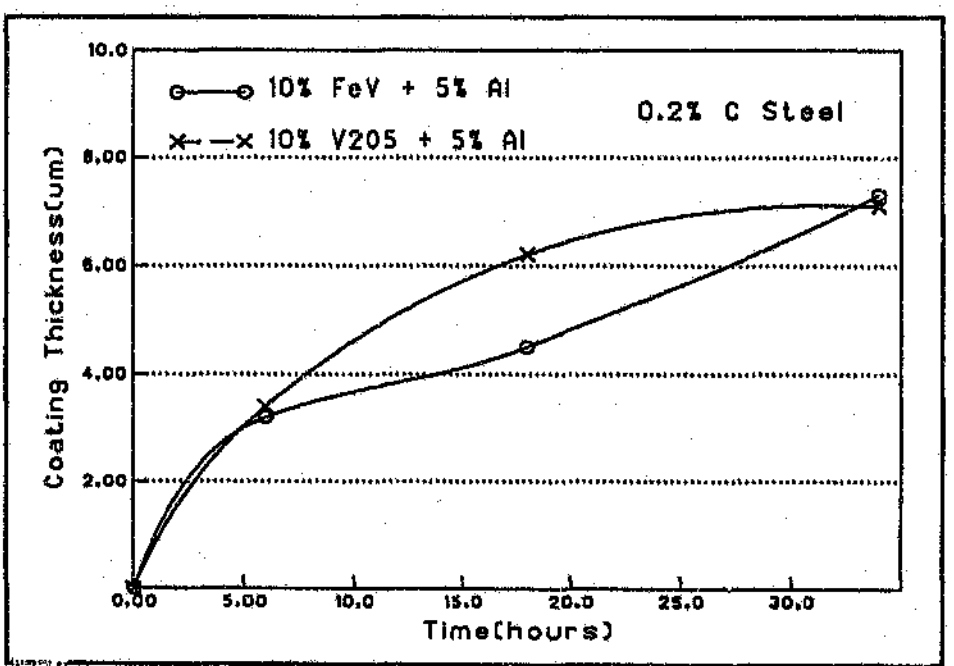


Figure.4.2. Comparison of the activities of baths containing FeV and V_2O_5.

4.2. Analyses of VC Coated Specimens

4.2.1. Microstructure of VC Coated Specimens

A number of interesting features were observed as far as the microstructure of coated specimens was concerned. As shown in **Table.4.1**, 0.2% C and 0.5% C steel specimens were treated. The micrographs presented in this section provide an overview of the microstructural characteristics observed in these specimens. Attention is drawn to those aspects of the microstructure which were found to be typical of the VC coated steel substrates, as well as, any salient features. The appearance of the VC coating on 0.5% C and 0.2% C steel substrates is shown in **Figures 4.3** and **4.4** respectively. These samples were air-cooled after treatment at 950°C.

The difference in the microstructure of the two substrate materials can be easily distinguished. The micrographs (**Figures 4.3** and **4.4**) are typical of the microstructure of VC coated samples. The uniformity of the carbide layer is noteworthy. It should be noted that the surfaces of the substrate materials were machine ground prior to coating. From these two micrographs it appears that the carbide layer formed by this process is fully dense. In the 0.5% C steel, the microstructure below the carbide layer consisted mainly of large pearlitic grains. In some instances, small areas of ferrite were found directly beneath the carbide layer(**Figure.4.5**). Below this region, the microstructure was typical of a 0.5% C steel, ie. large pearlitic grains surrounded by a ferritic network(**Figure.4.6.(a)**).In the 0.2% C steel, large grains of ferrite were present beneath the carbide layer. This was also followed by a more normal structure of mild steel comprising areas of pearlite surrounded by grains of ferrite(**Figure.4.6.(b)**).

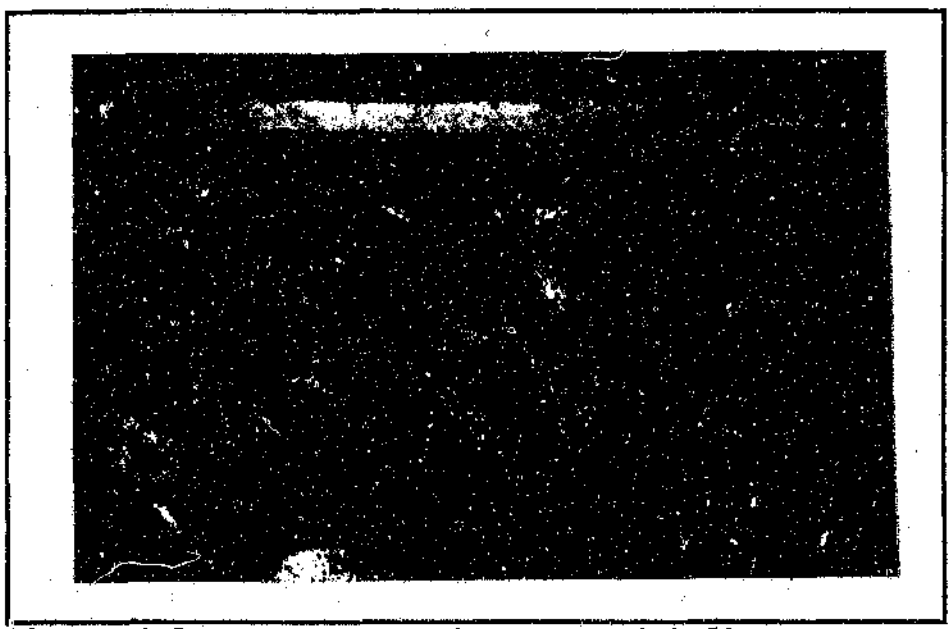


Figure.4.3. Appearance of VC coated 0.5% C steel.
Etched nital, 400X.



Figure.4.4. Microstructure of VC coating on 0.2% C steel.
Etched nital, 400X.



Figure.4.5. Microstructure of VC coated 0.5% C steel showing areas of ferrite directly beneath carbide layer. Etched nital, 3000X.

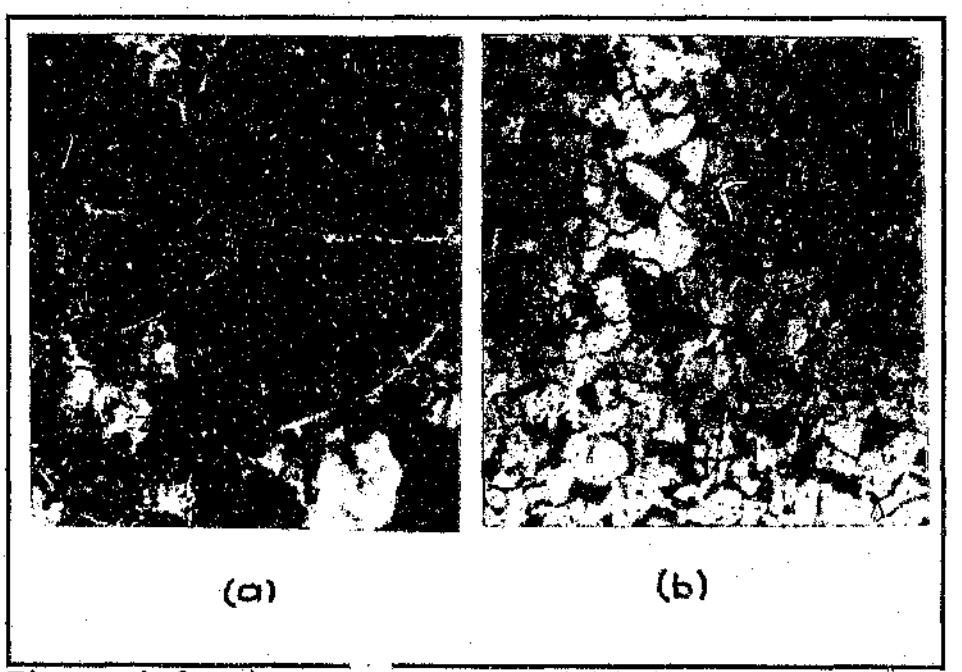


Figure.4.6. Microstructure of (a)0.5% C(400X) and (b)0.2% C(400X) steel towards the core of treated samples, nital etch.

Examination of the carbide layer at higher magnifications using electron microscopy revealed what appeared to be porosity in the layer. To confirm that this apparent porosity was not an etching effect, coated samples were examined in the as-polished condition. The appearance of the carbide layer on a 0.5% C steel before etching in nital is shown in **Figure.4.7**. This micrograph clearly shows that the VC layer contained very little porosity. The appearance of the morphology of the carbide layer as observed normally on coated samples is shown in **Figure.4.8**. One of the advantages of the carbide coating process used here is that articles can be through hardened by suitable quenching after removal from the bath. In some tests, 0.5% carbon steel samples were quenched in water or oil from the treatment temperature(950°C). Thereafter, these samples were examined to determine the extent of hardening. The microstructure of a VC coated 0.5%C steel specimen oil quenched after treatment is shown in **Figure.4.9**. One can see from this figure that the substrate microstructure below the carbide layer comprised a fairly coarse martensitic structure. Further in towards the core of the sample, the microstructure consisted of coarse martensitic needles indicating that the sample had been through hardened.

4.2.2. Determination of Coating Hardness

It was stated in Section.3.2 that the hardnesses of these VC coatings were determined from tests done on the cross section of the carbide layer. Mention was also made of the fact that the loads used had to be high enough to produce a measurable indentation and low enough to avoid breakage of the carbide layer. To give an indication of this, **Figure.4.10** shows how too large a test load caused breakage of the carbide layer(about 10μm thick in this case). The large indentation to the left of **Figure.4.10** was made at a

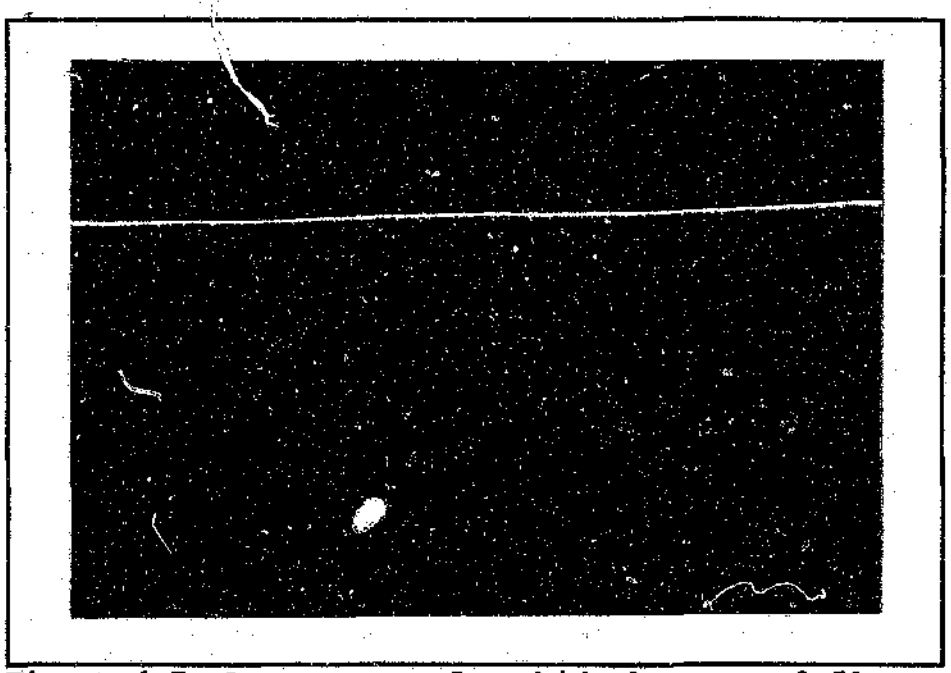


Figure.4.7. Appearance of carbide layer on 0.5% carbon steel before etching in nital.

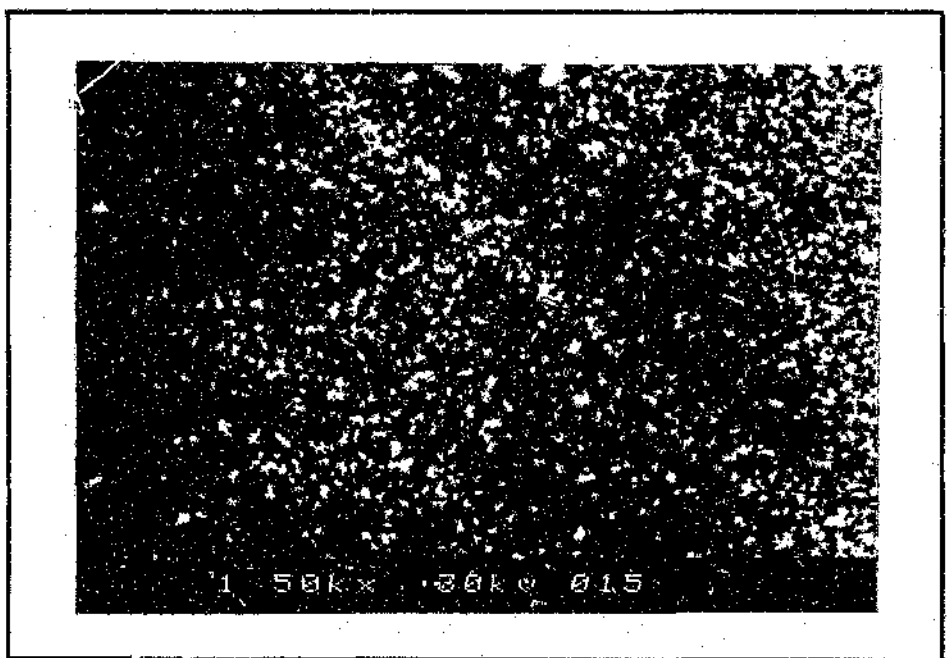


Figure.4.8. Morphology of carbide layer on coated steel surface.

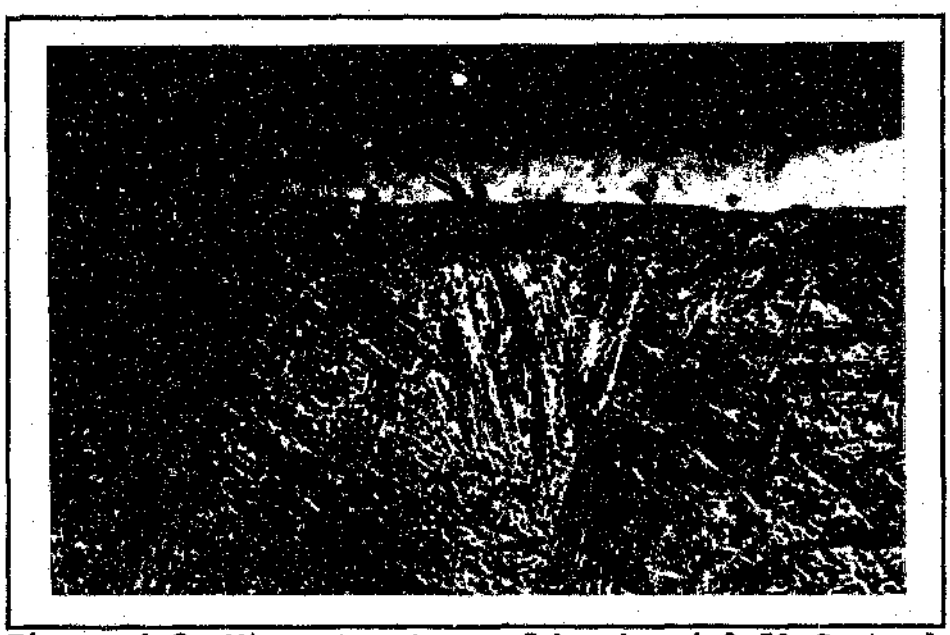


Figure.4.9. Microstructure of hardened 0.5% C steel after coating at 950°C.
Etched nital, 1000X.

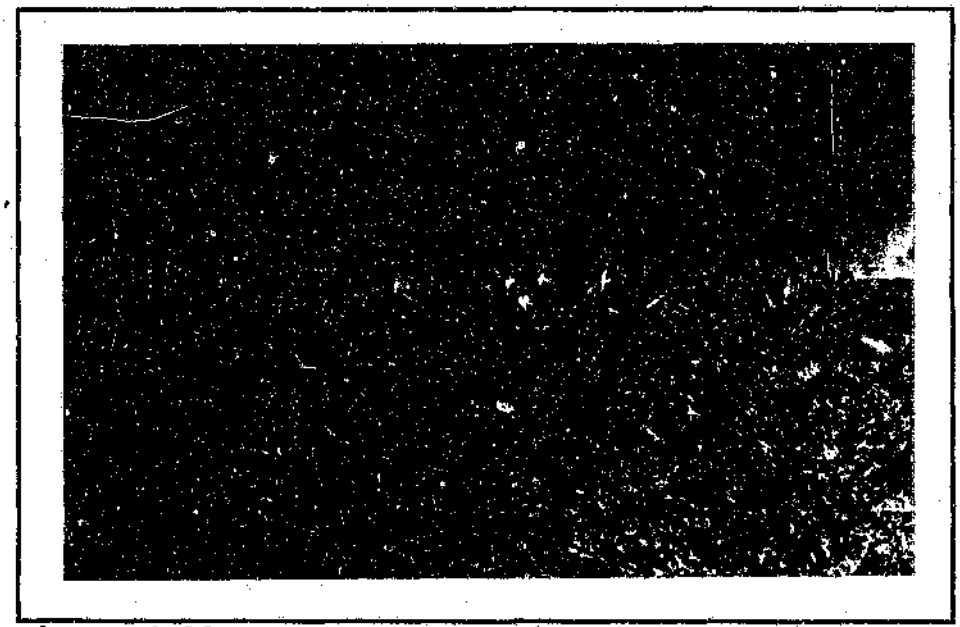


Figure.4.10. Appearance of microhardness indentations made at varying loads on carbide coating.
Etched nital, 1000X.

100gf load, while the indentation roughly in the middle of the layer was made at a load of 50gf. The smaller indentations visible on the layer, and, on the coating/ substrate interface were made at loads of 10gf and 25gf. It is clear from this figure that 10gf and 25gf loads could be used for testing the hardness of a carbide layer about 10μm thick. Using loads of 10gf and 25gf, hardness tests done on samples with average coating thicknesses between 10 - 11μm produced the results listed in **Table.4.2.**

Table.4.2. Results of Hardness Tests on VC Layers.

TEST NUMBER	HV0.25	HV0.10	Average Layer Thickness (μm)
1	2245	2375	10.6
2	2534	2646	11.8
3	2187	2343	10.4
4	2425	2465	11.3

For Test No.4, the individual hardness values were plotted against indentation number in **Figure.4.11** which shows that little variation in hardness occurred with the loads used. Furthermore, this variation was consistent and within acceptable limits.

One of the areas of interest, was the variation in hardness from the surface of the carbide coating to the core of the substrate material (**Figure.4.12**). In this regard, hardness profiles were determined on two VC coated 0.5%C steel samples. The first sample had been air-cooled from a treatment temperature of 950°C, whereas the second sample was oil quenched from the same temperature. The average

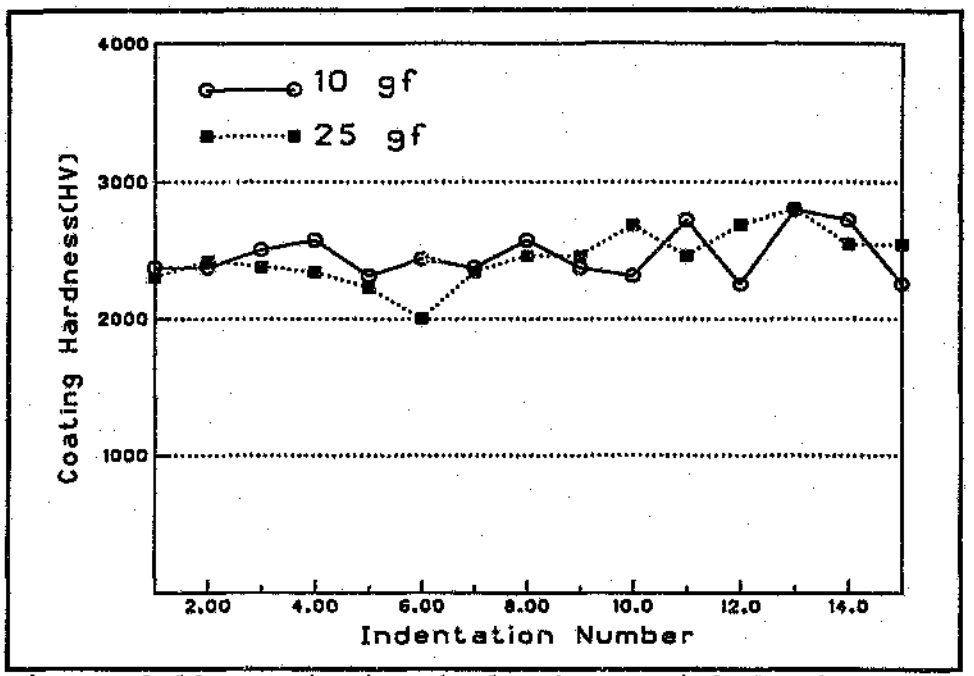


Figure.4.11. Variation in hardness with load. Average coating thickness = 11.3 µm.

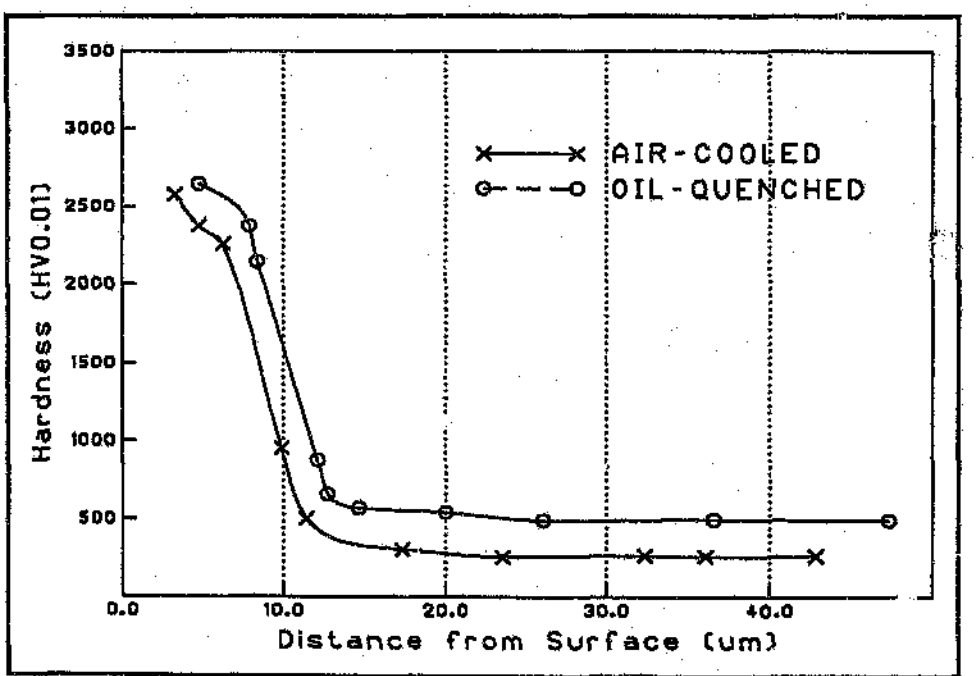


Figure.4.12. Hardness profiles on VC coated 0.5% carbon steel samples(Load = 10gf).

layer thicknesses on these samples were about 11.0μm and 10μm respectively. The oil quenched sample showed a somewhat higher hardness both at the surface and towards the core (**Figure.4.12**).

Tests were carried out to determine the "composite" hardness of the VC coating, ie. the hardness obtained from tests performed directly on the VC coated surfaces. It was mentioned in Section.3.3 that hardness values obtained by this method were likely to be influenced by the substrate material, thereby resulting in lower hardness values. In this regard, hardness tests were carried out on three different sample types as listed in **Table.4.3.**

Table.4.3. Samples used for measuring "Composite" Hardness of VC Coated Surfaces.

SUBSTRATE MATERIAL	AVERAGE COATING THICKNESS	TREATMENT CONDITIONS	SUBSTRATE HARDNESS
0.5% C	12 μm	Air-Cooled from 950°C	270HV10
0.5% C	10 μm	Oil-Quench from 950°C	600HV10
0.2% C	5μm	Air-Cooled from 950°C	220HV10

These samples were all treated in a bath containing 10% V_2O_5 plus 5% Al. Loads of 300gf, 500gf, and 1000gf were used as these loads gave indentations which were easily measurable. It must be mentioned that at loads below 300gf, the indentations made were not very clear, thus making accurate measurement difficult. The average hardness values obtained using this procedure on the three specimens were plotted against load in **Figure.4.13** which shows how the measured hardness drops with increasing load. It is clear that the

hardness measured is influenced by the hardness of the substrate. The harder the substrate the higher the combined hardness measured.

4.2.3. Determination of Coating Composition

EDS and XRD analyses were carried out to determine the chemical nature of the coating.

4.2.3.1. EDS analyses of Coated Specimens

A typical EDS spectrum of the VC coating(taken midway across the thickness of the layer) is illustrated in **Figure.4.14.** The high vanadium peak and low iron peak indicate that the major constituent of the coating was V while iron was present in appreciable concentration. Similar spectra were obtained from spot and area analyses carried out on the surfaces of coated specimens.

Quantitative EDS analyses of coated specimens were also carried out to obtain information regarding the concentrations of the elements present in the coating. **Table.4.4** lists the results of the quantitative EDS analyses on samples treated in V_2O_5-containing baths. The type of analyses, ie. spot, area, or line, is also indicated. It can be seen that the amount of Fe ranged between 0-5%.

4.2.3.2. XRD of Coated Specimens

The results obtained from XRD scans on VC coated specimens are presented in **Table.4.5.** Experimental results were

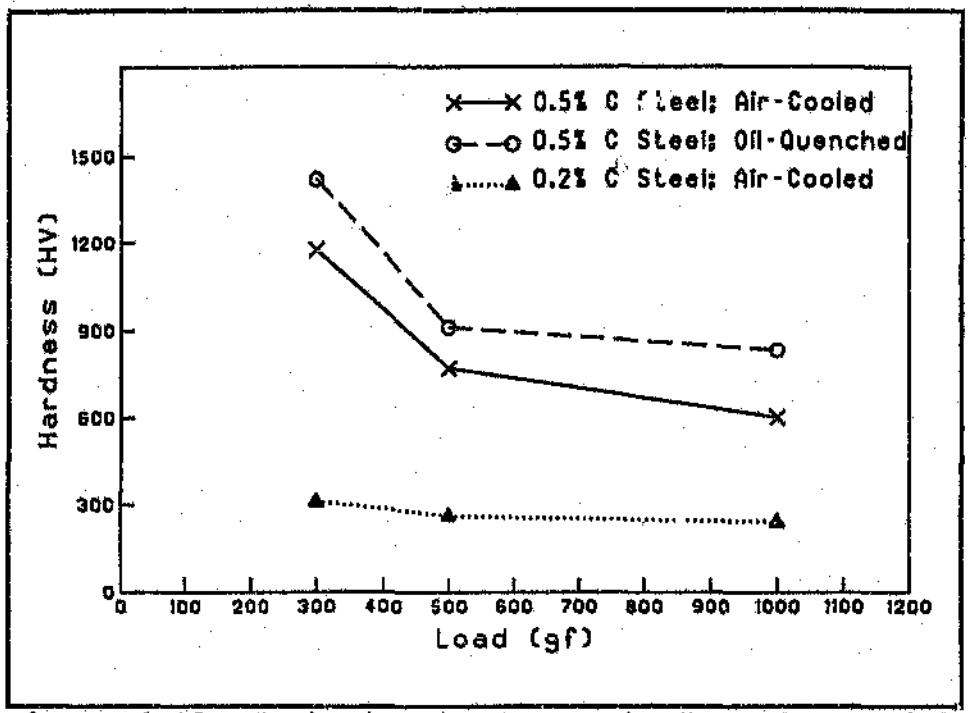


Figure.4.13. Variation in "composite" hardness with load of VC coated 0.5% C steel and 0.2% C steel.

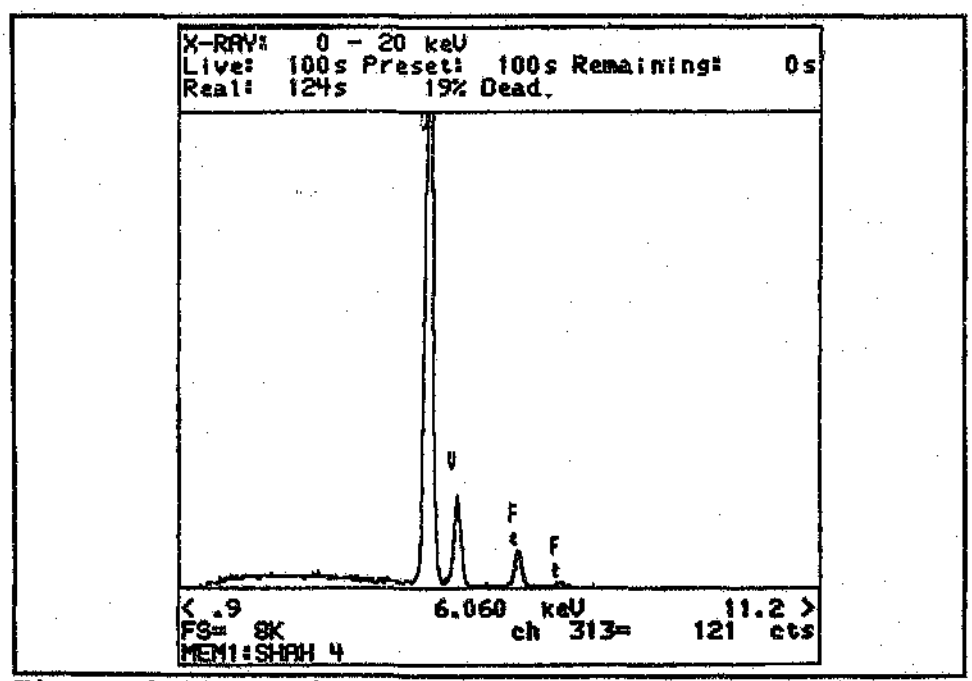


Figure.4.14. Typical EDS spectrum of VC Coating.

Table.4.4. Results of Quantitative EDS analyses on samples treated in baths containing V_2O_5 and Al.

SCAN NUMBER	TYPE OF SCAN	PERCENTAGE of ELEMENT		
		V	Fe	Total
1.	spot	96.19	3.81	100.00
2.	area	95.42	4.58	100.00
3.	line	96.85	3.15	100.00
4.	spot	99.04	0.96	100.00
5.	area	95.81	4.19	100.00

Table.4.5. XRD Data of VC Coated Specimens.

Peak No.	$VC_{0.88}$				VC(14%C)			
	Powder File Data		Diffraction Data No.1		Powder File Data		Diffraction Data No.2	
	d	I/Im	d	RPH	d	I/Im	d	RPH
1.	2.401	80	2.40	85	2.40	100	2.404	100
			2.39	75			2.40	80
2.	2.079	100	2.077	100	2.07	100	2.08	90
			2.071	90			2.073	80
3.	1.472	80	1.474	25	1.47	50	1.475	20
			1.469	30			1.471	30

d = Interplanar spacing; **I/Im** = Relative Peak Intensity; **RPH** = Relative Peak Height.

compared with results from the powder diffraction file. Two types of vanadium carbide were listed in the file, namely $VC_{0.88}$ and VC(14% C). The experimental data listed in **Table.4.5** were derived from two separate XRD scans. The first scan(No.1) was obtained with a 0.2% C steel sample with an average coating thickness of 5μm. Scan No.2 was obtained with the same sample at a slower scanning speed. This specimen was treated in a 10% V_2O_5 and 5% Al bath. As shown, the experimental peaks correlate well with those listed in the diffraction file. Only the major diffraction peaks are listed here for convenience. A full listing of experimental data obtained is provided in the **Appendix.A.1** which is a sample list of experimental data obtained on VC coated samples, For reference purposes, the relevant parameters and diffractometer settings used during scans are included in the list. The major peaks in the list are highlighted in bold print. It is also evident from the data in **Table.4.5** that the carbide formed on the specimens was very similar crystallographically to $VC_{0.88}$ and VC(14% C) despite its significant iron content. It would seem also that the crystallographic differences between $VC_{0.88}$ and VC(14% C) are small and would require sophisticated techniques to study these.

Figure.4.15 is a typical diffractogram of the VC coated specimen. The dashed lines under each peak correspond to the position of major peaks according to the powder diffraction file. This also shows good correlation between the experimental and established data indicating that the coatings were crystallographically similar to vanadium carbide.

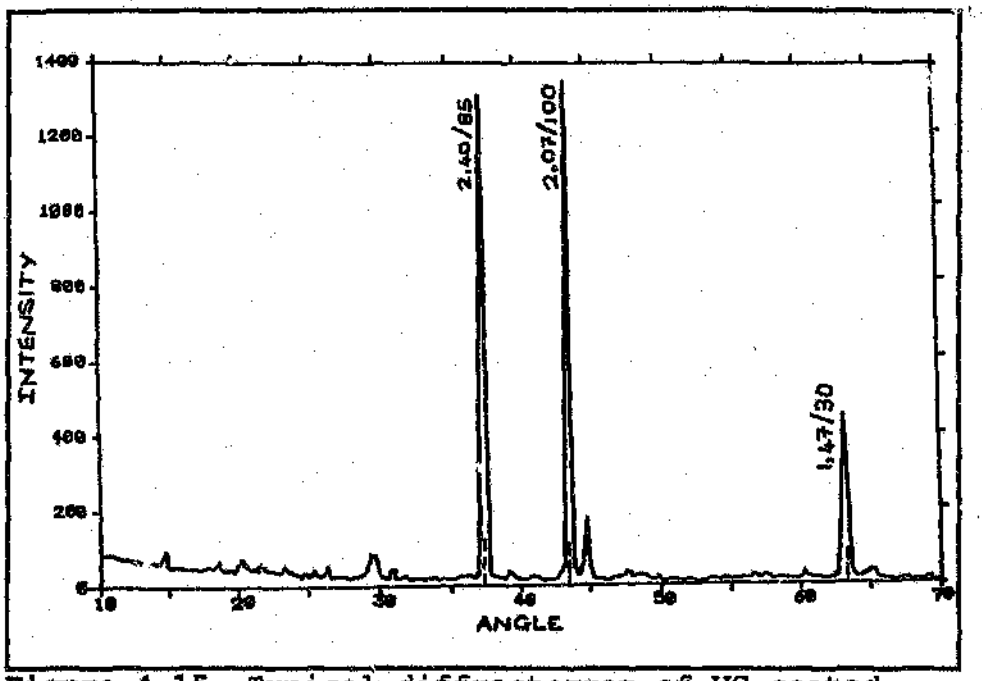


Figure.4.15. Typical diffractogram of VC coated sample.

4.3. A Detailed Study of Baths containing V_2O_5 and Aluminium

The reasons for deciding to study baths containing only V_2O_5 and Al were touched upon in Section.3.4. It was also pointed out that a number of process variables were controlled in order to isolate the effects which different variables, for example temperature and bath composition, may have on coating conditions. The outcome of each of the steps taken in this regard is presented in the relevant sections below.

4.3.1. Effect of Temperature on Coating Thickness

The effect of the three temperatures tested is shown in **Figure.4.16** where it can be seen that the thickest coatings were produced at the highest temperature. The difference in coating thickness between the three curves was more marked initially. However, by the end of a 9 hour period this difference was reduced.

4.3.2. Influence of Substrate Carbon Content on Coating Thickness

As expected, the higher carbon substrate formed a thicker coating in a given time period(**Figure.4.17**). The difference in coating thickness between the two steels became more marked towards the end of the test period.

4.3.3 Effect of V_2O_5 Content on Bath Activity

In this case, the V_2O_5 content of three separate baths was varied by 5, 10, and 20%, while the amount of aluminium was kept constant at 5%. Figure 4.18 summarises the results of

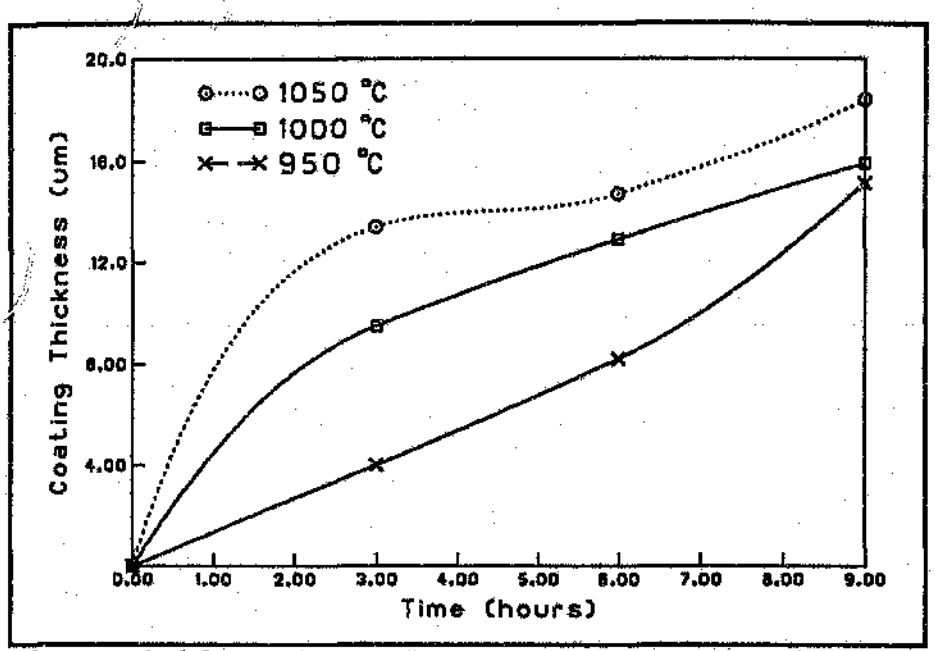


Figure.4.16. Effect of temperature on coating thickness produced in a bath of 10% V_2O_5 plus 5% Al.

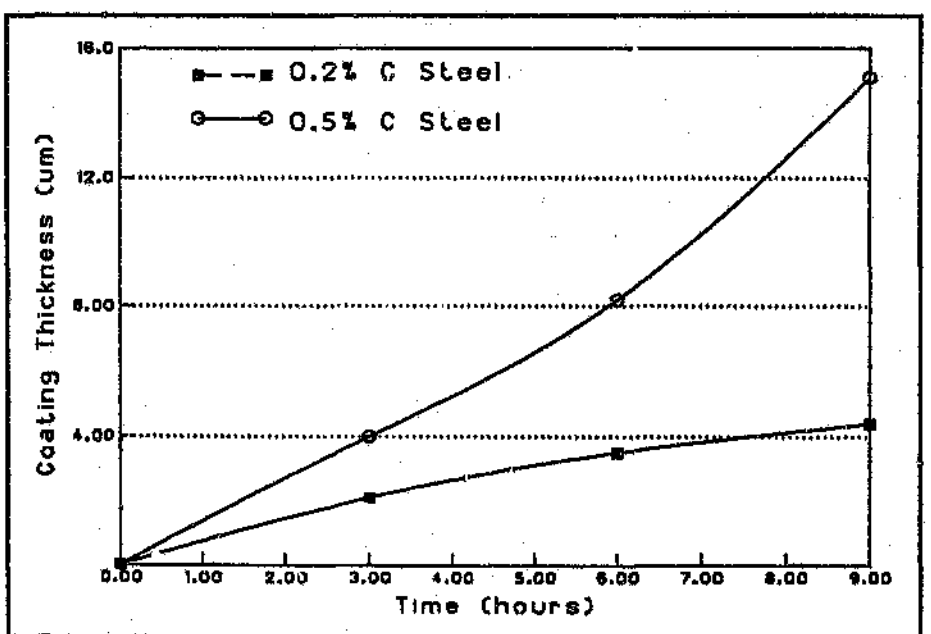


Figure.4.17. Comparison of carbide layer growth on 0.2% and 0.5% C steels treated at 950°C for 3, 6, and 9h.

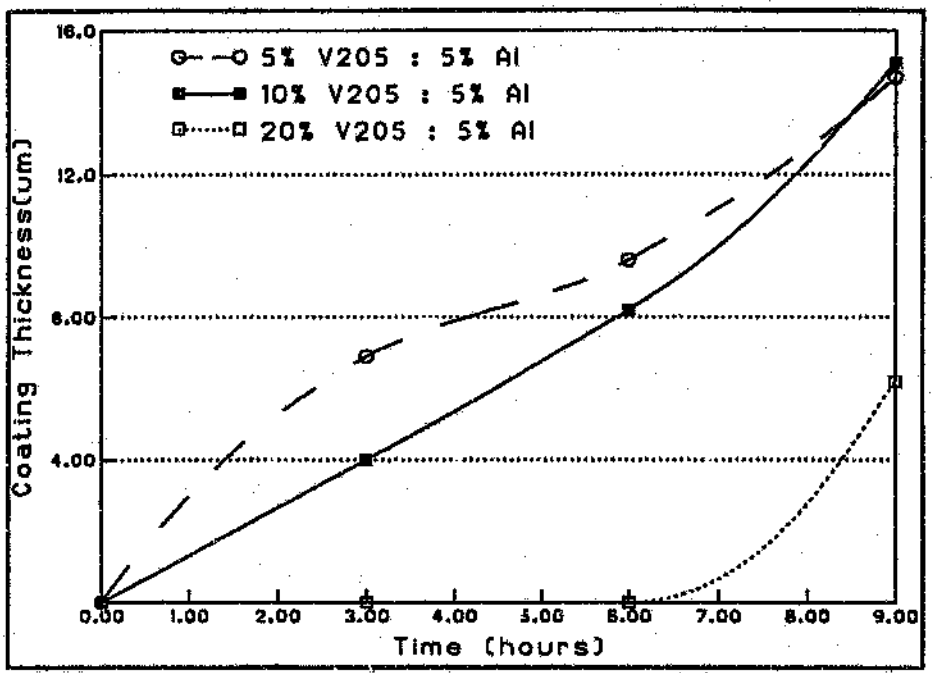


Figure.4.18. Effect of $\%V_2O_5$ on the thickness of coatings produced at 950°C and 3, 6, or 9h of treatment.

these tests. As can be seen, the activity of the bath containing 5% V_2O_5 was slightly higher than that of the 10% V_2O_5 bath initially. At the 9 hour period, the activity of the 10% bath had risen above the level of the 5% bath. It is interesting to note that in the case of the 20% V_2O_5 containing bath, no coating was formed in the first six hours of treatment.

4.3.4. Effect of Aluminium Content on Bath Activity

The results obtained by varying the concentration of aluminium while keeping the amount of V_2O_5 constant are shown in **Figure.4.19.** Initially, the bath with the 10% Al content exhibited a higher activity than the bath containing 5% Al. After about 8h, the two baths appeared to reach similar activities, but by the end of the 9h period,

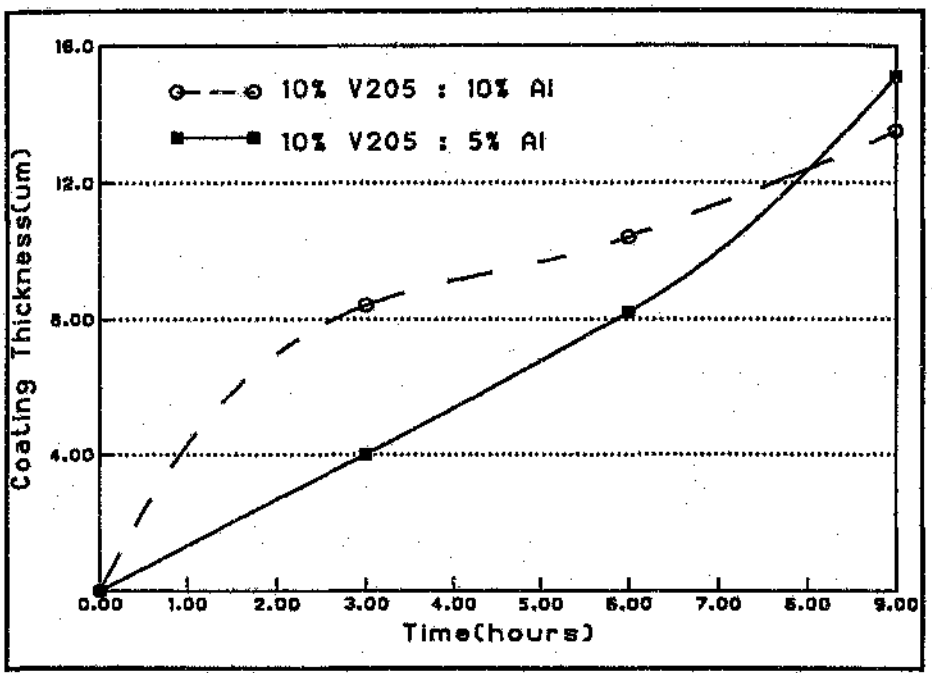


Figure.4.19. Effect of %Al on bath activity at 950°C for 3, 6, 9h of treatment.

the activity of the bath containing 5% Al was appreciably higher than that of the bath containing 10% Al.

4.3.5. Effect of Bath Composition on Coating Thickness

Changing the concentration of reactants while maintaining their ratio in the bath constant had the effect shown in **Figure.4.20.** Overall, the bath with the highest amount of additives had the highest activity whereas no layer was formed in the bath with the lowest concentration of reactants. The activities of the baths containing 20% V_2O_5 plus 10% Al and 10% V_2O_5 plus 5% Al were similar at the end of the 9h test period. It appears from these results that a minimum concentration of V_2O_5 plus Al must be exceeded for a coating to form.

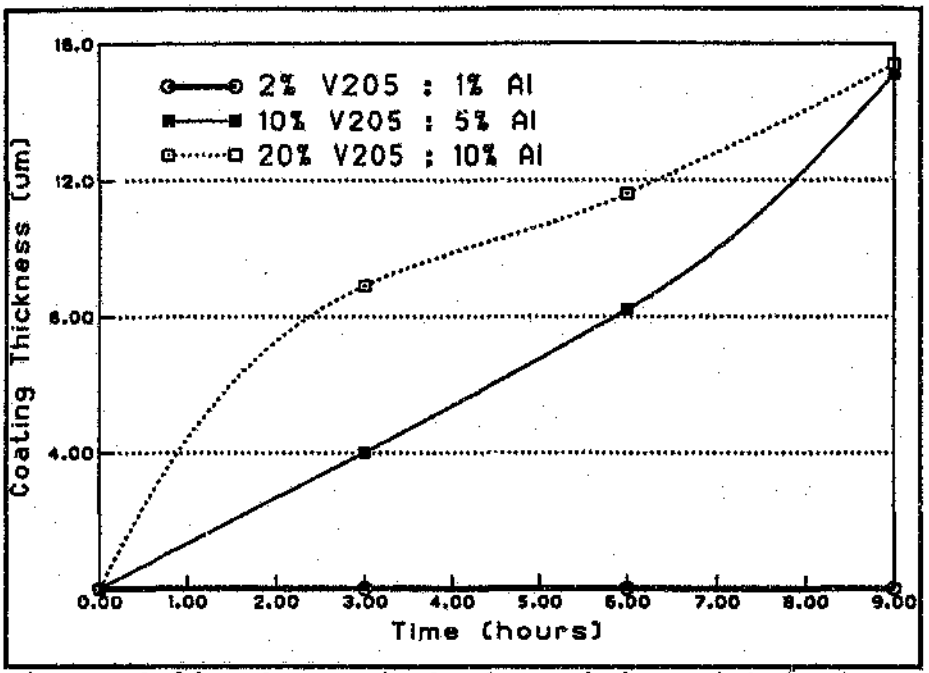


Figure.4.20. Change in bath activity with bath composition at 950°C (V_2O_5:Al = 2:1).

4.3.6. Influence of Particle Size of V_2O_5 on Bath Activity

As stated in Section.3.4.6, the particle size of the reactants was expected to have an influence on the activity of the bath. **Figure.4.21** is a plot of the results obtained on the four particle size ranges tested. As can be seen, the finest particle size produced the highest bath activity. The two intermediate sizes gave similar growth rates, which were lower than that obtained with the finest size. Using the V_2O_5 in the as-received condition, ie. as flakes, produced no coating in the first 3 hours.

4.3.7 Change in Bath Activity with Time

The influence of bath age on bath activity is shown in **Figure.4.22**. It can be seen that the activity rose rapidly

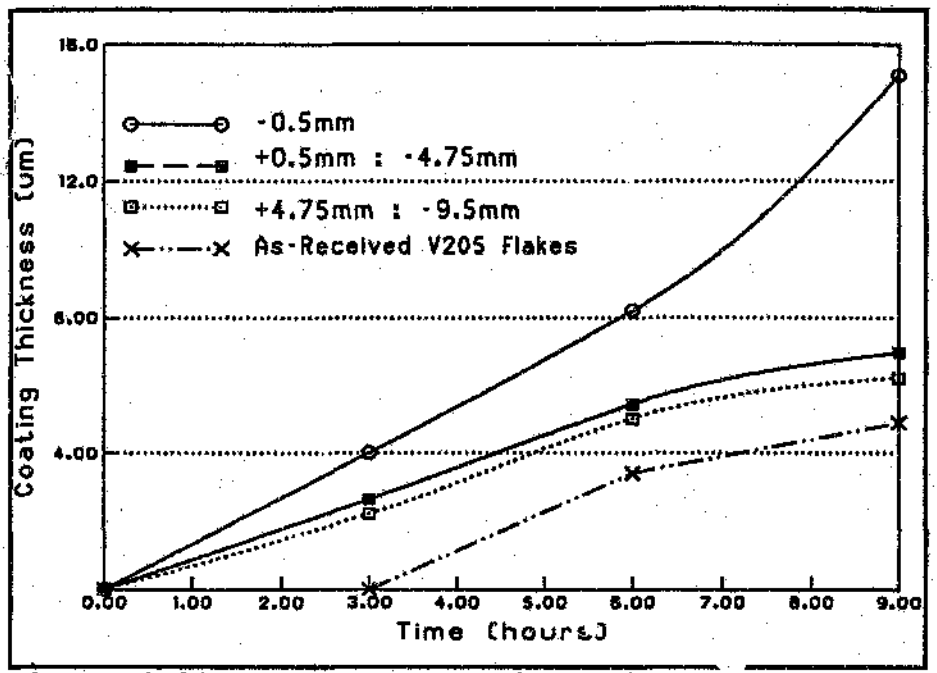


Figure.4.21. Effect of particle size on bath activity at 950°C for 3, 6, and 9h of treatment.

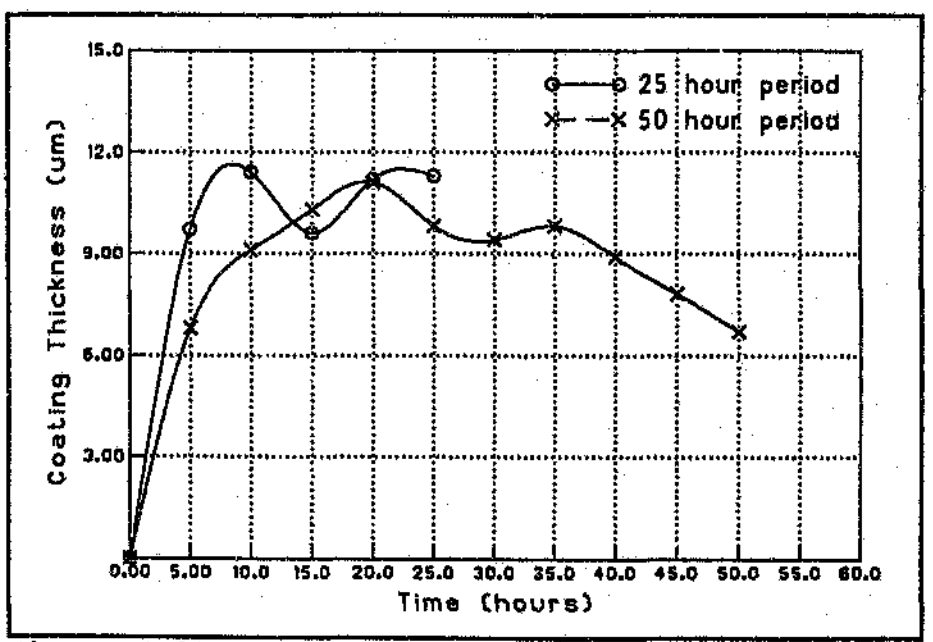


Figure.4.22. Change in bath activity over 25h and 50h periods at 950°C. Samples treated in 5h intervals.

during the first 10h of bath life. Thereafter, it remained reasonably constant and appeared to decline after about 25h.

4.3.8. Effect of Bath Depth and Bath Age on Coating Thickness Produced

The coating thicknesses measured at different points along the length of the coated 0.5% C steel rods were plotted against distance from the bottom of the bath. The curves in **Figure.4.23** show the variation in coating thickness with bath depth for rods treated in the baths aged for 8h and 16h. It can be seen that there appears to be some variation in coating thickness with bath depth for the baths aged for 8h and 16h. Towards the bottom half of these baths, the coating thicknesses produced were similar with the 16h bath appearing to have slightly higher activity than the 8h bath. Towards the top half, however, rods treated in the 8h bath produced significantly thicker coatings especially those treated for 9h and 12h. It should be noted that the rod treated for 12h in the 16h bath had oxidised at the 90mm level. The average depth of the melts varied between 90-100mm.

In order to assess the differences between the 8h and 16h baths in greater detail, the coating thickness produced at distances of 30mm, 50mm, and 70mm above the bath bottom on rods treated in either bath was plotted against treatment time in **Figure.4.24**. For treatment times of up to 6h, the activities of the two baths were similar. For treatment time of 12h the bath aged for 8h was definitely higher. Based on this result, it was decided to compare the coating thickness produced on samples immersed at the "standard" level (about 30mm from the bottom) with that produced on rods treated in the 8h and 16h bath (**Figure.4.25**) at the

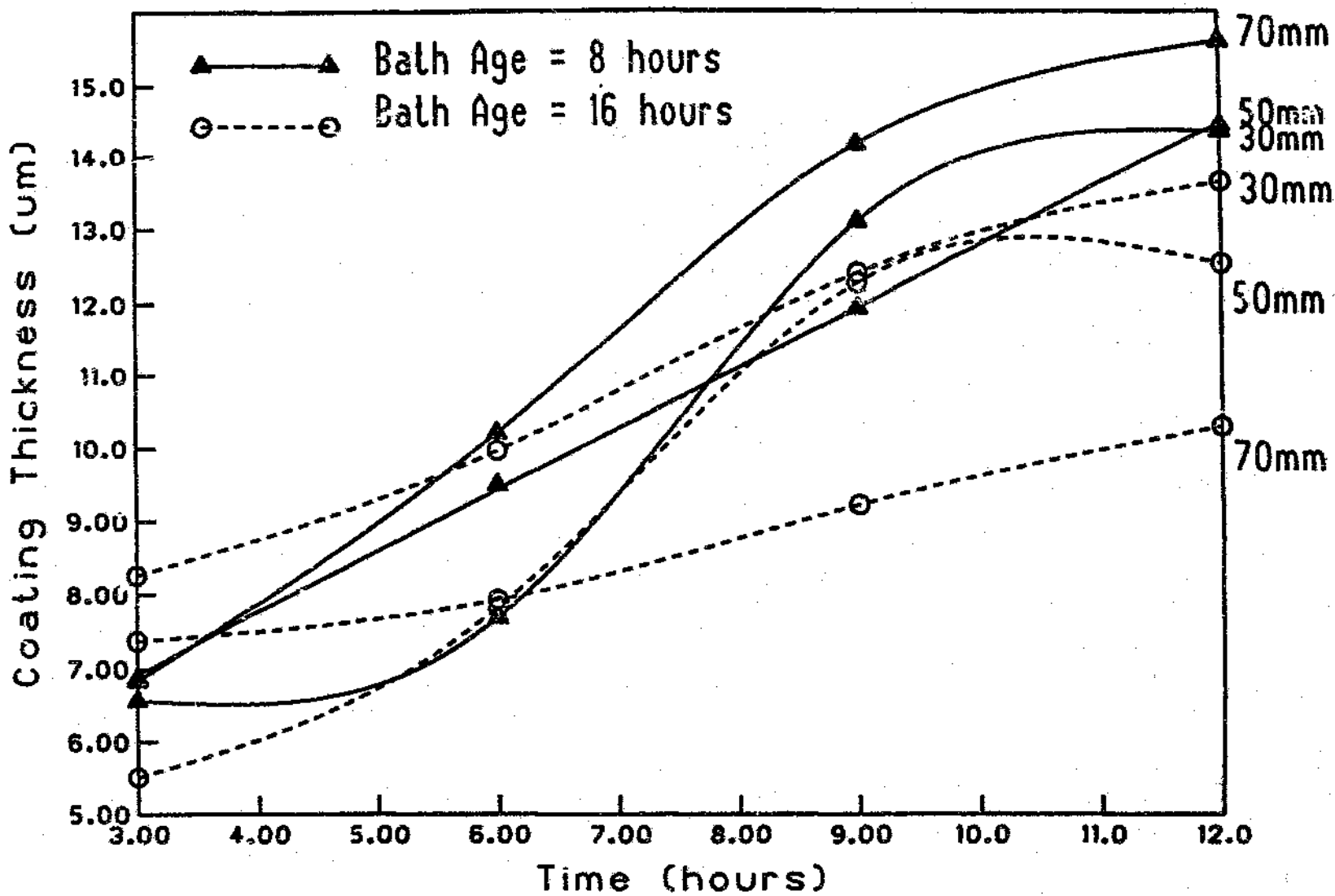


Figure.4.24. Comparison of coating thicknesses at distances of 30mm, 50mm, and 70mm above the bath bottom on rods treated in baths aged

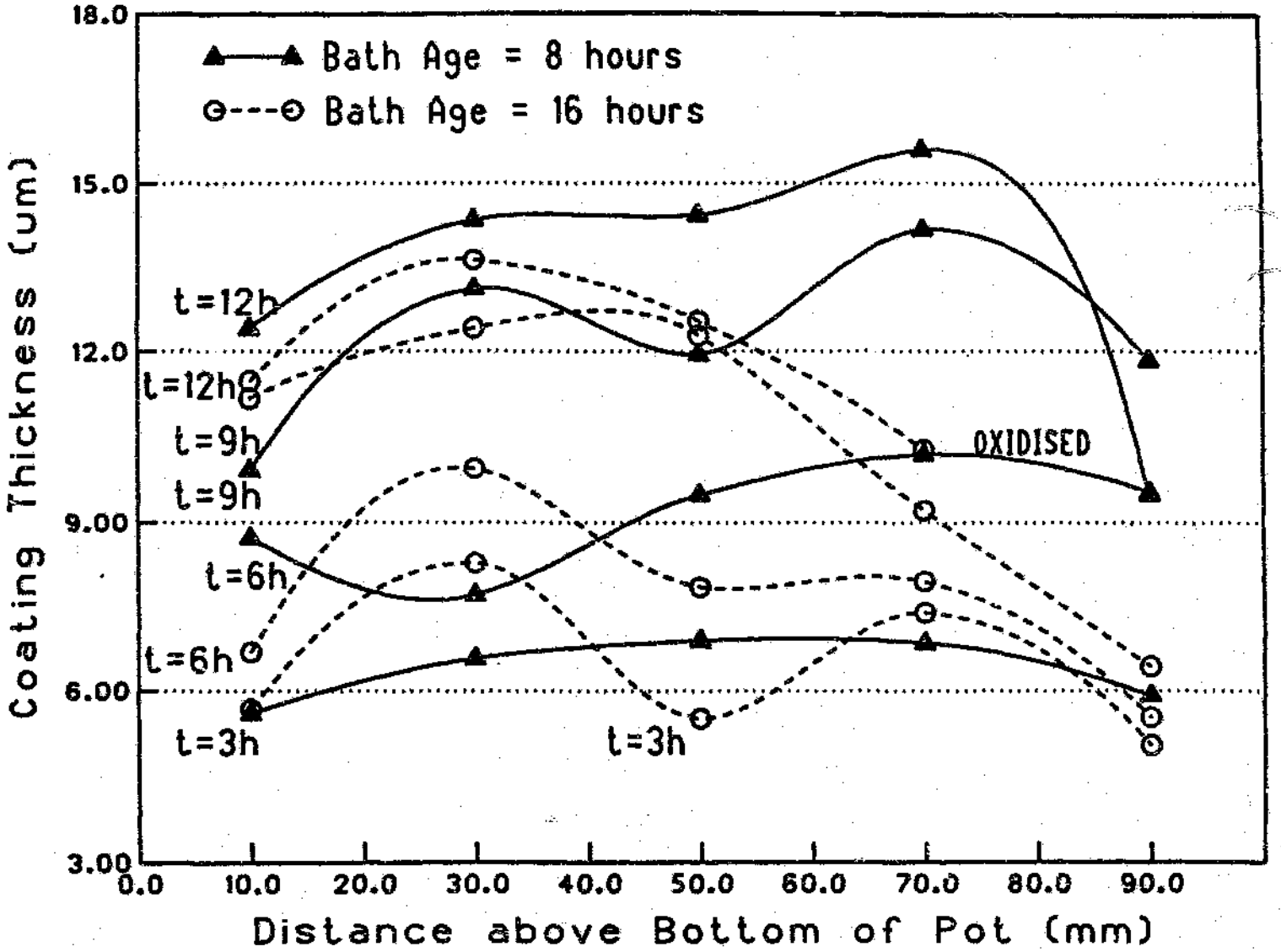


Figure.4.23. Variation in coating thickness with distance above the bottom of the bath for rods treated in baths aged for 8h and 16h.

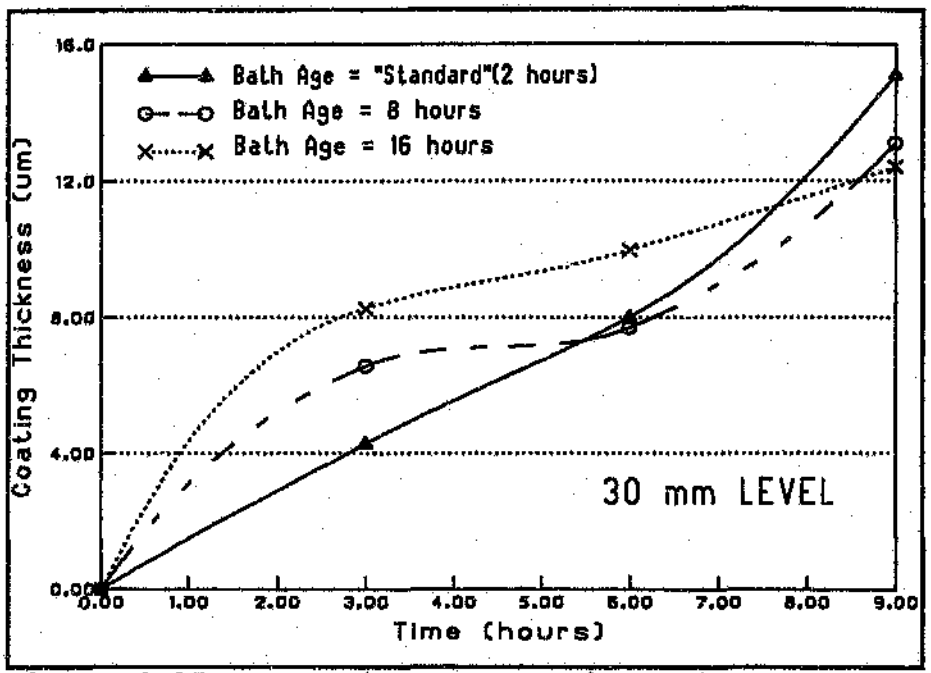


Figure.4.25. Comparison of coating thicknesses produced on 0.5% C steels treated in three 10% V_2O_5 and 5% Al baths aged for 2h, 8h, and 16h respectively.

same level for treatment times of 3, 6, and 9 hours. It can be seen that the 16h bath was most active during the first 6h of treatment after which the "standard" bath which had aged the least(about 2 hours) prior to the immersion of samples became the most active.

It must be noted at this stage that under normal conditions, the bath was kept at temperature for a period of 1.5 - 2.5 hours prior to the immersion of samples. Samples were only immersed in the bath once the colour of the borax melt had changed from black to green. A period of 1.5 - 2.5 hours, with little variation, was found to be sufficient for a freshly made bath to achieve the required greenish colour. Baths which were not of "standard" composition, ie. containing 10% V_2O_5 and 5% Al, were kept at temperature for 2.5 hours on average prior to the immersion of any samples in order to compare the activity

of such baths with the "standard" bath.

4.3.8.1. Macroscopic Appearance of Coated Rods

Examination of the coated rods after cleaning revealed a couple of noteworthy features. Firstly, the extent of oxidation which took place at the top of the melt is clear from the appearance of the rods (**Figure.4.26**). One can see the increase in the length of the oxidised portion with increased immersion time. Among the salient features noted on the treated rods was that of aluminium droplets which became attached to a number of the rods during treatment. The appearance of aluminium on these rods is shown in **Figure.4.27.**

4.3.9. Influence of Surface Finish

Macroscopic examination of the VC coated 0.5% C steel samples which had been given three different surface finishes revealed little difference in the appearance of the samples, except that the sand blasted sample was rougher. Microscopic examination provided further evidence of this (**Figure.4.28.(a)-(c)**). It can be seen from **Figure.4.28** that the roughness of the interface between the coating and the substrate increased from the diamond polished to the ground to the sand blasted surfaces as might have been expected. A noteworthy feature from this micrograph is that the surface roughness of the sand blasted surface was reduced by the carbide layer in contrast to the diamond polished surface where it appeared to increase slightly. This was due to the tendency of the carbide layer to grow faster at surface irregularities and in so doing smooth the surface progressively.

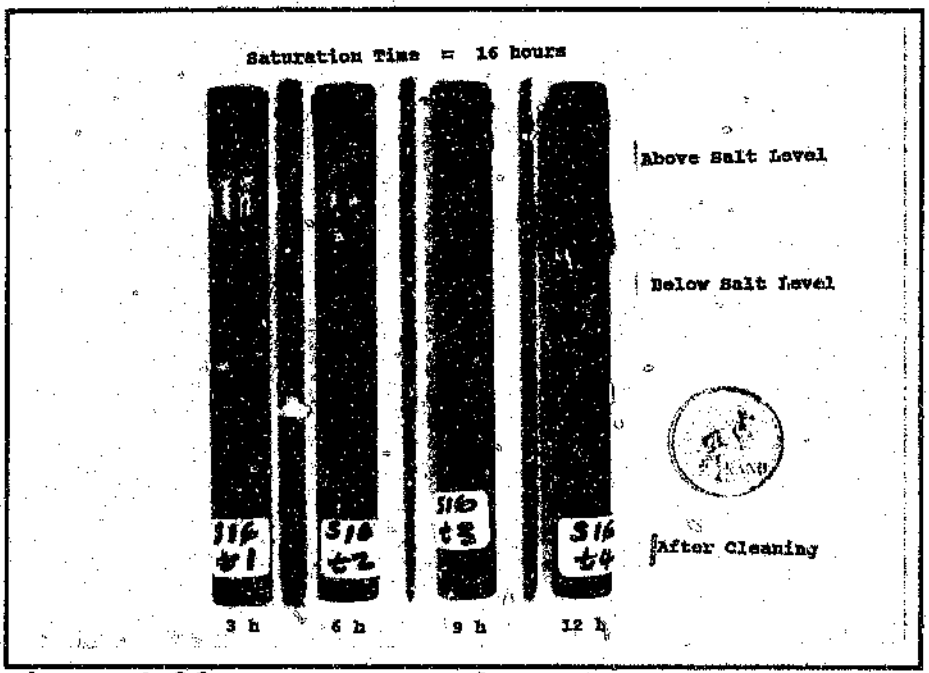


Figure.4.26. Appearance of sample rods after cleaning.

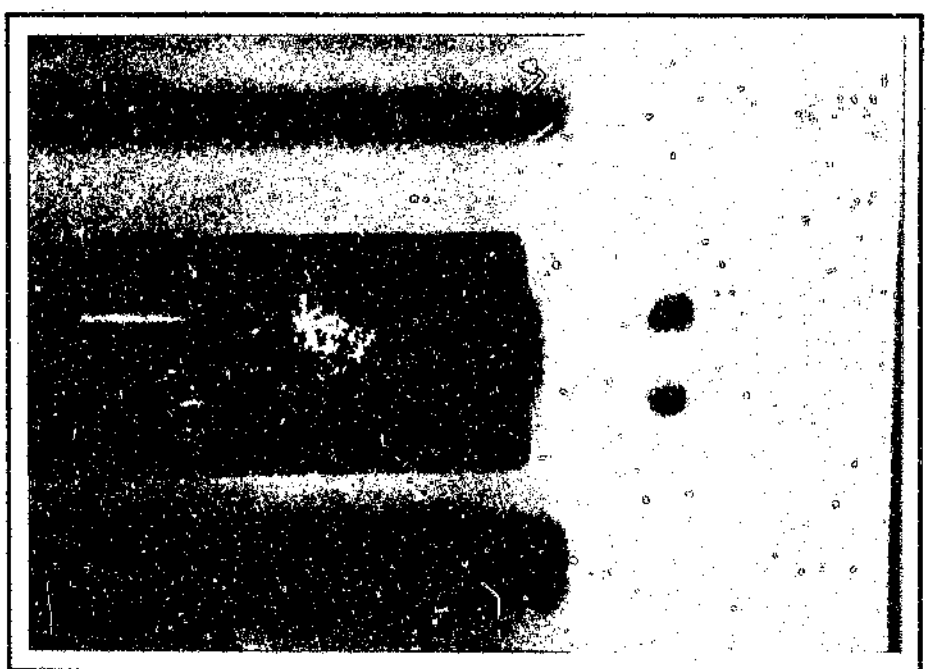


Figure.4.27. Appearance of aluminium attached to treated rod.

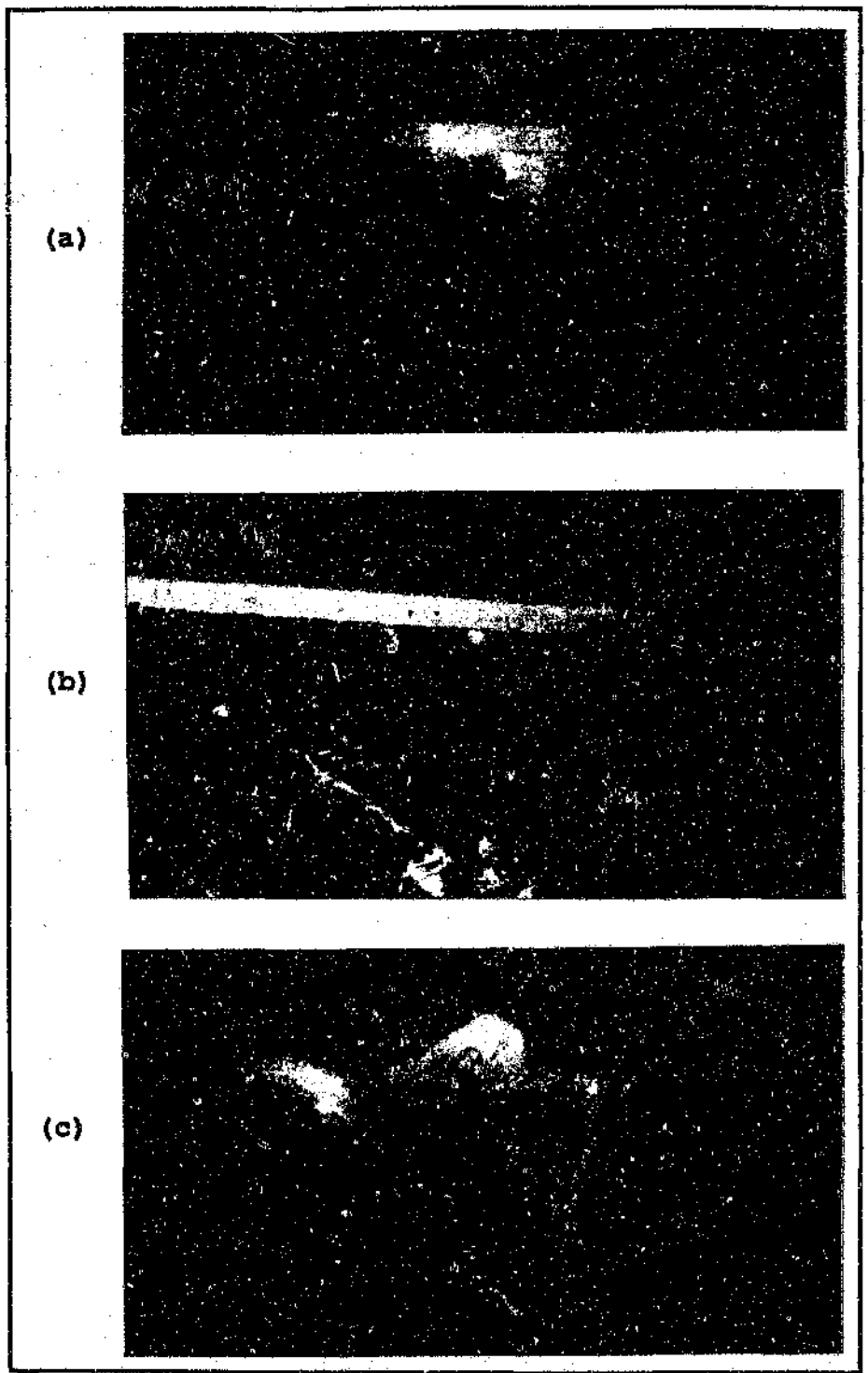


Figure.4.28. Nature of carbide layer on (a) Diamond polished (b) Ground (c) Sand Blasted Surfaces. Etched nital, 400X.

4.3.10. Analyses of Baths containing 10% V_2O_5 and 5% Aluminium

The experimental data from XRD analyses on pulverised glass samples taken from baths containing 10% V_2O_5 plus 5% Al were compared to data listed in the powder diffraction file. The experimental data correlated well with the file data for V_2O_3 as shown in **Table.4.6** which compares the data obtained from two scans. Only the major peaks are listed in **Table.4.6.** A typical diffractogram acquired from XRD analyses of bath samples is shown in **Figure.4.29.** The high background radiation was due to the glassy borax in the sample.

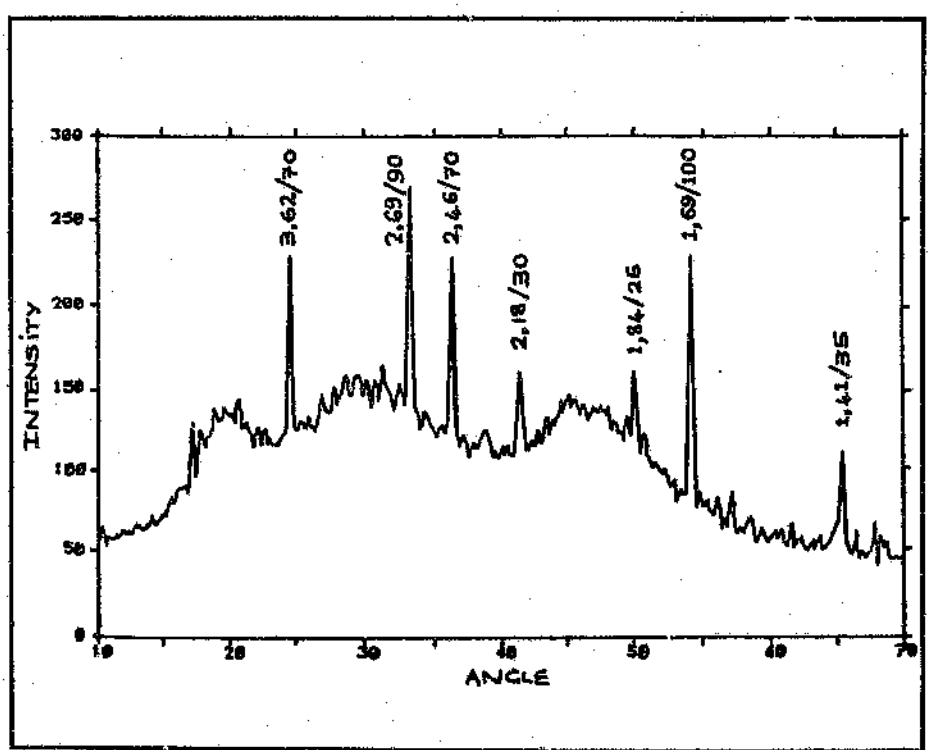


Figure.4.29. Typical diffractogram of bath sample.

Table.4.6. XRD Data of Bath Sample.

Peak No.	V_2O_3					
	Powder File Data		Diffraction Data 1		Diffraction Data 2	
	d	I/Im	d	RPH	d	RPH
1.	3.65	60	3.62	70	3.66	70
2.	2.70	80	2.69	90	2.71	100
3.	2.47	60	2.46	70	2.48	50
4.	2.18	20	2.18	30	2.18	15
5.	1.83	25	1.84	25	1.83	20
6.	1.69	100	1.69	100	1.69	100
7.	1.43	30	1.41	35	1.438	13
					1.432	18

d = Interplanar Spacing;
I/Im = Relative Peak Intensity;
RPH = Relative Peak Height.

It is evident that good correlation existed between established and the experimental data. A sample of the full listing of the XRD data obtained from bath samples is shown in the **Appendix.A.2.** The major peaks are highlighted in bold print.

4.4. Corrosion Test Results of VC Coated Specimens

The types of samples prepared for corrosion testing were described in **Table.3.5.** From the dummy samples treated with these samples, the average coating thickness for the four sample types was evaluated. The coating thicknesses on these samples were also estimated using **Figure.4.17.** These results are listed in **Table.4.7** where it can be seen that the estimated and measured values correspond fairly well.

Table.4.7. Measured and Estimated Coating Thicknesses of Corrosion Samples.

SUBSTRATE MATERIAL	ESTIMATED Thickness (μm)	MEASURED Thickness (μm)	Standard Deviation
0.2% C(4h)	2 - 3	3.7	0.20
0.2% C(6h)	3 - 4	4.9	0.21
0.5% C(4h)	6	6.5	0.14
0.5% C(6h)	8	9.1	0.39

As stated in Section.3.5, three coated and three uncoated samples of mild steel(0.2% C) and EN9(0.5% C) steel were subjected to potentiodynamic and cyclic polarization tests. Typical scans obtained from potentiodynamic testing of mild steel and EN9 steel samples are reproduced in **Figure.4.30** and **Figure.4.31** respectively.

Figure.4.30 and **Figure.4.31** compare the corrosion behaviour of the coated substrate with that of the uncoated substrate as indicated in the figures. For both mild steel and EN9 steel, it can be seen that the coated substrate responded quite differently to the test conditions than the uncoated substrate. Above Ecorr, which is the corrosion potential

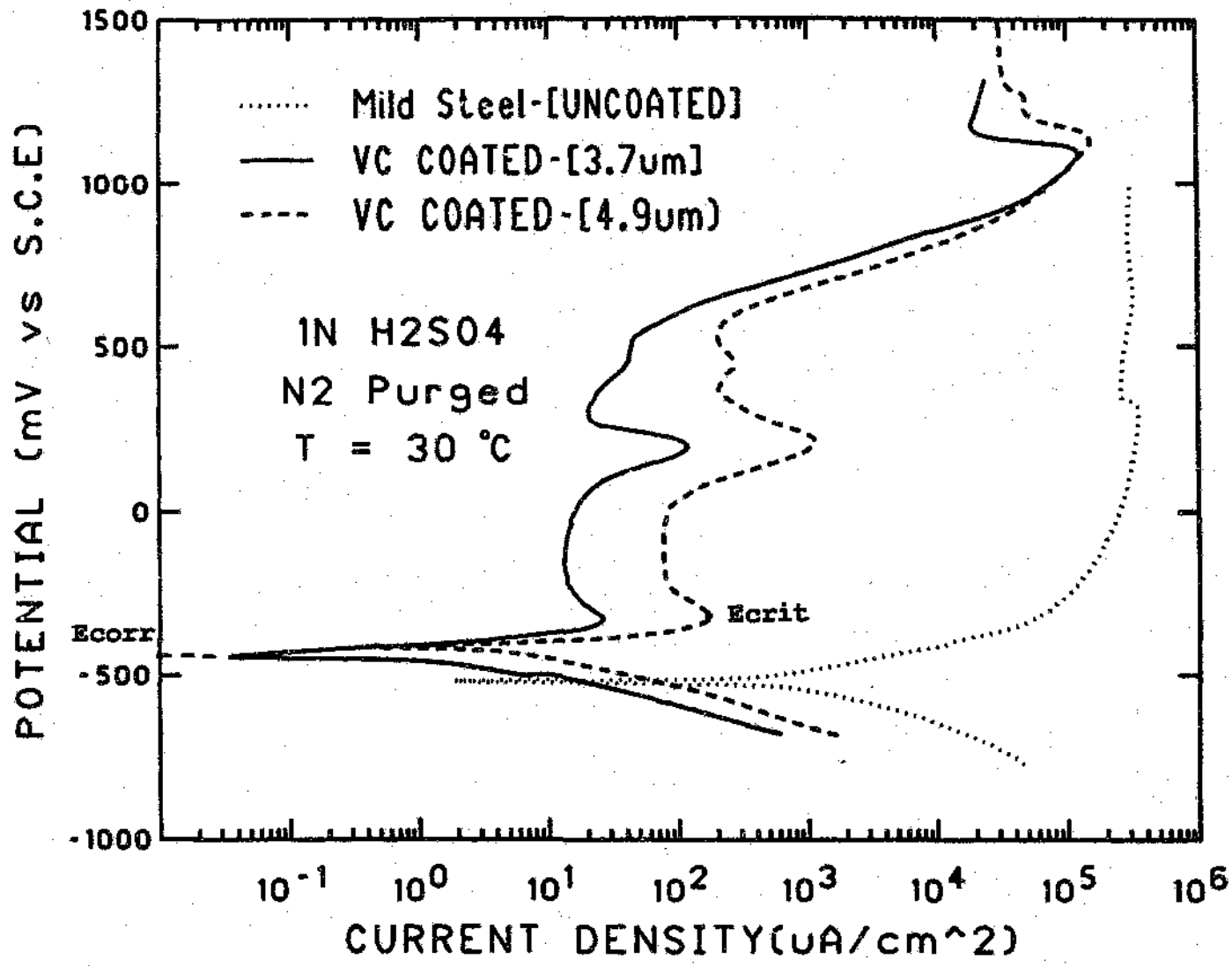


Figure.4.30. Typical potentiodynamic curves for mild steel samples.

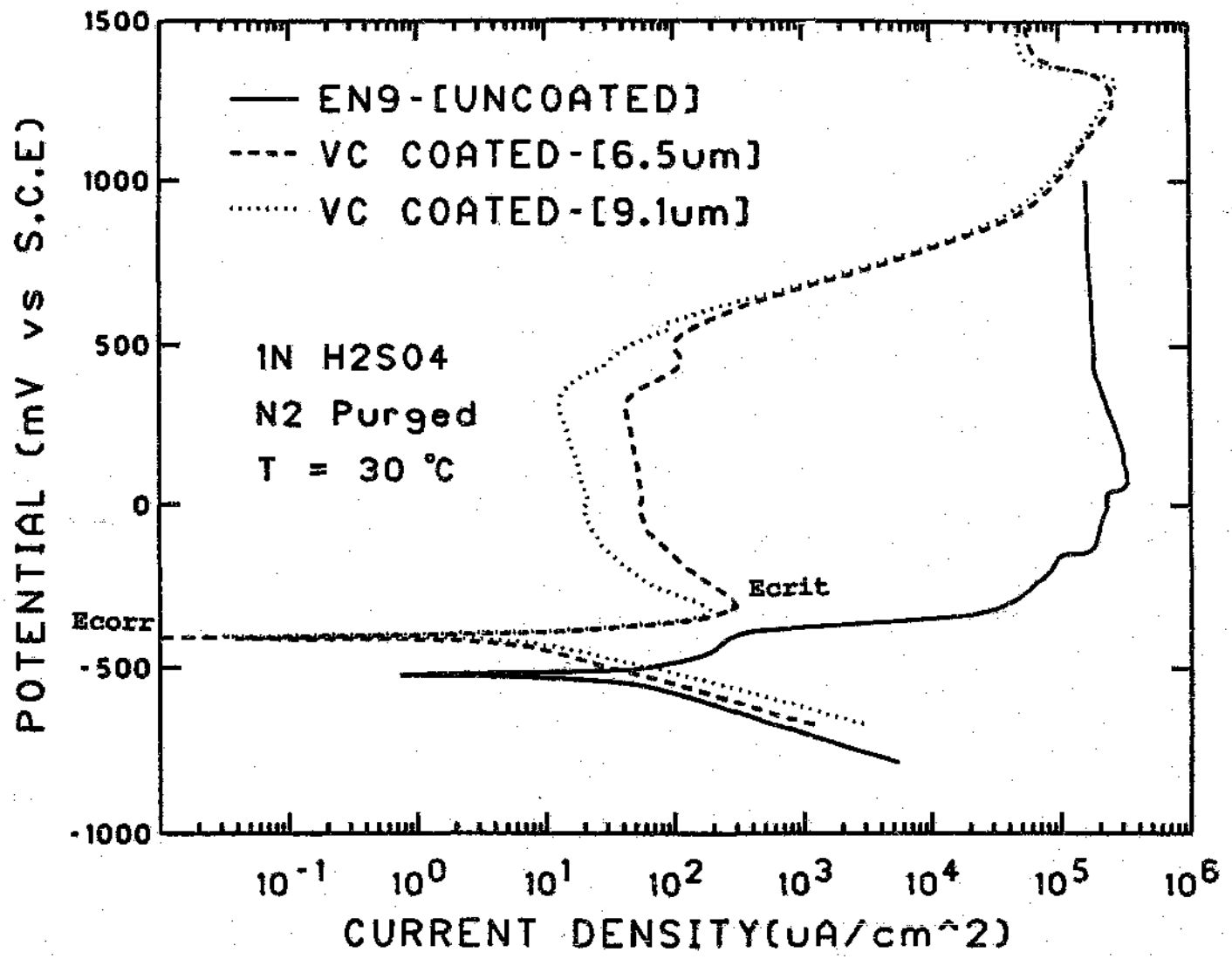


Figure.4.31. Typical potentiodynamic curves for EN9 steel samples.

(the potential to which the system would stabilize after a certain time period if no current was passed through it), the current density of VC coated samples increased rapidly up to icrit, the critical current. Beyond icrit, the current density decreased slightly and then varied little with a large increase in potential indicating that these samples had passivated and thus little or no corrosion of the samples was occurring. Above about 500 mV, the current density increased rapidly again. By contrast, the uncoated samples showed a large increase in current density over a similar potential range indicating that the samples underwent extensive corrosion.

Relevant corrosion data was extracted from each potentiodynamic scan and compiled in **Table.4.8**. The data extracted was as follows[79,80].

1) **Ecorr** - The corrosion potential which is the potential of the system in the absence of an impressed current. A more negative Ecorr signifies that the metal or alloy is less resistant to corrosion in that system.

2) **Icorr** - The corrosion current density at Ecorr.

3) **Corrosion Rate(C.R.)** - The corrosion rate in mpy(one mpy = 25.4 μm per year) is one of the more significant variables indicating the amount of dissolution which a material undergoes in a particular system within a year. The larger this value the greater the loss of material.

4) **Ecrit and Icrit** - The critical potential, and, critical current density which indicate the point at which passivation is initiated. Non-passivating materials do not display Ecrit and Icrit;

5) **Passive Range** - The potential range over which the sample effectively shows passivation. The larger this

Table.4.8. List of Potentiodynamic Test Results

SPEC. No.	Ecorr (mV)	Icorr ($\mu A/cm^2$)	(mpy)	r	Icrit ($\mu A/cm^2$)	Ecrit (mV)	Passive Range (mV)
M41	-442.3	31.4	8.61	1	217.6	-363	998
M42	-448.1	17.1	3.89	1	146.7	-344	900
M43	-439.8	6.7	1.52	1	225.7	-323	956
M61	-431.8	6.4	1.45	1	91.1	-326	1112
M62	-456.5	22.4	5.08	1	86.7	-357	956
M63	-422.2	9.7	2.20	1	63.6	-315	922
MS1	-520.4	536.0	247.8	1	-	-	-
MS2	-519.2	819.6	379.0	1	-	-	-
MS3	-523.1	1022	472.5	1	-	-	-
E41	-421.1	11.9	2.69	0.99	160.5	-319	918
E42	-424.7	10.4	2.37	0.99	290.0	-306	914
E43	-413.4	12.9	2.94	1	158.5	-318	916
E61	-423.8	14.5	3.30	1	190.0	-327	937
E62	-404.5	10.4	2.37	0.99	54.7	-300	850
E63	-389.6	4.8	1.09	1	19.7	-218	758
EN1	-540.6	921.4	397.0	1	-	-	-
EN2	-536.8	887.6	356.4	1	-	-	-
EN3	-526.1	1022	472.5	0.99	-	-	-

r = Correlation coefficient for linear polarization;
Ecorr = Corrosion Potential; **Icorr** = Corrosion Current;
C.R. = Corrosion Rate;
mpy = milli-inches per year;
Icrit = Critical Current Density; **Ecrit** = Critical Potential;
MS4/6 = Mild steel samples treated for 4h or 6h;
E4/6 = EN9 steel samples treated for 4h or 6h;
MS/EN = Uncoated Mild steel or EN9 steel samples.

range, the more corrosion resistant the material over a larger potential range implying that corrosion of the material is more unlikely to occur within a given system. Non-passivating materials do not display a passive range.

Icorr, Ecrit, and Icrit do not provide much information about the corrosion resistance of a material. However, the consistency of these values from one test to the next is an indication of the reproducibility of the test results. The potentiodynamic data from **Table.4.8** was then averaged. The average values are presented in **Table.4.9.**

Table.4.9. Average Potentiodynamic Test Data.

SUBSTRATE MATERIAL	E_{corr} (mV)	Icorr ($\mu A/cm^2$)	C.R. (mpy)	Passive Range (mV)
MS4	-443.4	18.42	4.67	951.3
MS6	-436.8	12.80	2.91	996.7
MS	-520.9	694.00	301.2	-
E4	-419.7	11.73	2.67	916.0
E6	-405.9	9.90	2.25	848.3
EN9	-534.5	943.67	408.6	-

Ecorr = Corrosion Potential;
C.R. = Corrosion Rate;
mpy = milli-inches per year;
MS4/6 = Mild steel samples treated for 4h or 6h;
E4/6 = EN9 steel samples treated for 4h or 6h.

The data presented in **Table.4.8** show that fairly consistent results were obtained for each group of samples. From the average values in **Table.4.8** it is clear that the corrosion rates of the coated substrate(2 to 5 mpy) were far lower than those for the uncoated material(200-400 mpy). Also, the VC coated samples all displayed considerable passive ranges(800-900 mV). There was also a significant increase in the values of Ecorr(-400 to -460 mV) for the coated samples compared to the uncoated samples(-500 to -550 mV) in this system.

Cyclic polarization(pitting) scans obtained with mild steel and EN9 steel specimens are shown in **Figure.4.32** and **Figure.4.33** respectively. Cyclic polarization tests also revealed that the behaviour of the VC coated substrate was significantly different to that of the uncoated base material. This is evident from **Figure.4.32** and **Figure.4.33** which compare the pitting behaviour of the two substrates. In both cases, the VC coated steel substrate displayed passivation similar to that observed in potentiodynamic tests whereas the uncoated material showed a uniform corrosion behaviour.

For the coated samples, the current density remained fairly constant till Ep, the pitting potential(which indicates the potential at which pitting is initiated), after which point it increased quite rapidly. The higher Ep, the greater the resistance of a material to pit initiation in a specific system. Upon reversal of the pitting scans at about 5000 $\mu A/cm^2$, it can be seen that the current density decreased almost on the same path along which it had increased. At Epp, the protection potential(the potential at which pits that have formed repassivate), the reverse scan intersects the forward scan. The closer Epp is to Ep the more likely it is that pits which have formed will repassivate thereby preventing the continuation of pitting.

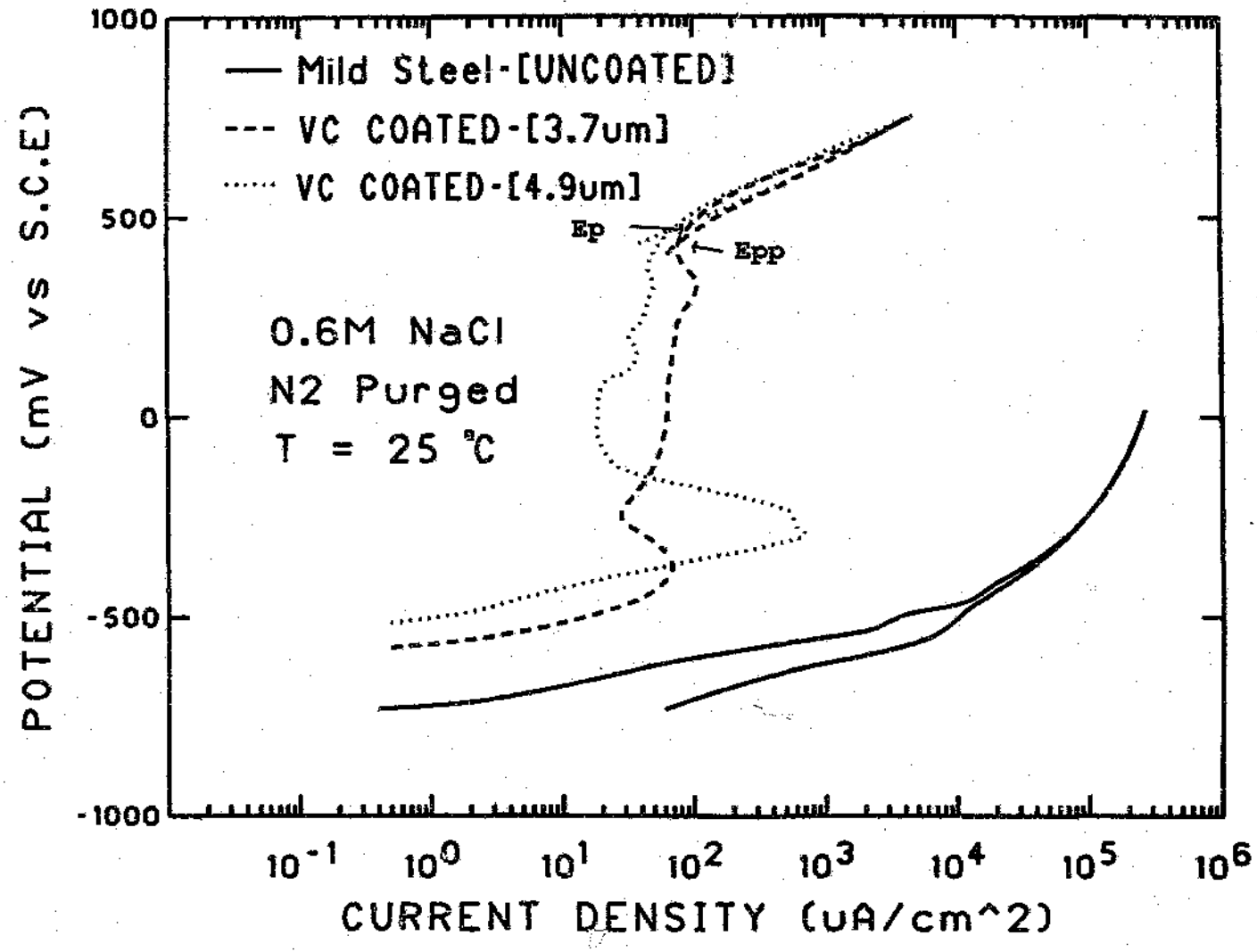


Figure.4.32. Typical cyclic polarization curves for mild steel samples.

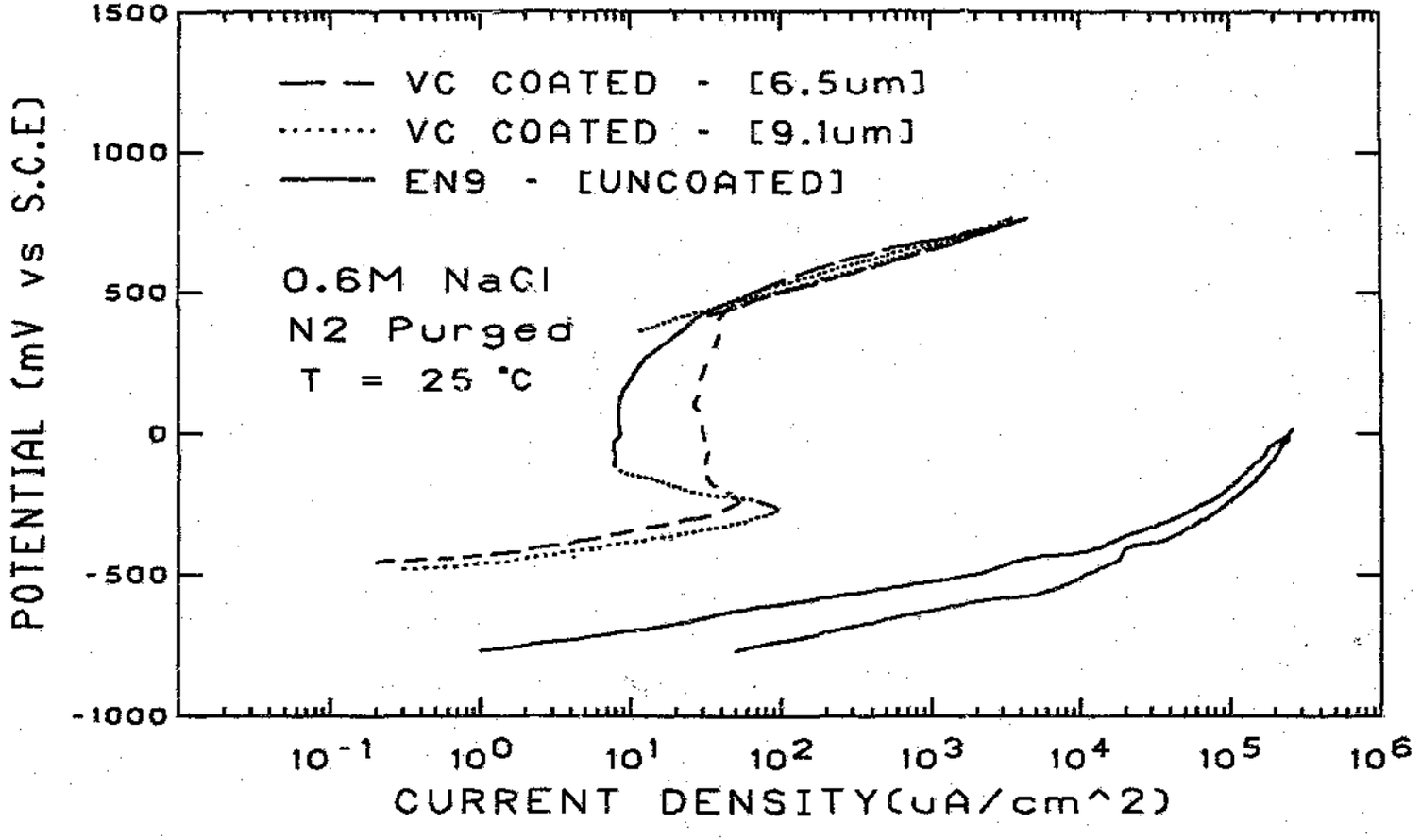


Figure.4.33. Typical cyclic polarization curves for EN9 steel samples.

Thus it appears that the coated samples were able to repassivate pits which had formed on the surface. It should be noted also, that the coated samples also showed a large passive range before pitting was initiated at Ep. As with the potentiodynamic data, the cyclic polarization curve obtained from each sample was used to extract relevant corrosion data. In this case, the values of interest were as follows[79,80].

1) Ecorr and Icorr;

2) **Ep** - The pitting potential which is the potential at which pitting is initiated. The higher this value the more resistant a material is to pitting attack within a specific system.

3) **Epp** - The protection potential which denotes the potential at which pits repassivate. In this respect, it is clear that the closer this potential is to Epit, the greater the likelihood of pit repassivation.

3) **Passive Range** - Similar to that evaluated from potentiodynamic testing, except that the test conditions used here were different. A large passive range in this case signifies a decrease in the chances of pit initiation.

The pitting test data are listed in **Table.4.10** where it can be seen that the results obtained for each group of specimens are quite consistent. **Table.4.11** lists the average values calculated from **Table.4.10**. It is evident from the average values that the coated samples had large passive ranges. The uncoated specimens did not display any significant corrosion behaviour since plain carbon steels are not susceptible to localized corrosion.

Table.4.10. List of Cyclic Polarization Test Results

SPEC. No.	Ecorr (mV)	Icorr ($\mu A/cm^2$)	Ep (mV)	Passive Range (mV)
M41	-535	0.34	390	801
M42	-575	1.55	414	833
M43	-535	0.50	421	785
M61	-479	0.34	406	737
M62	-513	0.47	436	729
M63	-472	0.14	397	755
M[illegible]	-732	0.39	-	-
E41	-510	0.55	483	781
E42	-449	0.84	440	837
E43	-457	0.24	420	709
E61	-533	0.13	416	833
E62	-480	0.29	421	793
E63	-515	0.37	442	729
EN3	-759	1.20	-	-

Ep = Pitting potential;
M4/6 = Mild steel samples treated for 4h or 6h;
E4/6 = EN9 steel samples treated for 4h or 6h;
MS/EN = Uncoated mild steel or EN9 steel samples.

Table.4.11. Average Results from Pitting Tests.

SUBSTRATE MATERIAL	Ecorr (mV)	Ep (mV)	Passive Range (mV)
MS4	-548.3	408.3	806.3
MS6	-488.0	413.0	740.3
MS	-732	-	-
E4	-472.0	447.7	775.7
E6	-509.3	426.3	785.0
EN9	-759	-	-

The average corrosion rates for coated and uncoated samples were plotted against the sample type in **Figure.4.34.** The remarkable reduction in corrosion rate of VC coated samples is clear from this figure.

4.4.1. Appearance of Corrosion Surfaces

Electron microscopy of corroded samples highlighted several important points regarding the response of the VC coated specimens to the corrosive media. The appearance of the corroded surface of a VC coated steel sample after potentiodynamic testing is shown in **Figure.4.35.** The appearance of a coated specimen after a pitting test is shown in **Figure.4.36.** It must be pointed out that little difference was found between the appearance of coated mild steel or EN9 steel samples after either potentiodynamic or cyclic polarization tests. The photomicrographs presented

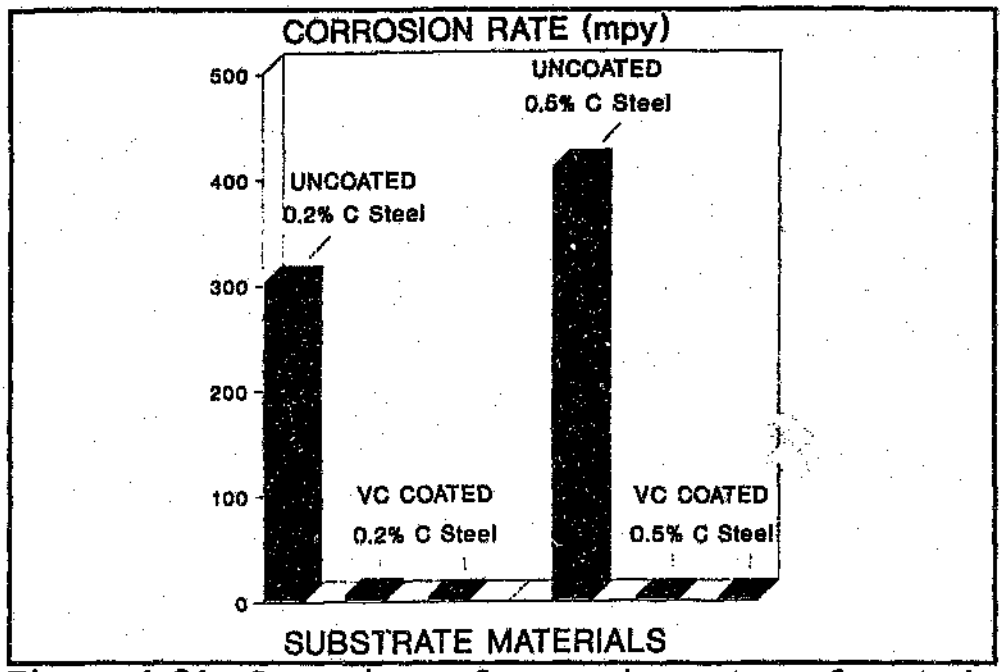


Figure.4.34. Comparison of corrosion rates of coated and uncoated substrate.

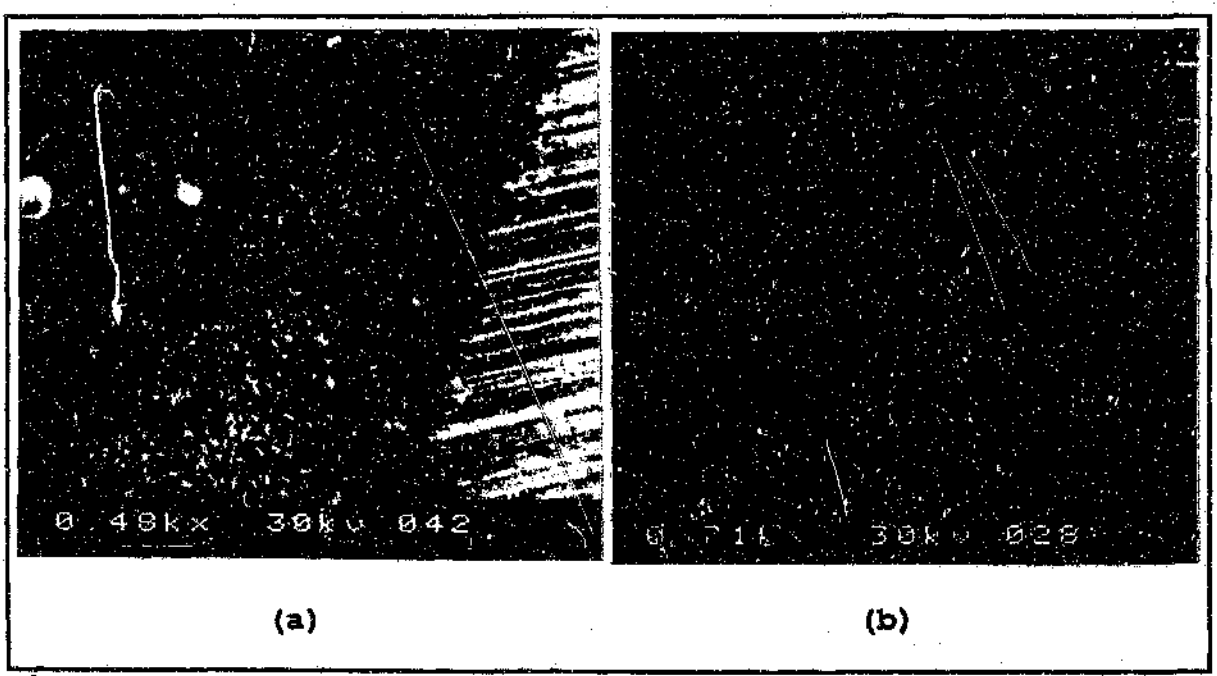
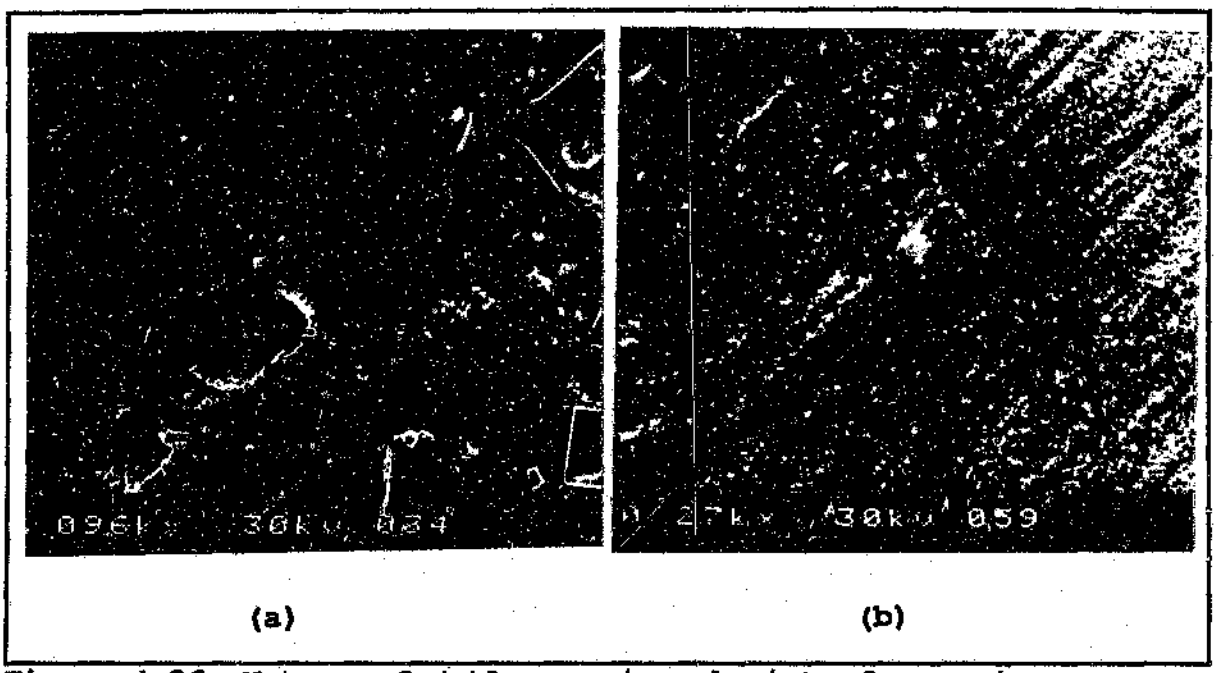


Figure.4.35. Nature of (a) lacquer/sample interface and (b) general surface corrosion of coated steel sample after potentiodynamic test.



(a) (b)

Figure.4.36. Nature of (a)Lacquer/sample interface and (b) General surface corrosion of coated steel sample after pitting test.

The photomicrographs presented here give an overview of the corroded surfaces observed. In both **Figure.4.35.(a)** and **Figure.4.36.(a)**, the lacquer/sample interface can be seen. These figures show that penetration by the corrosive media occurred between the lacquer/ sample interface, more so in the case of the potentiodynamic test sample. As mentioned previously, such penetration usually promotes the occurrence of crevicing at the lacquer/sample interface. Some NaCl crystals are evident on the surface of the specimen in **Figure.4.36.(a)**.

Figure.4.35.(b) and **Figure.4.36.(b)** indicate the difference between the two types of corrosion surfaces more clearly. It is clear from these micrographs that the coating had undergone complete dissolution in the potentiodynamic test

samples. By contrast, the VC coating still remained intact on pitting test samples. A striking feature in the case of the potentiodynamic test sample were the grooves on the corrosion surface running parallel to each other. These grooves are the marks caused by grinding of the specimen surface prior to coating. This contrasts with the appearance of the pitted surface which still had the coating intact. Comparing these two corrosion surfaces with that of the uncoated steel substrate which is shown in **Figure.4.37**, there was a substantial difference. As can be seen, the uncoated steel substrate had undergone severe corrosion in both potentiodynamic and pitting tests.

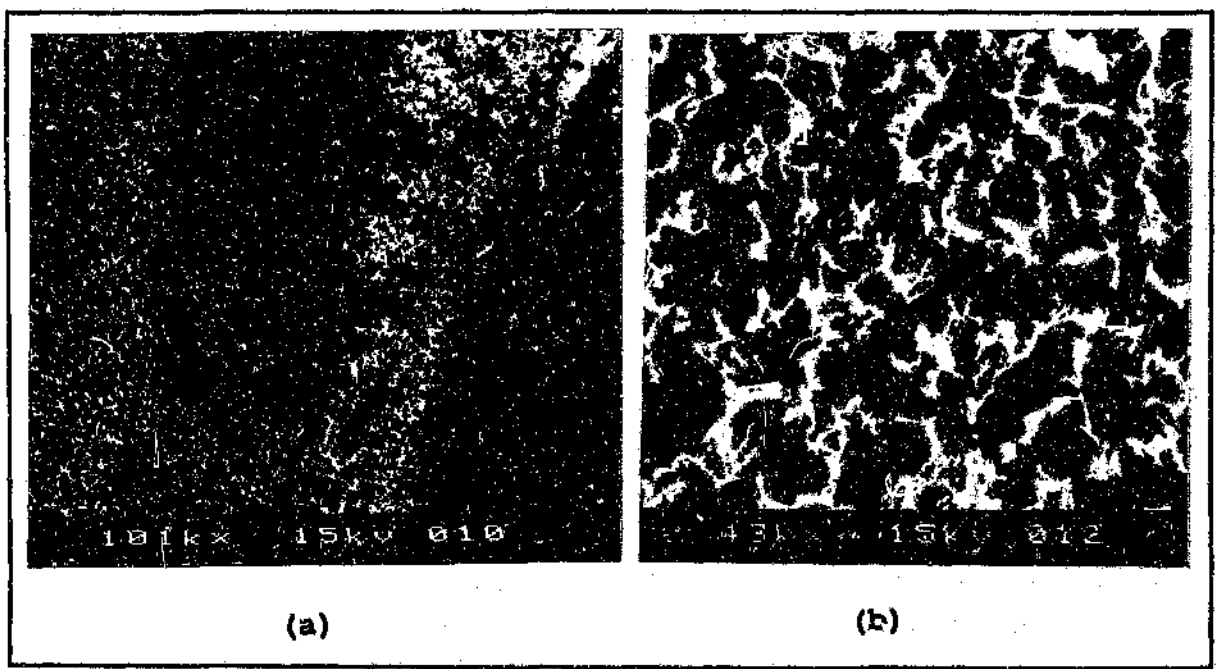


Figure.4.37. Extensive corrosion of uncoated steel substrate: (a) Lacquer/sample interface (b) General surface corrosion.

4.5. Treatment of Tool Steels

The composition of the tool steels in the as-received condition is shown in **Table.4.12.** For comparison purposes, the nominal composition of these steels is also listed in **Table.4.12.** The hardness of the as-received materials is shown in **Table.4.13.** It can be seen that the composition of the as-received materials compared well with their nominal compositions. The carbon content of the D3 tool steel was however markedly lower than the nominal value. It is clear from these values that the materials were in the annealed condition. Further evidence of the initial condition of the tool steels is given by their microstructures as shown in the **Appendix.A.3.** These consisted of alloy carbides in a matrix of ferrite, hence the very low hardness. The orientation of the eutectic carbides particles indicated that the bulk materials had been worked. This was also evident from the cavities associated with coarse eutectic carbide particles in the D2 and D3 steels.

In the first test, two samples of each tool steel were treated for 3h and 6h respectively in a 10% V_2O_5 plus 5% Al bath at 950°C. The average coating thickness on these samples was evaluated and is plotted against treatment time in **Figure.4.38.** Included in **Figure.4.38** are the carbon contents of the various tool steels. The coatings produced on the D2 and D3 steels which had the highest carbon contents were the thickest. As expected, thinner coatings were formed on samples of the H series of steels apparently due to their lower carbon contents. The coating thickness on the M2 steel was surprisingly low despite the high carbon content(1.04%) of this steel.

To determine how substrate carbon content had influenced coating thickness, the average coating thickness was

Table.4.12. Composition of Tool steels.

EL.	TOOLSTEEL									
	D2		D3		H13		H21		M2	
	N	S	N	S	N	S	N	S	N	S
C	1.5	1.46	2.25	1.69	0.3	0.37	0.3	0.41	0.8 to 1.5	1.04
Cr	12	14.05	12	15.05	5.0	5.60	3.5	3.04	4.3	4.56
Mo	1.0	0.70	-	0.18	1.5	1.23	-	0.22	3-9	1.23
Ni	-	0.37	-	0.3	-	0.38	-	0.22	-	0.34
Mn	-	0.34	-	0.27	-	0.45	-	0.37	-	0.37
Si	-	0.62	-	0.47	-	1.27	-	0.42	-	0.68
V	-	NA	-	NA	1.0	NA	-	NA	1-3	NA
W	-	NA	-	NA	-	NA	9	NA	1-7	NA
Co	-	NA	-	NA	-	NA	-	NA	5-12	NA

EL. = Element; **N** = Nominal Composition;
S = Spark analyses; **NA** = Not analysed.

Table.4.13. Hardness of As-Received Tool Steels.

MATERIAL	AVERAGE HARDNESS (HV10)
D2	247
D3	224
H13	220
H21	226
M2	249

plotted against carbon content (**Figure.4.39**). The two lines shown correspond to the two treatment times, ie. 3h and 6h. Included in **Figure.4.39** are the thickness values obtained on the 0.2% C and 0.5% C steels under similar treatment conditions. This graph clearly shows an increase in coating thickness with carbon content.

In the second treatment done on the tool steels, both annealed, and, hardened and tempered samples were coated to compare the coating thicknesses produced on either sample type. The microstructures of the hardened and tempered tool steels are shown in the micrographs of **Appendix.A.3**. The structure of all the heat treated steels consisted of alloy carbides in a tempered martensite matrix, except that of the H13 steel which appeared to have been inadequately hardened. The hardnesses of the tool steels in this condition are shown in **Table.4.14** from which it can be seen that all the steels except the H13 steel had been adequately hardened and tempered. The hardness of the H13 steel had increased only slightly above its initial value (**Table.4.13**). This steel was not coated.

Table.4.14. Hardness of Hardened and Tempered Tool Steels.

MATERIAL	AVERAGE HARDNESS (HV10)
D2	629
D3	590
H13	294
H21	433
M2	563

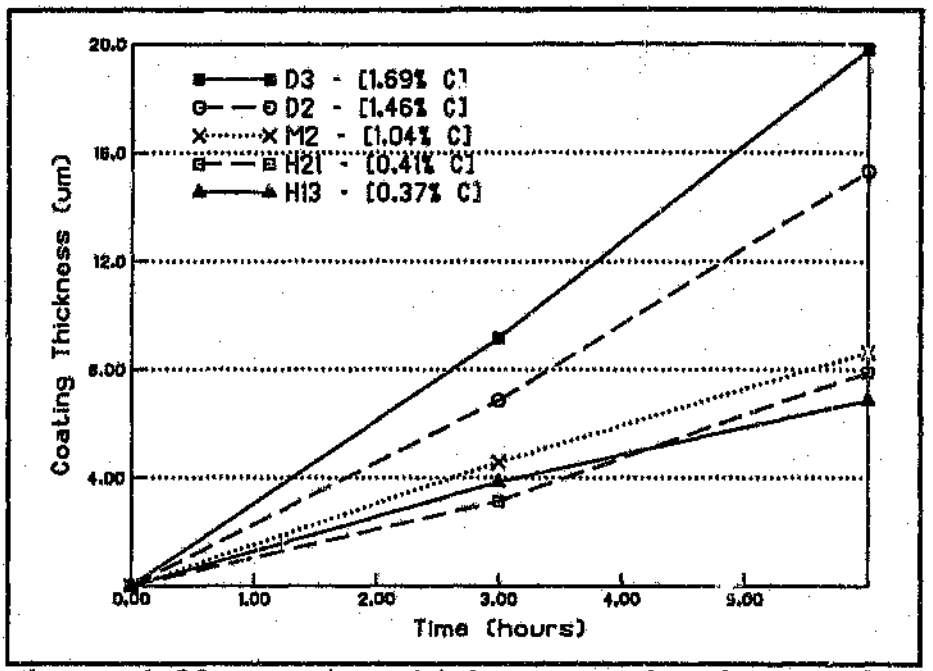


Figure.4.38. Coating thickness produced on tool steels treated for 3h and 6h at 950°C.

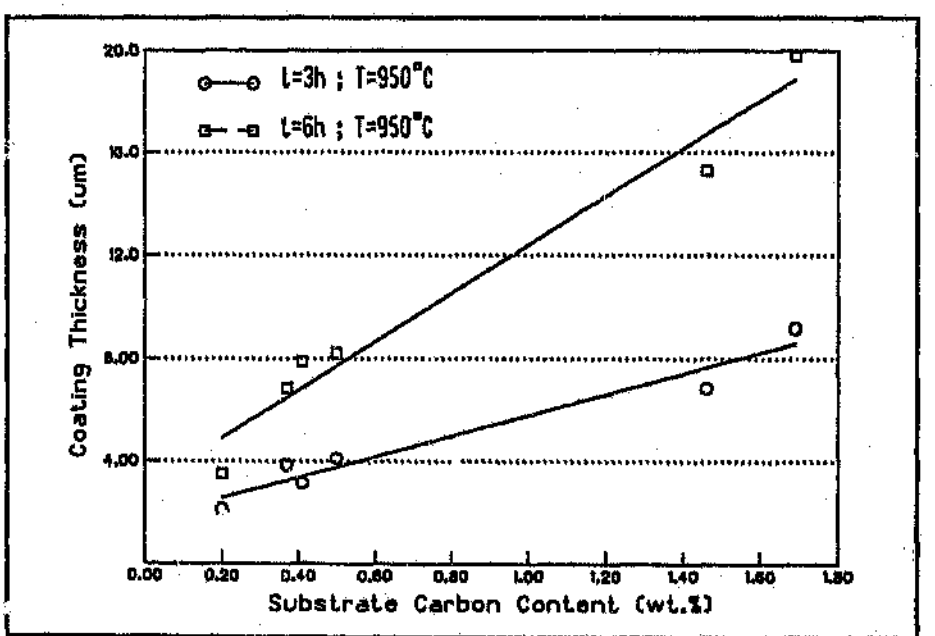


Figure.4.39. Variation in coating thickness with substrate carbon content for 3h and 6h treatment times at 950°C.

Evaluation of the coating thicknesses on the annealed, and, hardened and tempered samples, which were treated for 3h at 950°C in a 10% V_2O_5 and 5% Al bath produced the bar graph shown in **Figure.4.40.** It can be seen that the difference in coating thickness between annealed and hardened and tempered samples was similar for the four steels coated.

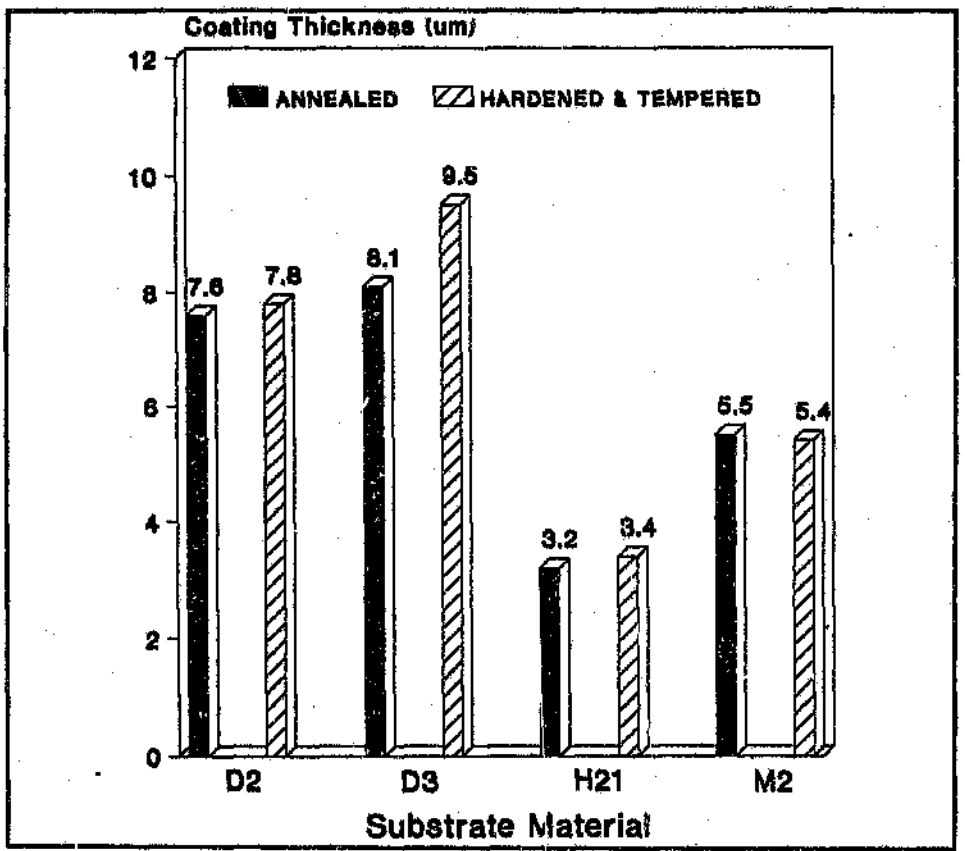


Figure.4.40. Comparison of average coating thicknesses produced on annealed and heat treated substrate treated for 3h at 950°C.

As pointed out previously, the core hardness of the VC coated toolsteel samples was measured in order to assess the extent to which these samples had hardened, since these samples were oil quenched or air-cooled after removal from the bath. The hardnesses of these samples in the untempered

Table.4.15. Core hardness of oil-quenched or air-cooled VC Coated Samples.

SAMPLE*	INITIAL CONDITION	TREATMENT TIME (hours)	QUENCHING MEDIUM	AVERAGE HARDNESS (HV10)
D2	AR	3	air	705
	AR	6	oil	699
	AR	3	oil	690
	HT	3	oil	729
D3	AR	3	air	850
	AR	6	oil	862
	AR	3	oil	770
	HT	3	oil	746
H13	AR	3	air	525
	AR	6	oil	548
	AR	3	oil	500
	HT	3	oil	483
H21	AR	3	air	416
	AR	6	oil	457
	AR	3	oil	493
	HT	3	oil	479
M2	AR	3	air	690
	AR	6	oil	694
	AR	3	oil	644
	HT	3	oil	642

* All samples treated in a 10% V_2O_5 and 5% Al bath at 950°C; **AR** = As-Received; **HT** = Hardened and Tempered.

condition are presented in **Table.4.15.** As can be seen, all the steels had hardened considerably although the treatment temperature used was 950°C, which is below the austenitizing temperature of all the tool steels except that of the D3 steel which is in the range 920-980°C. It is interesting to note therefore that the D3 steel had achieved the greatest hardness in all the cases shown. This was probably due to the relatively low stability of the carbides in this steel. Second to this was the D2 steel followed by the M2 steel and the H series steels. The hardness of the last three steels was low considering the fact that these values corresponded to the hardness of the untempered samples. This will be discussed in greater detail in Section.5.6.

The results of hardness tests on the cross section of the VC coating are presented in **Table.4.16.** The D2 and D3 steels were used for the cross-sectional tests since the thickest VC layers were produced on these steels. Because of the average thickness of the coating on the D3 steel, ie. 19.8 μm, hardness tests could be done at loads of 50 gf as well without damaging the layer.

Table.4.16. Hardness of VC Coatings on Tool steels.

SUBSTRATE MATERIAL	COATING HARDNESS			Average Layer Thickness (μm)
	HV0.01	HV0.025	HV0.05	
D2	2834	2639	-	15.3
D3	3105	2520	2046	19.8

4.5.1. Microstructure of VC Coated Tool Steels

The micrographs in **Figures 4.41.(a)-(e)** show the appearance of the VC layer on the D2, D3, H13, H21, and, M2 tool steels respectively. These micrographs illustrate the uniformity of the VC coating which can be achieved with this process. In addition, the coating appears to be dense in all cases. The roughness of those surfaces which were not ground prior to coating appeared to be reduced by the VC coating (**Figure.4.41.(d)**). The difference in coating thickness shown in these micrographs is also quite marked.

The microstructure of the substrate below the carbide layer varied for the different tool steels. The VC coated D2 and D3 steels both contained large alloy carbides in the matrix below the VC layer. The directional orientation of the carbides, as pointed out earlier, was quite evident. There was no evidence of decarburization below the VC coating in either steel. The H13 and H21 substrates which contain tiny carbide precipitates - not easily seen at the magnifications used here - had decarburized directly below the carbide layer (**Figure.4.41.(c) and (d)**). This decarburized zone(light area) consisted mainly of ferrite grains. Below the decarburized zone the microstructure comprised tiny carbide precipitates in what seemed to be a martensitic matrix. The VC coated M2 steel showed little evidence of decarburization with small spherical carbide precipitates visible in the matrix.

The salient microstructural features observed with respect to the coated samples are presented below. The formation of the carbide layer around the corner of a D2 steel is shown in **Figure.4.42.(a)**. The appearance of the inside of a VC coated 3mm hole which was drilled through a D3 steel sample is shown in **Figure.4.42.(b)**. The uniformity and continuity

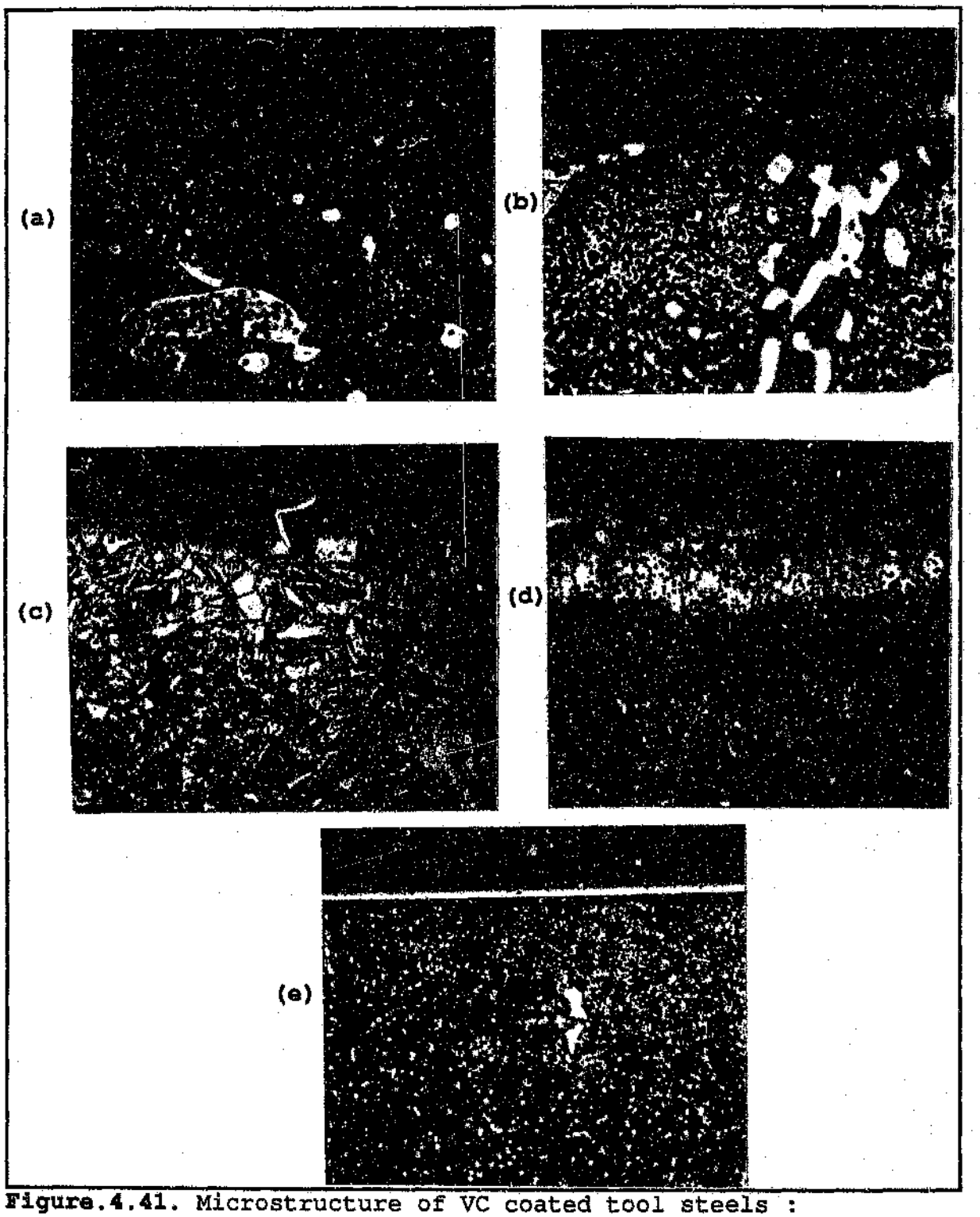


Figure.4.41. Microstructure of VC coated tool steels :
(a) D2[400X] (b) D3[1000X] (c) H13[400X]
(d) H21[1000X] (e) M2[400X]. Etched nital.

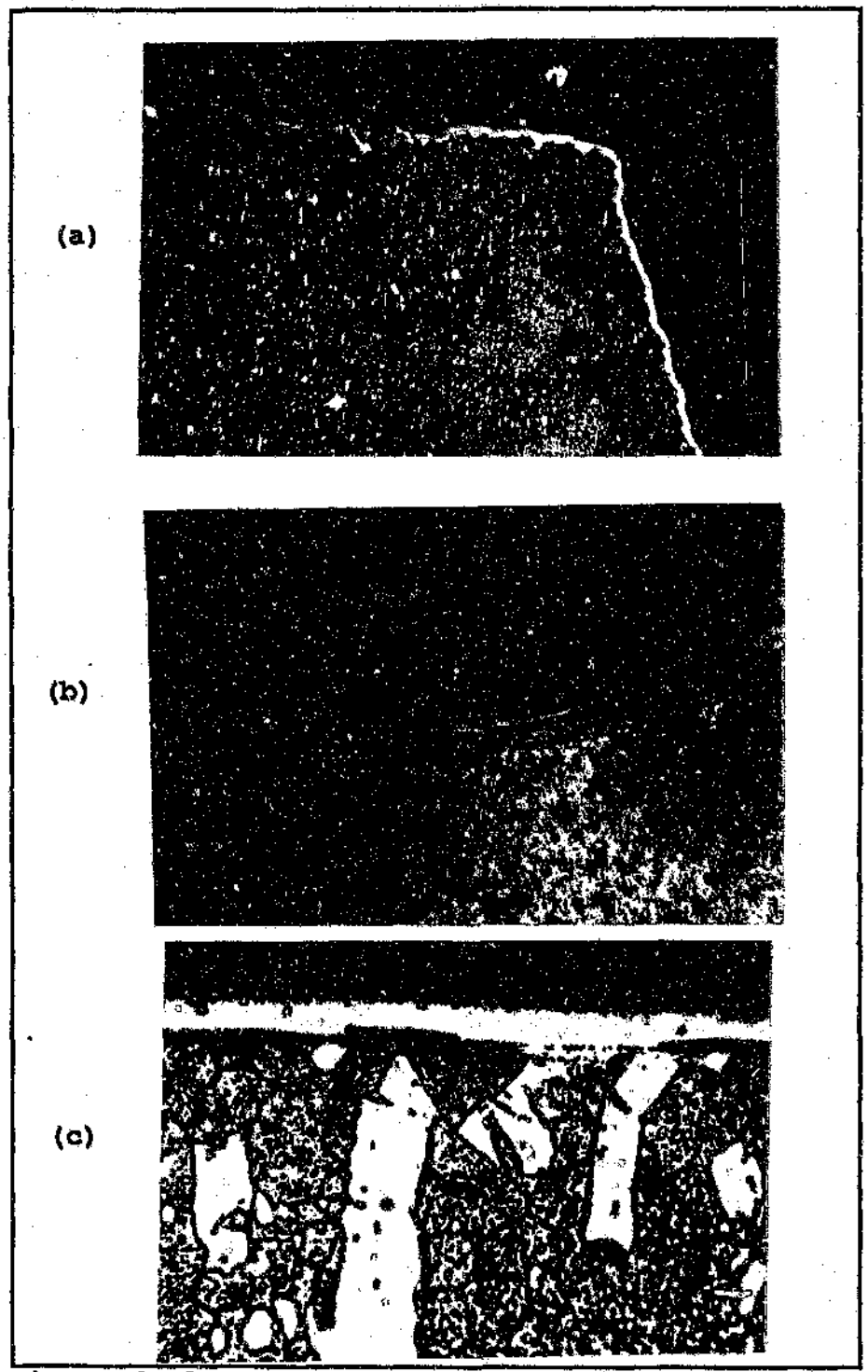


Figure.4.42. Appearance of VC coating (a)round corner[200X] (b)inside a hole[200X] (c)on D2 toolsteel[1000X]. Etched nital.

of the VC coating is clear. **Figure.4.42.(c)** highlights an interesting feature with respect to the way the coating grows. It appears from this figure that carbides at the surface of the substrate material tend to be "consumed" by the growing carbide layer. This is probably the reason why there is no apparent decarburization of steels containing eutectic carbide particles.

4.6. Problem Areas and Solutions

4.6.1. Method of Immersion of Samples in the Melt

Among the various experimental problems encountered, one of the first was the method by which samples are suspended in the borax melt. As discussed in Section 4.1, it was found that oxidation occurred in molten borax baths, especially those containing no aluminium. Samples immersed in such baths showed weight loss consistent with oxidation effects after removal from the bath as shown in **Figure.4.43.** From **Figure.4.26** it could be seen that oxidation occurs to a large extent at the surface of the melt. The suspension of samples in the borax melt by means of wire proved ineffective since the wires oxidised at the melt/air interface causing them to break off.

A variety of steel wires were tried with no success. The use of monel wire or kanthal wire which have high oxidation resistance also proved ineffective. To overcome this problem, a frame(**Figure.4.44**) was made from 316 stainless steel. This frame was then submerged below the surface of the melt thereby avoiding the oxidation effects which occur at the surface. Samples could be hung with wire on the frame and the entire frame then submerged. Using this technique, ordinary mild steel wire could be used to suspend samples in the bath without any oxidation taking place since the entire workpiece was placed below the surface of the melt.

An exception to this method had to be made in tests where samples were removed one at a time at set time intervals. In this case, each sample was hung on a 316 stainless steel rod. The rods (diameter = 6mm) were then supported by means



Figure.4.43. Oxidation of steel sample.

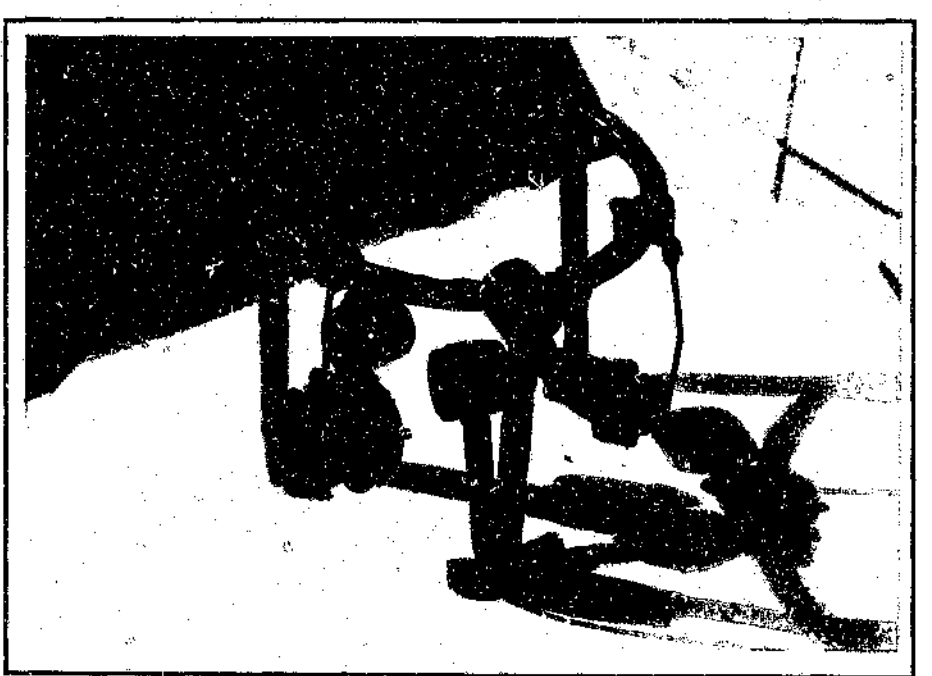


Figure.4.44. Immersion of samples using a frame.

of a cross bar made of the same material. Samples could then be removed individually as required. However, after a number of tests new rods had to be used as the old rods oxidised excessively in the region of the melt/air interface.

4.6.2. Cleaning of Samples after Treatment

One of the problems encountered with treating articles using salt bath processes is the cleaning of samples after treatment. This arises mainly because of the salt which remains attached to treated articles. As such, an appropriate cleaning procedure is required. In the case of samples treated in molten borax baths, quite a large amount of salt can remain attached to treated articles. This is illustrated in **Figure.4.45.(a)**. However, articles treated by this process can be easily cleaned(**Figure.4.45.(b)**). This is achieved by immersing the treated article in boiling water to dissolve adhering borax. An immersion time of about half an hour was adequate. Thereafter, the article is rinsed in cold water to wash off any residue and dried.

4.6.3. Cleaning of Steel Pots used for Baths

As was the case with cleaning treated samples, the stainless steel pots which were used as baths also had to be cleaned. Although a few pots were made, each pot had to be used a number of times since these pots were expensive to fabricate. For this reason, the pots had to be cleaned properly after each test. This was done by heating the old melt and dumping the molten borax into a steel bin. After the pot cooled down over a period of a few hours, the salt which remained attached to the inside of the container had to be removed. This was done by filling the metal pot with water and boiling.

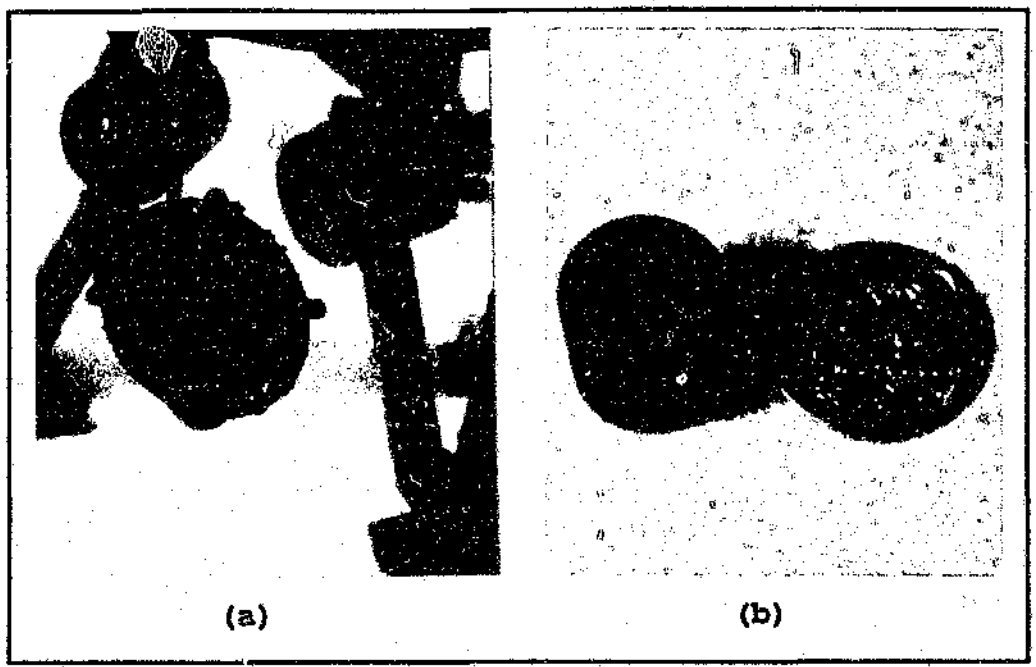


Figure.4.45. Appearance of treated samples (a) before (b) after cleaning.

The boiling procedure had to be repeated 2-3 times depending on the amount of salt remaining. Any remaining salt was removed by lightly grinding the inside surface of the pot. Oxide scale which formed above the level of salt in the bath, due to the high oxygen potential, tended to be a problem also. Grinding helped to remove some of this. Overall, the above procedure took a day to complete, but nonetheless rendered the pot fit for another melt.

4.6.4. Formation of Degenerate Carbide Layers

In the exploratory stages of this work, FeV was also used as one of the carbide-forming compounds added to the bath. It was found that samples treated in baths containing FeV only, produced what appeared to be a "two phase" coating in some cases. The microstructure of such a "two phase" coating is shown in **Figure.4.46.** It was not certain whether

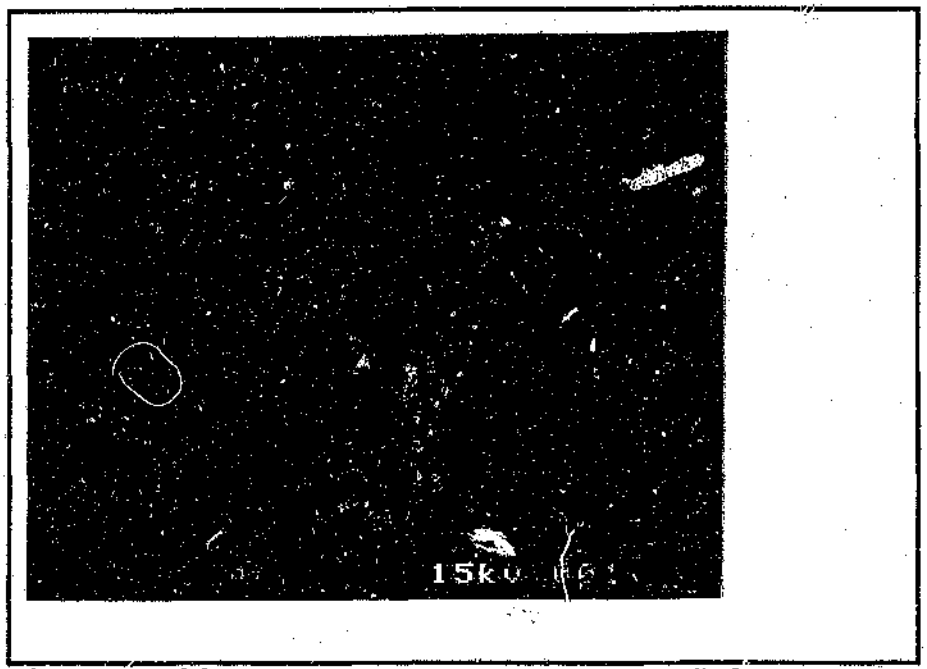


Figure.4.46. Appearance of "two phase" layer.

this layer was a carbide layer. To confirm this, qualitative and quantitative EDS analyses were performed on such layers. Spot analyses were done on the two areas of the layer, namely the light areas and the surrounding darker area to assess the difference in composition of the two areas. A typical spot analysis of the light area in the layer is shown in **Figure.4.47.** The high Fe peak and lower V peak in this spectrum indicated that the light area was Fe-rich. By contrast, spot analyses of the darker region surrounding these light patches produced the spectrum shown in **Figure.4.48** which indicates that the V content of this region was higher.

Quantitative EDS analyses done on such a "two phase" layer at the top, middle, and bottom of the layer, as well as in the substrate just below the carbide layer produced the results listed in **Table.4.17.** These results also show that the proportion of Fe in the "two phase" layers was excessively high. Compared to the Fe contents of carbide

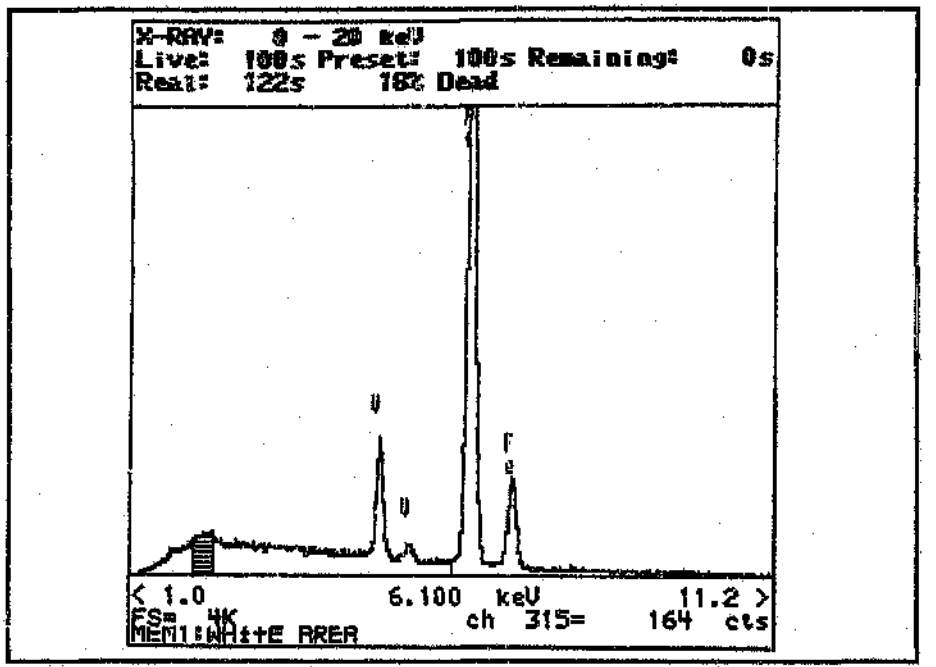


Figure.4.47. Typical EDS spectrum of light area using spot analyses.

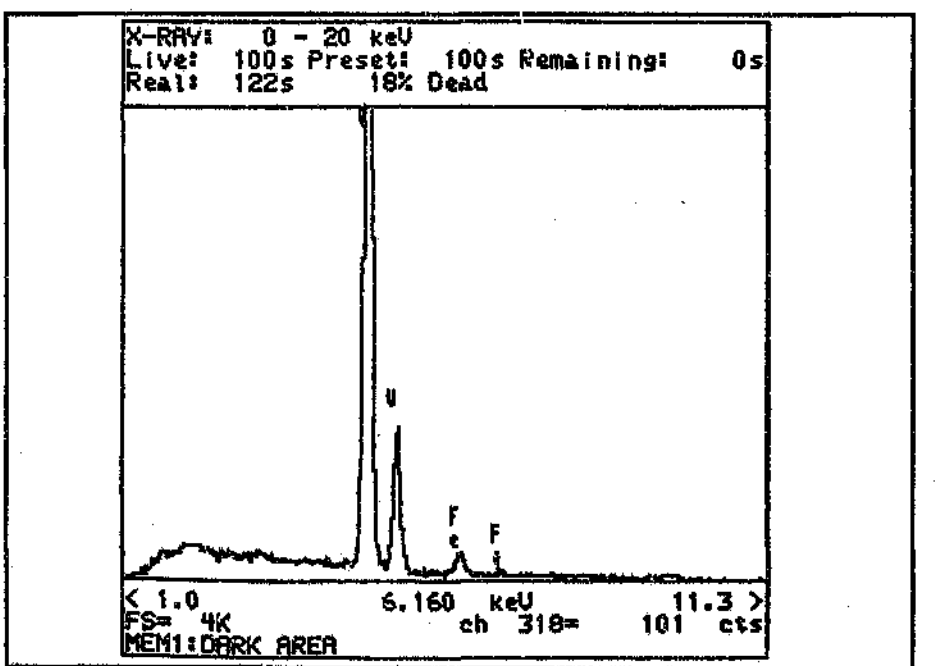


Figure.4.48. Typical EDS spectrum of darker area using spot analyses.

Table.4.17. Quantitative EDS of "Two phase" Layer from Surface to Substrate.

ELEMENT	ATOMIC PERCENT			
	TOP	MIDDLE	BOTTOM	SUBS.
V	92.47	68.60	76.60	2.93
Fe	7.53	31.40	22.69	96.16
Si	-	-	0.71	0.42
Mn	-	-	-	0.49
TOTAL	100.00	100.00	100.00	100.00

layers produced in V_2O_5 plus Al baths(Section.4.2.3), these proportions were excessively high. The reason for the formation of such layers was uncertain, but possible reasons are discussed in Section.5.6. However, it must be pointed out that these "two phase" layers were found to occur only on samples treated in baths containing FeV. In some cases, samples treated in FeV plus Al baths also produced a two phase layer, but less frequently. In this case, there seemed to be less of the Fe rich phase present. The problem appeared to be related to the use of FeV as the bath additive. This was one of the main reasons that the decision was made to perform a detailed study of V_2O_5 containing baths.

4.6.5. Spalling of Coated Samples

Another problem encountered was that of the spalling of the vanadium carbide layer on some coated samples. The

observation was made that the surface of coated samples became patchy soon after removal from the bath. This is illustrated in **Figure.4.49**. The lighter areas on the surface of the sample are the patches referred to here. Upon closer examination, it became evident that these patches were in fact areas where the carbide layer had spalled off. Electron microscopy provided further evidence that the carbide layer was spalling. Spalled samples were examined both on the surface and in cross-section to investigate the nature of this spalling.A number of photomicrographs are presented which provide some idea of the nature and extent of the spalling.

The surface of a spalled sample is shown in **Figure.4.50** which illustrates how the carbide layer spalled off. **Figure.4.51** and **Figure.4.52** are cross-sectional views of samples which displayed spalling indicating that the extent to which the carbide layer had broken off from the substrate varied, ie. the layer may be partially or completely detached from the substrate. Cracks propagating in the plane of the sample surface may initiate from the surface of the carbide layer, or, from the coating/ substrate interface. **Figure.4.53** is a close up view of a spalled area showing what appears to be cleavage planes (**Area 1**) within the spalled area. The appearance of this area compared to the smooth surface(**Area 2**) of the carbide layer suggests that spalling occurred by a brittle fracture mechanism.

Spalling was probably due to residual stress in the coating possibly due to differential contraction between the coating and substrate during cooling. Spalling occurred frequently on samples which were air-cooled after treatment. To overcome this problem samples were quenched after treatment and it was found that this alleviated the problem. This may be of significant benefit as far as coating and hardening of components are concerned. However,



Figure.4.49. Patchy appearance of spalled sample[10X].

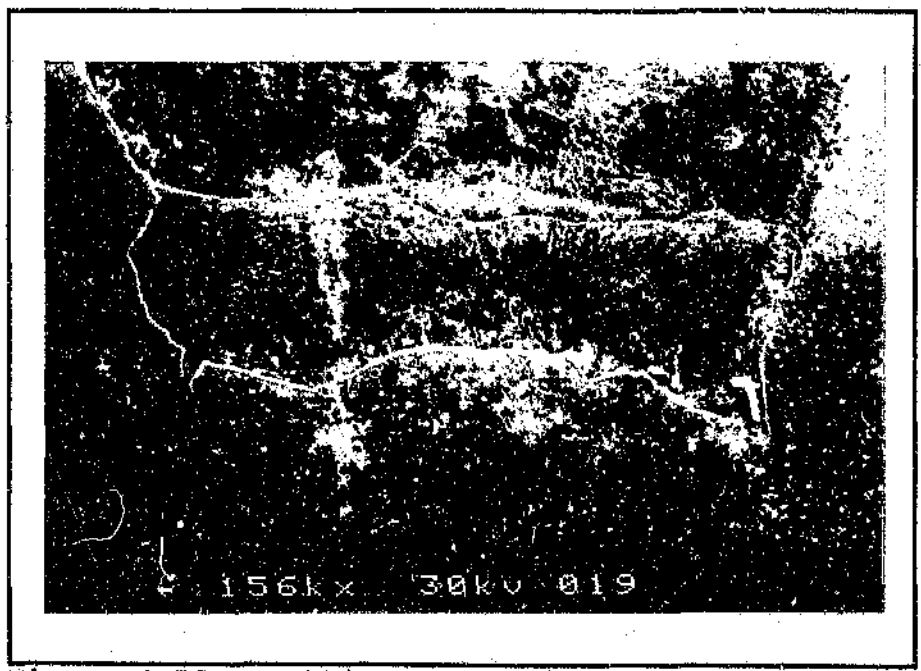


Figure.4.50. Spalling of carbide layer.

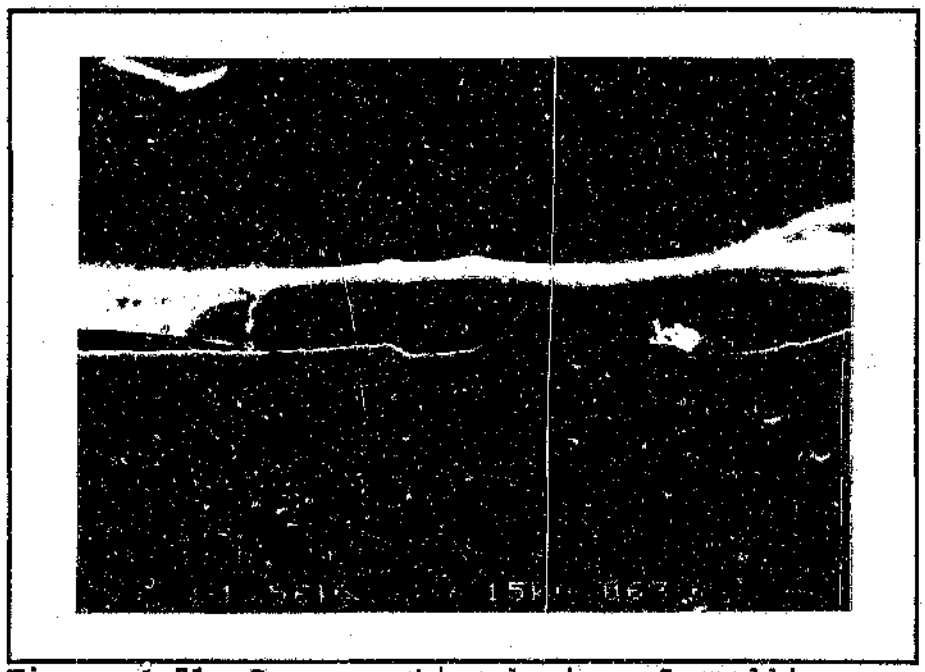


Figure.4.51. Cross-sectional view of spalling carbide layer typifying varying extent to which spalling occurred.

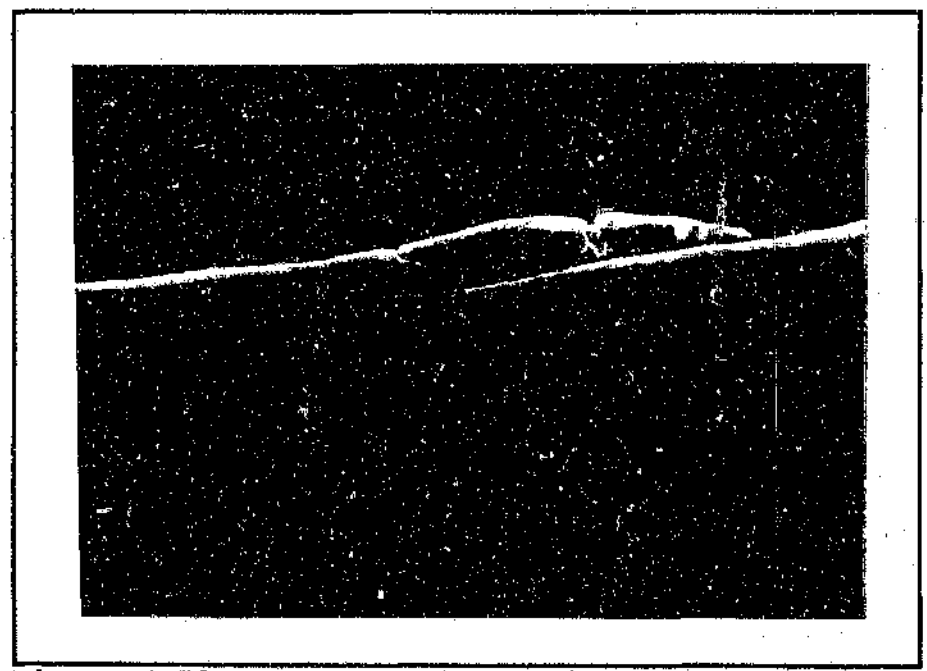


Figure.4.52. Cross-sectional view of spalled carbide layer.

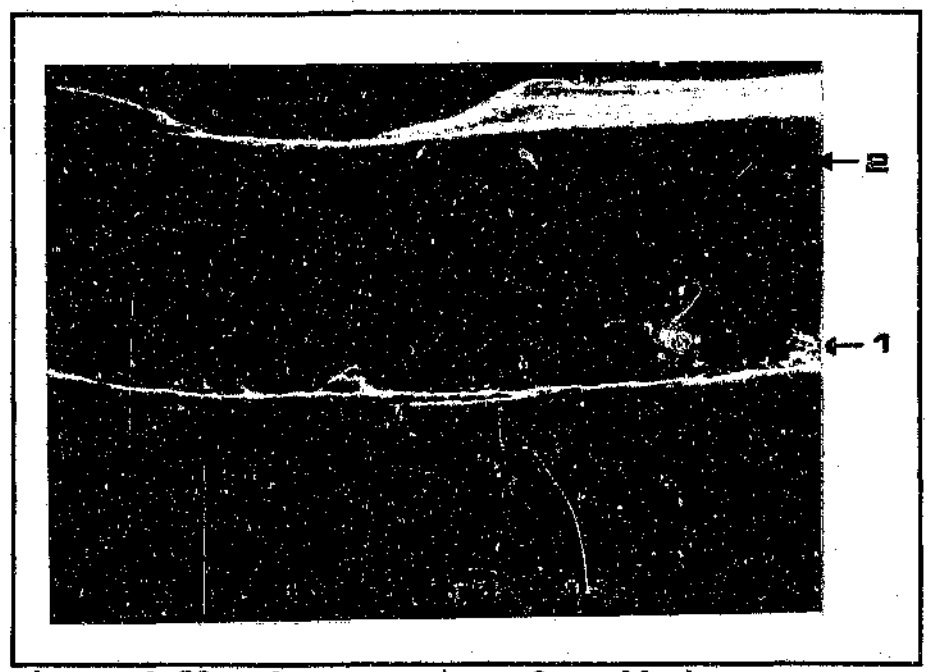


Figure.4.53. Close-up view of spalled area displaying apparent brittle fracture surface.

4.6.6. Quench Cracking of Treated Samples

Although quenching of treated specimens appeared to alleviate spalling, in many cases this caused cracking of specimens. A typical quench cracked sample is shown in **Figure.4.54.** The extent of such cracking can be seen to be the bath temperature may have to be regulated in order to bring treated components to their correct quenching temperature.quite severe. Cracks were found to initiate more easily from areas of high stress concentration, namely drilled holes and rough machined edges. Poor surface preparation of samples, especially at the edges also contributed to this problem. A detailed view of the crack which extended through the carbide layer is shown in **Figura.4.55.** Quenching samples in oil, instead of water, decreased the occurrence of quench cracking as expected.

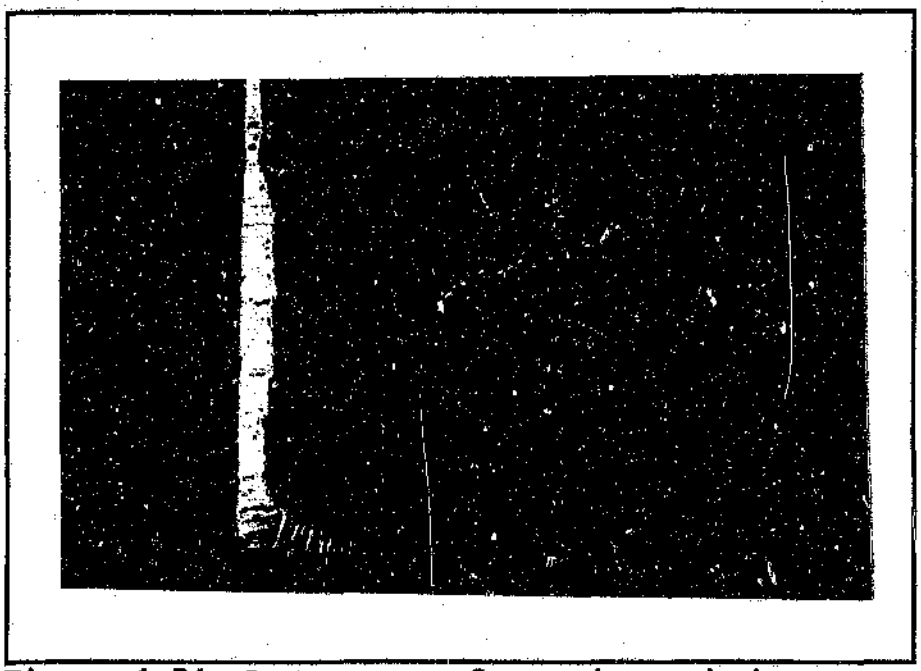


Figure.4.54. Appearance of quench cracked specimen[8X].

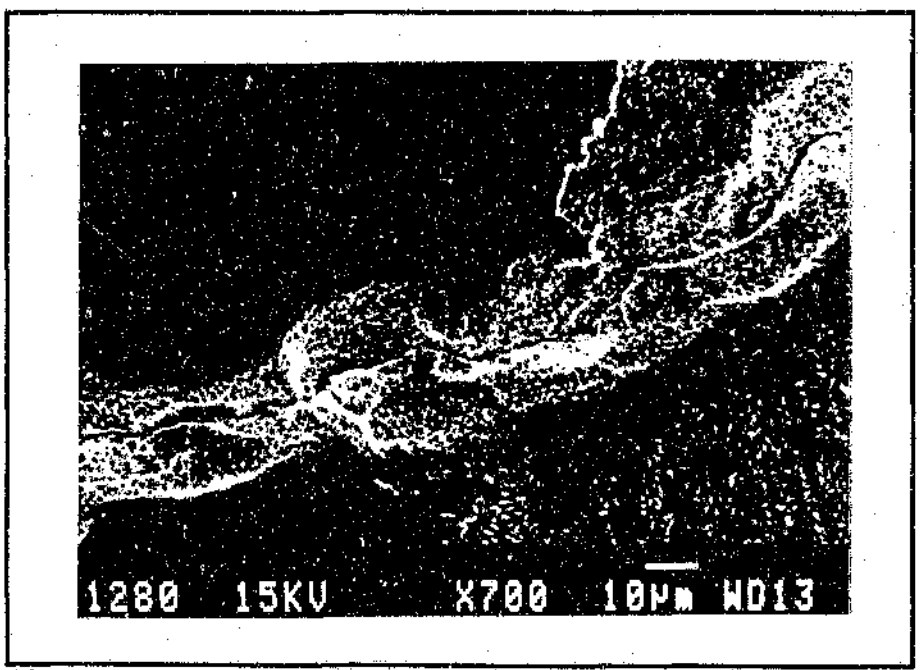


Figure.4.55. Extension of quench crack though carbide layer.

From this it is clear that the appropriate quenchant and quench temperatures have to be selected when treating articles. The problem of cracking is expected to be minimised with coated alloy or tool steels which do not require severe quenching for hardening.

4.6.7. Staining of Coated Samples

A more serious problem experienced was the appearance of black patches on the surface of coated samples which occurred quite often on treated samples. Dark "stains" on the surface of a sample are shown in **Figure.4.56**. "Staining" diminished the aesthetic appeal of coated specimens. Microscopy was carried out on samples to establish the nature of the "stains".

The appearance of a stained area at higher magnification is shown in **Figure.4.57**. Qualitative EDS analyses was also done on these areas producing the spectra such as the one shown in **Figure.4.58** which shows a high V peak typical of that obtained with the VC coating. From **Figure.4.57** and **Figure.4.58** it seems that these dark areas were in fact areas where the vanadium carbide layer had grown with a different morphology or orientation. The morphology of the "stained" area is shown in greater detail in **Figure.4.59**. Comparing this morphology to that observed normally (**Figure.4.8**), it can be seen that the carbide layer grew in cubic form or as lathes in the "stained" area.

The reason for the formation of these "stained" areas was not clear, although it seemed that these "stains" occurred more frequently on the edges of samples than on any other areas. Possible reasons for the formation of these "stains" will be discussed in Section.5.6.

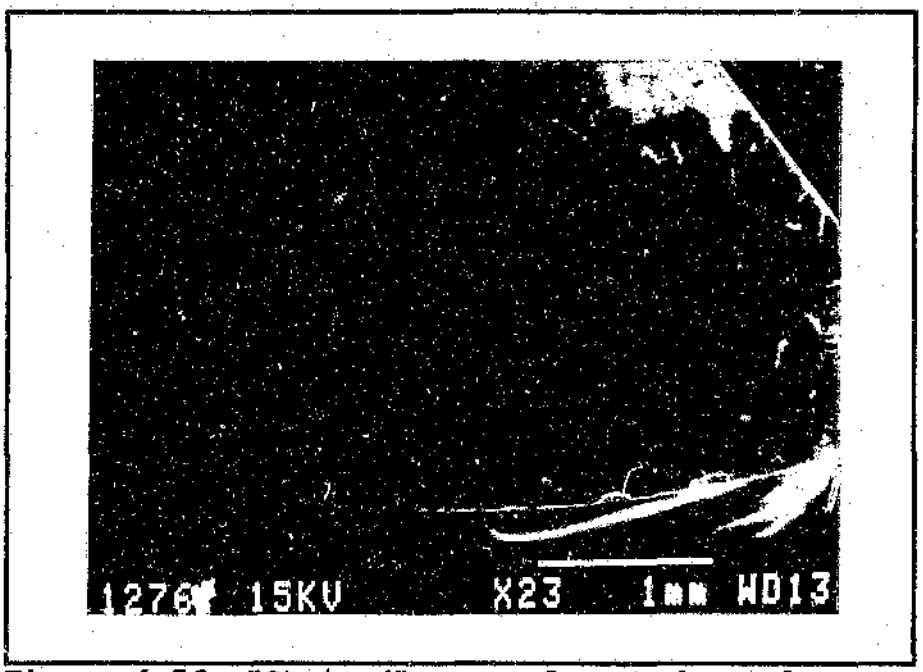


Figure.4.56. "Stained" area of coated sample.

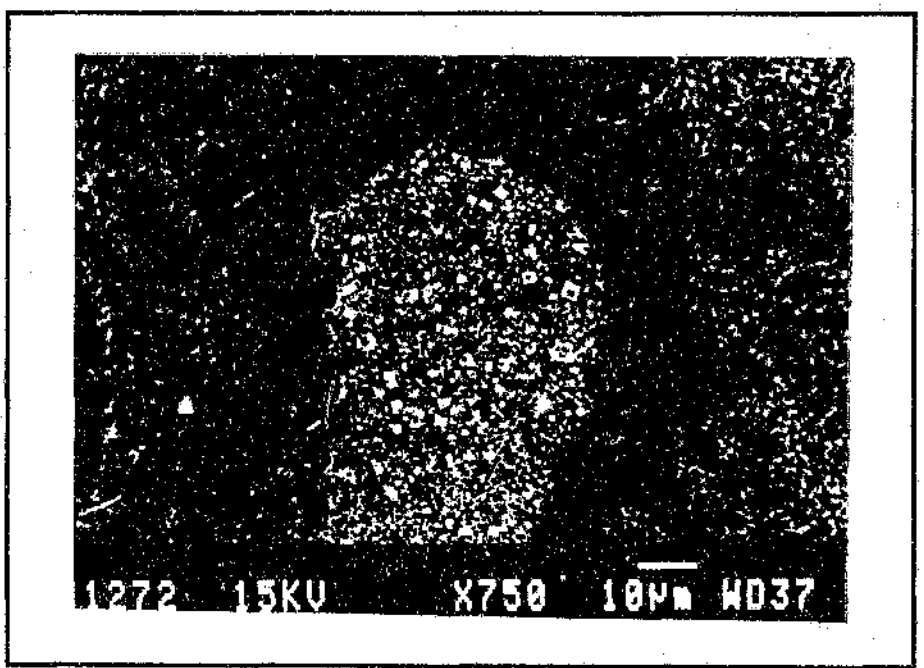


Figure.4.57. Morphology of carbide layer in "stained" areas.

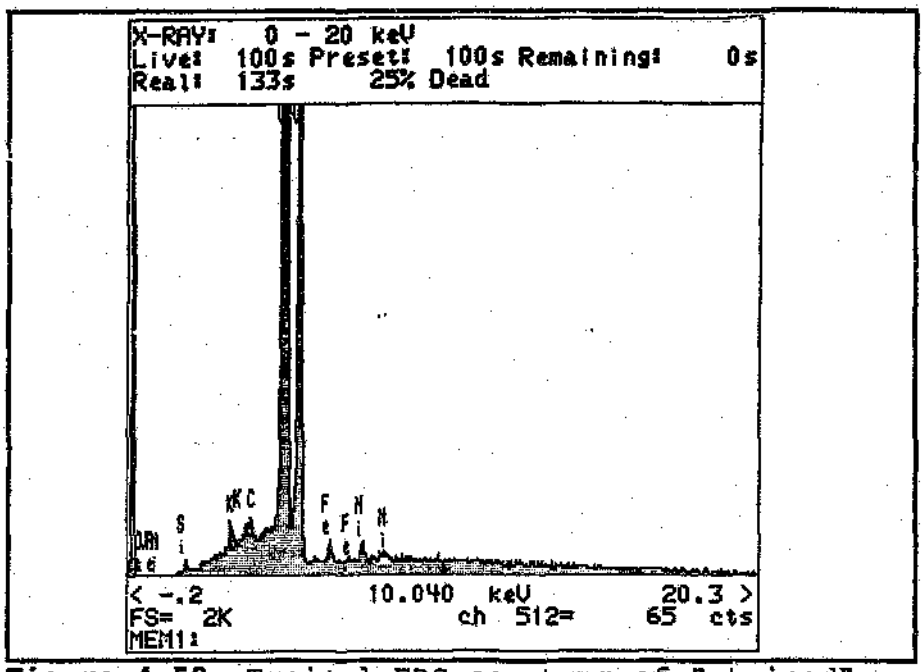


Figure.4.58. Typical EDS spectrum of "stained" area.

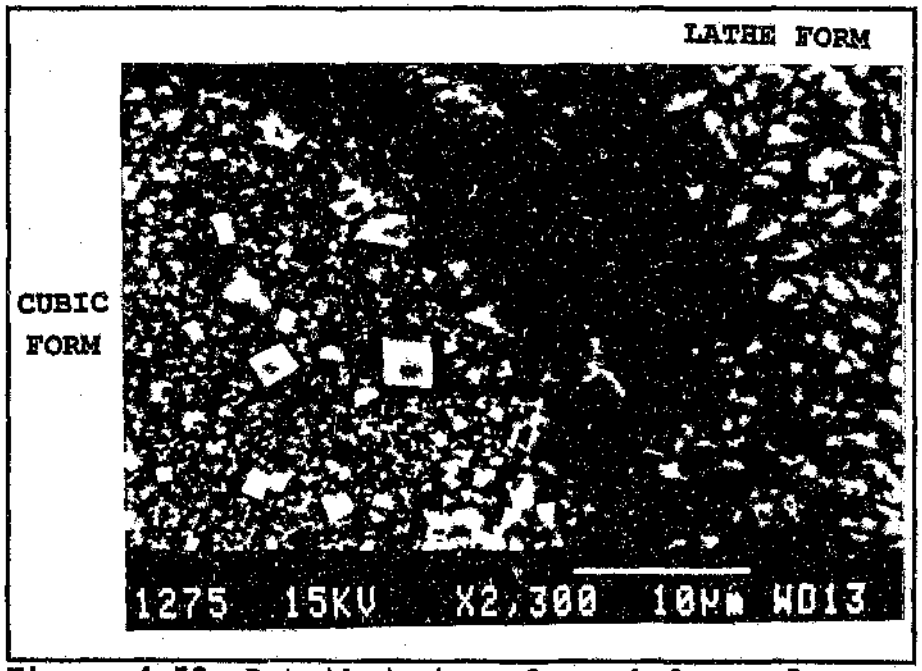


Figure.4.59. Detailed view of morphology of "stained" area.

4.6.8. Moisture in Borax

One of the less critical problems experienced was that of moisture in the borax. Using the hydrated form of the borax($Na_2B_4O_7.10H_2O$) it was found firstly, that the bath took longer(3-5 hours) to achieve the green colour which indicates that the bath is active. Secondly, the mass of borax weighed out had to be adjusted since about 40% of this mass comprised water which contributed to the measured weight. Upon melting this borax the level of the melt dropped to about a quarter of its initial value because the water component of the borax vaporised. Under these conditions, the level of the melt was too low to treat samples in the bath. It should be noted also that borax is hydroscopic and can exist in pentahydrate ($.5H_2O$) or decahydrate form.

5. DISCUSSION

5.1. Choosing between FeV and V_2O_5 in the bath

It was mentioned in Section.3.1 that in the as-received form, the FeV chunks were much harder to crush and pulverise than the V_2O_5 flakes. This was one of the reasons for deciding to study V_2O_5 containing baths in detail. Furthermore, the amount of carbon in the FeV(0.12% C - **Table.3.1**) was quite high compared to that in the V_2O_5 (0.015% C - **Table.3.2**). It was thought that this carbon could produce side reactions with other bath constituents. Of particular concern was the possibility that the carbon would react with Fe or V to form complex carbides in the melt. In so doing, the activity of the bath was likely to be affected.

The presence of Si(1%) and Al(1.6%) in the FeV could be regarded as beneficial since both of these elements are excellent deoxidising agents which could help prevent excessive oxidising conditions in the bath. Another noteworthy fact was the higher percentage of V(80.5%) in the ferro-alloy compared to the pentoxide(99.7% V_2O_5) which contained 56.4% V by mass suggesting that the ferro-alloy would be a more lucrative bath additive. However, the FeV did contain a larger amount of Fe(13.8%) and a fairly high percentage of unknown components(about 3%) unlike the V_2O_5(0.04% Fe; 0.059% unknown). Besides, the use of FeV did pose particular problems as discussed in Section.4.6.4.

5.2. Exploratory Tests

From **Table.4.1**, it can be seen that coatings could be

produced in baths containing borax and FeV only. By contrast, no coatings were formed in baths containing borax and V_2O_5 only. This suggested that the addition of FeV to the bath was sufficient to produce VC coatings in ambient atmosphere. However, it must be mentioned that in most cases, specimens treated in FeV baths did not display a coating. Instead, many of these specimens showed weight loss after removal from the bath(Section.4.6). This weight loss was attributed to oxidation effects occurring in the bath.

From exploratory work, it appeared that under certain circumstances, reducing conditions could exist in baths containing only borax and FeV. In the general case however, oxidising conditions seemed to prevail in such baths under ambient conditions. This appears to have been related to the size of the bath. Child et al.[26] pointed out that oxidation is very likely to occur in small baths (Section.2.5.3). It is interesting to note therefore that the largest bath in use(as at 1984) in Japan was 700mm in diameter and 150mm deep. It appears therefore that the oxidation observed in this study was due to the limited size of the bath(1.5kg of borax). Much of the early work patented by Arai[26] was done in small graphite crucibles and this probably prevented excessive oxidation. Child et al.[26] also state that baths heated under strongly oxidising conditions, eg. a gas-fired furnace, did not produce coatings. It seems therefore that the prevailing bath condition, ie. oxidising/reducing is critical to the formation of coatings.

It became obvious from exploratory work that bath conditions had to be well-controlled in order to achieve the conditions necessary for producing coatings. Attempts at maintaining a blanket of argon over the surface of FeV containing melts to reduce excessive oxidation proved

unsuccessful. By contrast, Child et al.[26] claim that VC coatings formed satisfactorily on carbon steels using the same approach. The reason for this discrepancy is not certain.

The finding that no coatings formed on steels treated in baths containing borax and V_2O_5 was consistent with the findings of other workers[26]. As shown, the addition of 5% Al to the bath in Test No.3(**Table.4.1**) rendered the bath active after about 10 hours(Test No.4). The fact that this bath contained V_2O_5 suggests that the Al acted as a reducing agent. This would confirm the claims by Arai[26] that V_2O_5-containing baths require reducing agents to produce carbide layers. This can be substantiated by referring to the diagram in **Figure.2.5.3** which shows that the free energy of formation of Al_2O_3 is much more negative than that of B_2O_3 or V_2O_5. It can therefore be expected that oxides of B or V will be reduced in the presence of Al in a borax bath. It is worth noting at the same time that the free energy of oxide formation of other carbide-forming elements, ie. Cr, Nb, Ta or Ti(in decreasing order), are also more positive than that of Al. This may imply that oxides of these elements could also be reduced in the presence of Al and thereby produce carbide layers. However, it should also be noted that the free energies of formation of the oxides of Cr, Nb, Ta and Ti are similar to that of B_2O_3. It was pointed out in Section.2.5.3 (**Figure.2.5.3**), elements with free energies of oxide formation which are more negative than B_2O_3, eg. Ti, tend to form a mixed layer of boride and carbide.

The activities of the FeV and V_2O_5 baths as compared in **Figure.4.2** were similar. A noteworthy feature of this graph is that the addition of Al to the FeV bath rendered this bath active in a short time period. The growth rate of the carbide layer in both baths, and, in the bath used in Test

No.2 (**Figure.4.1**) followed a parabolic relationship However, it has been shown from subsequent results that layer growth appears to follow a linear relationship. Both Arai and Child et al.[26] have presented similarly conflicting results (Section.2.5.3). They state that a parabolic growth pattern indicates that layer growth is controlled by the diffusion rate of carbon through the substrate and the existing carbide layer. A linear relationship points to reaction rate controlled growth where the growth of the carbide layer is limited by the rate at which reactions occur in the bath. Thus, layer growth is controlled by the supply of active species to the surface of the existing carbide layer. On this basis, an ideally conditioned bath is diffusion rate controlled since the supply of active species to the steel surface would not be the limiting factor. Both workers claim that many baths are reaction rate controlled given the fact that the baths age with time, thereby becoming less active. In this respect, the age of the bath, its composition and homogeneity, as well as operating temperature, can all be expected to influence the growth of the carbide layer.

It is interesting to note from Test No.4 (**Table.4.1**) that the bath remained active for a 20 hour period, producing a layer 4.6 μm thick on a 0.2% C steel specimen in 5 hours. Al was effective both in generating active conditions in the bath and maintaining this activity for a fairly long time period.

From the results of these preliminary tests, it was clear that bath conditions had to be accurately controlled, and, that Al was suitable as a reducing agent. For this reason, Al was included as a bath additive in subsequent studies.

5.3. Analyses of VC Coated Specimens

5.3.1. Microstructure of VC Coated Specimens

From the photomicrographs in Section.4.2.1, it can be seen that the VC coatings were uniform. Examination of the polished layer (**Figure.4.7**) revealed that the VC layers were fully dense. The nature of the coating/substrate interface indicated that the layer grew from the substrate reproducing the surface on which it formed. Given these characteristics, one could expect these coatings to have excellent adhesion properties.

The presence of large ferrite grains below the layer in the 0.2% C (**Figure.4.4**) steel was consistent with the formation of the layer and the original microstructure of the steel. The diffusion of carbon from the substrate to form the surface layer depleted the substrate of carbon and resulted in transformation to ferrite during cooling. Further in towards the core of this steel, the ferrite grains were finer and the amount of pearlite greater (**Figure.4.6.(b)**).

With the 0.5% C steel the substrate below the coating comprised mainly large pearlitic grains (**Figure.4.3**). In some cases, small areas of ferrite were found beneath the VC layer (**Figure.4.5**) suggesting that decarburization had occurred in these areas.

The extent of hardening shown indicated by **Figure.4.9** and **Figure.4.10** is encouraging as it suggests that hardening of coated steels could be achieved easily. The large pearlitic areas observed in the 0.5% C steel are the result of grain growth arising from the long treatment times used, ie. 3h

to 9h. Such coarsening of the microstructure would be detrimental to the toughness and impact strength of the steel. This is discussed in greater detail in Section.5.6.

5.3.2. Hardness of VC Coatings

It was shown in **Figure.4.10** that loads in excess of 10gf and 25gf caused breakage of the carbide layer or produced indentations which were larger than the coating thickness. Hardness values obtained with the 10gf and 25gf loads ranged between 2000 and 3000HV which compared well with values quoted by other workers[25,26], or, values quoted in literature for the bulk material[4]. It should be noted that values quoted here are averages and that in some cases values in excess of 3000HV were measured. As a measure of consistency, **Figure.4.11** showed that there was little variation obtained with the the two loads used. In most cases, higher values were recorded using the lower load as one would expect. Variations in the thickness of the coating in different areas were probably the reason for any large variations in measured values.

The hardness profiles of the coated air-cooled and oil-quenched 0.5% C steel substrates(**Figure.4.12**) showed that the hardened sample was harder throughout. The slightly higher hardness of the coating on the hardened substrate is interesting to note and suggests that quenching has a beneficial effect on the hardness of the coating. It may also be that the harder substrate affects the hardness obtained. Nonetheless, as expected, the hardness dropped dramatically once the coating thickness was exceeded unlike carburised or nitrided components where the hardness usually varies more gradually with distance. The "composite" hardness values measured(**Figure.4.13**) were higher for the harder substrates but similar coating

thicknesses as might have been expected. For all three cases shown, there was a characteristic drop in hardness when the load was increased from 300gf to 500gf indicating that with the increase in load there was a significant increase in the contribution of the substrate to the measured hardness.

5.3.3. Composition of Carbide Coatings

Results obtained from EDS analyses showed in all cases that the coating contained small amounts of Fe(0 to 5% - **Table.4.4**). This is in good agreement with the claims of Child et. al.[26] and Arai[25]. The presence of Fe in the layer might have been expected given that the layer grows by a diffusion mechanism. Since the treatment temperature used in most cases, ie. 950°C, was well above the austenitizing temperature of the EN9 steel and the mild steel substrates, the presence of Fe in concentrations as high as 5% may be expected. Although Fe is atomically slightly larger than V, at the high process temperatures used, say 950°C, the diffusion of Fe into the layer may be expected to be significant. The diffusion of Fe would nonetheless be limited due to the fact that Fe diffuses substitutionally.

Confirmation that the coatings produced were of VC was provided by XRD analyses of coated samples as shown in **Table.4.5** and **Figure.4.15**. The experimental data correlated well with the indexed data for $VC_{0.86}$ and VC(14% C). Given these results, and the results of EDS analyses, it may be concluded that the composition of these coatings varies non-stoichiometrically from substrate to surface. Overall, these results indicate that the layers are VC with small amounts of Fe in the layers.

5.4. A Detailed Study of Baths containing V_2O_5 and Al

5.4.1. Effect of Temperature and Carbon Content on Coating Thickness

Among the first variables investigated were those of temperature (**Figure.4.16**) and substrate carbon content (**Figure.4.17**). An increase in either of these two variables increased coating thickness. As pointed out earlier, the probable reason for this behaviour was the dependence of diffusion rate on temperature and concentration.

For the higher temperature curves (1000°C and 1050°C), it can be seen that the initial growth rate is much higher than that of the 950°C bath. Specimens treated for 9h however showed similar coating thicknesses. It would seem that the thick coatings produced in a short time period in the higher temperature baths lengthen the diffusion path of C through the carbide layer and therefore reduce the layer growth rate. In the case of the 0.2% C steel (**Figure.4.21**) the growth rate levels off probably due to carbon depletion of the substrate, an increase in diffusion distance, and a decrease in the concentration gradient.

5.4.2. Effects of Bath Composition

From the results shown graphically in **Figures 4.18, 4.19,** and **4.20,** which relate to bath composition, it can be seen that Al had a pronounced effect on bath activity. This was especially so in the first 8 or 9 hours of bath life. In all three cases, the bath with the highest amount of Al had the highest activity. The 20% V_2O_5 plus 5% Al bath became active only after about 6 hours, whereas the 2% V_2O_5 and 1% Al bath remained inactive over the 9h test period. It seems therefore that the proportions of V_2O_5 and Al in the bath

have to be such that there is sufficient pentoxide to saturate the bath and enough Al to effectively reduce the pentoxide. Baths containing 10% V_2O_5 plus 5% Al appeared to give good results in this regard.

The reducing effect of Al appears to take place quite rapidly. It is important to note in this respect that Child et al.[26] mention that a 10% FeV bath, containing no Al, achieved activity after about 8 hours at a temperature of 1040°C. Also, the size of the FeV powder used here was -100 mesh (about -150μm). They also found in this particular case that the amount of V in the bath was approximately 1.7% which was below the saturation level of roughly 2.8% in borax at 1050°C (see **Table.2.5.2**).

From the above discussion it is clear that Al accelerates the rate at which the bath becomes active. This is also supported by the fact that the V_2O_5 and Al baths used were heated for at 1.5 to 2.5 hours before treating samples therein. , indicates that an active bath - not necessarily saturated with the active species - could be achieved within an hour of meltdown. Another noteworthy feature in **Figures 4.18 to 4.20** is that the growth of the VC layer followed a parabolic relationship in most cases. As discussed previously, this indicates diffusion rate controlled growth. From the experimental graphs shown up to this stage, and from results discussed at a later stage, it will be seen that growth of the coating mostly followed a parabolic behaviour. Essentially, this would suggest that most of these baths were ideally conditioned. This could be attributed to the relatively small size of the baths (1.5kg borax). Furthermore, the bath constituents were mixed quite intimately prior to meltdown which could have made the melt more homogeneous. Also, the relatively fine particle size (-500μm) probably influenced bath activity as shown in **Figure.4.21.**

5.4.3. Influence of Particle Size of V_2O_5 on Bath Activity

The particle size of the pentoxide used in the bath had considerable influence on the bath activity (**Figure.4.21**). The lower activity of the bath containing larger particles was attributed to kinetic and sedimentation effects. Larger particles take longer to react with bath constituents due to their smaller ratio of surface area to volume. In addition, larger particles settle to the bottom much faster. A fine particle size would be more effective in producing a layer of the required thickness in a practical time period.

One of the questions raised by the results of this test is what would be the effect of mechanical stirring on the bath activity containing a certain particle size. Stirring of the bath would probably raise its activity by improving contact between bath constituents and avoiding settling to the bottom. In this regard, Child et al.[26] state that stirring of the bath promotes oxidation particularly at the melt/air interface. At the same time they point out that frequent agitation of FeV baths is essential to keep the bath active. In this study, baths were agitated by hand using a carbon steel rod about half an hour prior to the immersion of any samples to improve the homogeneity of the melt. This however, is not considered to be as effective as mechanical stirring.

5.4.4. Change in Bath Activity with Time

Monitoring the bath activity over 25h and 50h periods revealed that the activity of baths containing 10% V_2O_5 and 5% Al, rose sharply in the first 5 hours and remained

fairly constant for the next 20 hours or so, after which time it seemed to drop. This behaviour compares well with the results shown by Child et al.[26] for the variation of layer thickness with bath age for 4h treatments of 0.4% C steel in a 10% FeV bath(see **Table.2.5.2**). Although they do not make mention of the temperature used, their results show that the bath became active after 8 hours. After 28 hours(a 20 hour interval), the activity dropped markedly and no layer formed after 32 hours.

From the above information, it would appear that the baths containing 10% V_2O_5 plus 5% Al remain active for much longer periods of time as indicated by **Figure.4.22**, since a layer of about 7μm was still produced at the end of the 50 hour period. Again, the question regarding mechanical stirring of the melt is raised. Based on reasons discussed previously(Section.5.4.3), the possibility exists that stirring of either bath at the end of the 25h or 50h period could have raised the activity of these baths.

5.4.5. Effect of Bath Depth and Bath Age on Coating Thickness Produced

Results obtained from the tests done to determine, simultaneously, the effect of bath depth and bath age on coating thickness were shown in **Figure 4.23, 4.24** and **4.25**. From **Figure.4.23** it can be seen that the 16h bath was more active towards the lower portion of the melt, whereas the 8h bath appeared to be more active in the upper portion of the melt. Further evidence of this was provided in **Figure.4.24** which showed that at 30mm above the bottom of the bath, the 16h bath produced thicker coatings, especially during the first few hours of treatment. At higher levels, ie. 50mm and 70mm above the bottom, the 8h bath produced thicker coatings especially on specimens

treated for 12h.

These results seem to suggest that the coating thickness produced at any depth in the bath is influenced by the bath age. As shown above, the bath age appeared to determine which portion of the bath was more active. In the cases shown here, the lower and upper portions varied in activity. From **Figure.4.25** it appears that this active portion or "zone" shifts position with age of the bath. At 30mm above the bottom of the bath, the bath containing 10% V_2O_5 plus 5% Al, which was aged the least, was initially least active and became most active at this level after about 7 hours. By contrast, the 16h bath was initially most active and became the least active by the end of the 9h period.

This effect is considered to be due to the diffusion of air/oxygen at the surface of the melt. With older baths, in this case the 16h bath, the surface of the melt becomes oxidised to a fair depth perhaps as much as 10-15mm(see **Figure.26**). It was indicated in **Figure.4.23** that the rod treated for 12h in the 16h old bath had oxidised at 90mm above the bath bottom. Also, the coating thickness produced on the other rods at this level decreased with increasing treatment time and bath age clearly implying that the oxidation at the surface of the melt had an effect. Thus, for a "younger" bath(8h), the top portion of the melt would not be oxidised to the same degree as the older(16h) bath.

Regarding the shift of this "active zone", with time the top portion of the melt becomes excessively oxidised, causing this "active zone" to move lower down the melt to a region of lower oxidation. The size of this "active zone" is also likely to be influenced by oxidising conditions prevailing at the top of the melt.

In practice, such oxidation of the melt surface may have to be prevented. The size of the bath is expected to play a significant role in this regard. As pointed out previously, excessive oxidation occurred more easily in small baths. Perhaps a suitably designed lid to reduce contact between air and the melt, or, the addition of suitable protective agents on the melt surface would help to reduce this effect. An alternative may be to stir the bath after certain time periods. As can be seen from **Figure.4.27**, some of the Al still remained unreacted in the bath although the bath was about 30 hours old. Stirring may move this Al to the top of the melt thereby reducing the effects of oxidation.

5.4.6. Influence of Surface Finish

Figures 4.28.(a)-(c) showed that rough surfaces tend to be smoothed by the VC coating, while the polished surface was roughened slightly. It was pointed out that the coating in regions of high plastic deformation on the sand blasted surface appeared to be thicker. This was probably due to the fact that the surface area of these regions is much larger than that available on a flat surface. As a result, the contact area between the molten salt and the steel surface was increased leading to an increase in coating thickness.

5.4.7. Analyses of Baths containing 10% V_2O_5 and 5% Al Aluminum

The detection of V_2O_3 by XRD on bath samples revealed significant information concerning the nature of the chemical reactions taking place in these melts. As mentioned previously, Child et al.[26] also found that a

lower oxide of the carbide forming element is the reactive species. They found V_2O_3 to be the reactive species in FeV baths, whereas samples analyzed here were taken from V_2O_5 and Al baths. On this basis it seems that in FeV baths V is oxidised to V_2O_3, while in V_2O_5 baths the pentoxide is reduced to V_2O_3 in the presence of Al which has a more negative free energy of oxide formation (**Figure.2.5.3**).

Child et al. attribute the formation of V_2O_3 to the fact that this lower oxide is less stable than V_2O_5 with respect to their free energies of oxide formation, ie. -456.1 J/mol compared to -518.8 J/mol. It would appear however, that the lower oxide forms only when conditions in the melt are not excessively oxidising. Important to note are the factors mentioned by Child et al.[25] in this respect. They state that active borax baths contain small percentages (2-4%) of oxide of the carbide-forming element, and stirring is needed to form replacement vanadium oxide in the melt and thereby keep it active. They also claim that ferro-alloys do not dissolve in borax baths but are first oxidised, and, that conditioning of the melt can be speeded up by bubbling air through it.

Thus, some oxidation in FeV baths appears to be necessary in order to form the active V_2O_3 species. However, the extent of this oxidation has to be controlled. Interestingly enough, controlled oxidation may not be necessary in V_2O_5 and Al baths as aluminothermic reduction of V_2O_5 is likely to occur anyway. An interesting area of study would therefore be to study the V_2O_5 and Al baths under conditions of little or no oxidation. The long term behaviour of such baths would also be of interest.

It is also apparent that layers produced in these baths form by a two stage process. Firstly, the active oxide

forms in the melt. In the second stage, this oxide then reacts with carbon on the metal surface to form the carbide layer. It is very likely therefore that the reaction occurring at the metal surface is one involving carbothermic reduction of the oxide. However, this is mere speculation and requires further investigation.

Child et al.[26] state that the V from the ferro-alloy is extracted by selective leaching. This would imply that the borax acts as a flux. On the other hand, in V_2O_5 plus Al baths the borax appears to be necessary only as a mass transfer agent. It would seem therefore that borax can play a dual role in these melts as a flux and mass transfer agent.

5.5. Corrosion Testing of VC Coated Specimens

The results in **Tables 4.8** and **4.10** showed that the sample preparation technique enabled fairly consistent data to be recorded. The consistency of these results stems from the preparation and testing technique used which yielded similar potentiodynamic and cyclic polarization curves for each group of samples.

The improved corrosion resistance of the coated steel substrate was clear from both the potentiodynamic (**Figures 4.30** and **4.31**) and pitting (**Figures 4.32** and **4.33**) curves. The average test data in **Tables 4.9** and **4.11** also showed this. The low corrosion rate of coated samples was highlighted in **Figure.4.34**. Arai et al.[27] showed that coated 304 stainless steel underwent no corrosion in various aqueous media (see **Table.2.5.4**). However, no mention was made of the type of corrosion test carried out, presumably these were weight loss tests.

As stated previously, the high Ep values of VC coated samples showed that they had marked resistance to pitting initiation in the 0.6M NaCl solution. One may argue that the pitting damage shown on the surface of coated samples (**Figure.4.38**) is greater than is apparent since pits tend to undercut the surface on which they form. This is unlikely since the the Epp values of the coated samples were close to that of the Ep values as shown in **Figures 4.32** and **4.33.**

The excellent corrosion resistance of the coated samples also bears testimony to the quality of the VC coatings. The results obtained indicate that the coatings are dense and uniform with no defects which would be detrimental to their corrosion properties. For example, the pitting resistance of coated samples would be reduced significantly by large pores or cracks where pitting could be easily initiated and allowed to proceed unhindered. This is substantiated further by the micrographs illustrating the different corroded surfaces. In potentiodynamic tests damage to the substrate surface was reduced markedly(**Figure.4.37**) while in pitting tests the coating remained intact (**Figure.4.38**).

It may appear from these results that the VC coating behaves quite independently of the substrate on which it forms. Arai et al.[27] observed that the type of substrate material had an effect on corrosion resistance, especially in aqueous media. This was attributed to the penetration of acid through micropores in the coating. It is worth noting in this regard that Van Bennekom[81] also carried out potentiodynamic and pitting tests on VC coated 304L(0.02% C) and 316L(0.02% C) substrates. He found that in general, the VC coated 316L had a lower corrosion rate than the uncoated 316L substrate. It was also more corrosion resistant than the coated 304L substrate. Van Bennekom[81] also found that the uncoated substrates had far higher

pitting potentials(Ep values) and much larger passive ranges than the VC coated substrates. This suggests that the substrates and the quality of the coating influenced the corrosion behaviour of the coated steels. It should be noted though, that Van Bennekom[81] attributed the low pitting resistance to the fact that the stainless steel substrate became sensitized during the coating treatment which was carried out at temperatures in the sensitization range of these steels. It can be deduced therefore that the corrosion behaviour of the coated substrate will be influenced by the type of substrate material, the coating quality and coating process.

5.6. Treatment of Toolsteels

EDS and spectrometric analyses as well as microscopy of the as-received toolsteels indicated that these materials were of acceptable quality. The only concern was that the V, W, and Co contents of these steels were not determined. Nonetheless, based on the percentages of the other elements, these materials were of acceptable composition.

From the outcome of the 3h and 6h treatment at 950°C (**Figure.4.40**) it was shown that the steels with the higher carbon contents formed the thickest coatings with the exception of the M2 steel(1.04% C). The comparatively thin coating produced on this tool steel was probably due to the high austenitizing temperature range of this steel, ie. 1100-1230°C. Also, this steel contains a fairly high amount of V(1-3%). Consequently, at 950°C the carbon content of the matrix is relatively low, since the carbon is trapped in the carbides. These carbides are stable to much higher temperatures. In fact the carbide of vanadium, ie. VC, remains stable up to temperatures of about 1300°C[76]. The low carbon content of the austenite at 950°C is therefore

responsible for the thin layer produced.

The hardness (**Table.4.12**) and microstructure (**Figures A.3.1.(b) - A.3.5.(b)**) of the hardened and tempered tool steels confirmed that all these samples were adequately heat treated, except for the H13 steel. Nonetheless, the coating thickness produced on the annealed, and, hardened and tempered samples showed little variation (**Figure.4.42**). The higher carbon content of the matrix in the hardened and tempered samples appeared to have little effect on the coating thickness produced. This seems contradictory, but it must be remembered that the treatment temperature of 950°C was below the austenitizing temperatures of all the tool steels, except the D3 steel. At the same time it is worth noting that the coating thickness on the hardened sample of this particular material was markedly higher than that on the annealed sample. This suggests that a treatment temperature in the austenitizing range of these tool steels would be most effective for producing thicker coatings.

From these results, it can be seen that coating thicknesses between 3-10μm, which is regarded as adequate in practice, were produced within 3-4 hours at 950°C. At higher temperatures, say in the austenitizing range of these toolsteels, such coating thicknesses may be expected to be produced much quicker, perhaps within an hour or two. The time taken to produce a layer of the required thickness is important since too long a treatment time could result in excessive grain growth which would reduce the impact resistance and toughness of the tool steel. Thus, shorter treatment times may be more suitable. On the other hand, the higher temperatures, sometimes in excess of 1100°C may pose problems for the borax melt.

The high core hardness of the tool steels quenched from

950°C was due to the fact that these steels are all austenitized to some extent at this temperature (**Table.4.13**). On quenching, the austenite transforms to martensite thereby increasing hardness to some degree. The D3 steel whose austenitizing range lies between 920-980°C had the greatest hardness because it was probably fully austenitized. The as-quenched hardness of these tool steels varies with austenitizing temperature. The Ms temperatures of these steels range between 200°C to 400°C, with some of the steels, eg. the M2 steel, showing marked secondary hardening[78].

From this discussion, it can be appreciated that the treatment of tool steels by this coating process requires careful planning and control. Too high austenitizing temperatures could cause incipient fusion, while too long treatment times will lead to some grain growth. Quenching at temperatures far below the Ms may result in quench cracks, and, improper tempering procedure will reduce toughness and impact properties.

The hardness of the VC layer (**Table.4.14**) from tests done on the cross-section of the layer compared well with the values obtained previously on coated EN9 steel substrate. In this case, the values appeared to be slightly higher overall, perhaps due to quenching or the higher hardness of the substrate. The drop in hardness at the 50gf load is noteworthy, but is expected for the higher load since hardness drops with load.

5.6.1. Microstructure of VC Coated Tool Steels

The appearance of the VC layer on the toolsteels resembled that of the coated carbon steels in terms of uniformity and

density. The salient features shown (**Figure.4.44.(a)-(c)**) were typical of those observed previously (Section.4.3.1). The highlight of the salient features shown is that this coating process is non-line of sight. The ability to coat small holes, corners, and fairly rough edges presents a number of practical advantages especially when one considers the limitations of the line-of-sight processes, eg. PVD.

The substrate microstructure below the carbide layer varied. In all cases, except in the case of the H series steels the alloy carbides in the matrix could be seen. The H series steels showed extensive decarburisation below the coating which was evident from the ferrite grains (white areas) below the coating. This is probably due to the low carbon content of these steels (0.3% C). It is not certain what steps would have to be taken in practice to overcome this, but the steel may have to be carburised prior to coating.

The structure of the matrix of these steels was not studied in any detail but the hardness test results indicate that the matrix probably comprised a mixture of martensite and retained austenite. The behaviour of the carbide upon quenching and its known stability at elevated temperature would enable the necessary treatments of tools steel or alloy steel substrates to be carried out in order to produce the required microstructure and properties in the substrate.

5.7. Problem Areas and Solutions

5.7.1. Method of Immersion of Samples

As shown previously, the method by which samples are immersed in the melt could pose problems. In practice, the size, weight and shape of articles will have to be considered carefully. A jig may prove to be suitable, but this will have to be looked into.

5.7.2. Cleaning of Samples

Cleaning of treated articles in boiling water proved to be a fairly effective procedure. Often, a thin surface layer of salt still remained attached to samples even after cleaning in boiling water. A suitable solvent may have to be found to remove this deposit.

5.7.3. Cleaning of Steel Pots used for Baths

The pots used in these tests were easy to clean, as described in Section.4.6.3, because of their relatively small size. The larger baths used in practice will be difficult to clean in a similar manner due to their size. An alternative cleanout procedure will have to be found, since the pots are expensive to fabricate.

5.7.4. Formation of "Two-Phase" Carbide Layers

Although undesirable, the formation of "two-phase" carbide

layers was an interesting phenomenon. As shown in **Figure.4.48**, the "two-phase" layer comprised an Fe-rich phase(**Figure.4.49**) surrounded by a V-rich phase (**Figure.4.50**). The Fe-content of this type of layer was also shown to be very high(**Table.4.15**). Microhardness tests revealed that the hardness of such layers was low compared with that of the normal VC coatings, ie. 1340HV0.025. Even more interesting was the fact that these layers seemed to form in either FeV baths, or, FeV plus Al baths, hence the deduction that this problem was related to the use of FeV.

It is thought that the formation of such layers may be due to the particle size of the FeV being used. Particles of FeV(-500μm = -32 mesh) may become attached to the surface of the growing carbide layer, combining with carbon to form a complex $(Fe,V)_xC_y$-type carbide phase. The surrounding V-rich phase, which is in essence the growing carbide layer, grows around these particles to form the "two-phase" layer. Vanadium from these Fe-rich areas may diffuse out to combine with carbon in forming VC, thereby making these areas Fe-rich.

It is also possible that the Fe originated from the substrate. One may argue that such high Fe contents could not have diffused from the substrate into the layer, but it is worth noting that in ferro-chromium baths, duplex layers of $(Fe,Cr)_7C_3$(outer layer) and $(Fe,Cr)_{23}C_6$(inner layer) are formed[26]. The theory that such layers are formed under certain bath conditions has not been discounted and this may be possible. However, the above discussion involves mere speculation and the formation of these "two-phase" layers remains unresolved at present. These layers are nonetheless regarded as a degenerate form of the carbide layer aimed for and their formation must be avoided.

5.7.5. Spalling of Coated Samples

The occurrence of spalling(see Section.4.6.5) was associated with the build-up of residual stress at the surface of coated samples due to the differential contraction of the layer and the substrate. As stated, quenching of treated samples appeared to alleviate this problem. Since residual stresses can arise from volume changes, which may be caused by thermal or structural changes in the specific volumes of neighbouring regions of a material(see Section.2.3.2), it seems likely that the residual stresses responsible for this spalling originate from thermal or structural changes between the coating and substrate. This is substantiated by the fact that quenching alleviates this problem. It would appear that the 3-4% specific volume increase in the substrate, brought on by the martensite transformation, compensates for the differential contraction between layer and substrate.

Without the volume compensation brought on by quenching, residual stresses would develop in the VC coating. The distribution of these residual stresses may vary. However, given the fact that the VC layer may be partially or wholly detached from the substrate, and that, cracks in the coating propagate along the length of the coating originating from the layer surface or the coating/substrate interface (**Figures 4.52**, **4.53**, and **4.54**), it is clear that the position of the maximum residual stress is situated at some point along the coating thickness. This point may be at the layer surface, the substrate/coating boundary, or at some intermediate point.

The sign of this stress, ie. negative or positive which indicates compressive or tensile residual stress respectively, is not certain. However, given the fact that

the volume expansion due to quenching alleviates this problem, it seems likely that the substrate contracts to more rapidly than t VC layer. Therefore, without quenching, the substrate would finally be in a state of compressive residual stress, while the VC coating which contracts more slowly during cooling, is finally in a state of tensile residual stress. Hence, the occurrence of spalling in the coating. With quenching, the volume expansion compensates for the differences in volume between substrate and coating which takes place during cooling.

5.7.6. Staining of Coated Samples

Micrographs presented in **Figures 4.58-4.61** showed the nature of the "stained" areas on samples, and, the morphology of these areas. As pointed out, such "staining" was of concern as it diminished the aesthetic appeal of the coated specimens. The interesting feature of the "stains" was that they were actually areas of VC as indicated by EDS analyses(**Figure.4.60**). The conclusion was therefore drawn that these dark areas were areas where the carbide layer grew with a morphology different to that observed normally(**Figure.4.8**). In some cases the stained areas consisted of cubic particles, whereas in other cases the layer seemed to grow in lath form (**Figure.4.59**). At present, the cause of "staining" is not known, but some possible reasons regarding the occurrence of these "stains" are listed below.

1) Oxidation of samples in these areas prior to immersion in the melt;

2) Decarburisation in these areas due to machining or in the bath itself;

4) A change in the growth orientation of the layer resulting from the infiltration of "foreign" elements, either from the substrate, the melt, or the steel pot, thereby giving rise to the formation of a less even carbide layer and therefore a different reflectivity;

5) Changes in the bath conditions, or, bath composition specifically in the areas where staining occurs.

6. CONCLUSIONS

1. VC coatings were formed in molten borax baths containing FeV or V_2O_5 as carbide-forming additives, when the conditions in the bath were sufficiently reducing.

2. Aluminium is effective as a reducing agent and a deoxidising agent in baths containing FeV or V_2O_5.

3. Small amounts - in relation to the mass of salt used - of bath additives were required to produce coatings of adequate thickness.

4. Growth of the carbide layer may be reaction rate controlled or diffusion rate controlled depending on bath conditions. Generally, processes in older baths tend to be reaction rate controlled.

5. The hardness of the VC coatings was consistent with values quoted by other workers, and values found in the literature for the bulk material.

6. Coatings produced by this process comprise VC with small amounts of Fe diffused into the layer.

7. Increasing temperature and substrate carbon content had a distinctly positive effect on the coating thickness produced in a given time period.

8. The particle size of the carbide-forming compound influenced the thickness of coating produced. The rate of coating growth increased with smaller particle size.

9. Rough surfaces tended to be smoothed by the carbide layer while polished surfaces were roughened slightly.

10. The detection of V_2O_3 by XRD analyses on bath samples confirmed the findings of other workers that a lower oxide of vanadium is the active species in the bath.

11. The corrosion rate of VC coated carbon steel substrates was reduced by 50-100 times in 1N H_2SO_4 at 25°C.

12. Pits formed on the surface of VC coated carbon steel substrates in 0.6M NaCl solution at 30°C tend to repassivate.

7. FUTURE WORK

It is clear from the findings presented in this report that much work is needed to overcome ceratin problems, and, produce treated components which are fit for service. Future work should cover the following areas.

1. A detailed study of reactions occurring in the bath, paying particular attention to the thermodynamic aspects of such reactions. In this regard, data such

as free energies of formation of the different species, activation energies, and rate constants, would be useful in modelling the process. This study could be extended to other bath types, such as baths for producing NbC or Cr-carbide coatings. The study could also be extended to include other types of melts, for example flouride melts. Such information could also lead to the development of other types of surface coatings.

2. An investigation into effective measures which could be taken to condition ageing baths, ie. stirring, bath additions, or other means.

3. Evaluation of the wear resistance of the VC coated materials.

4. Application of the VC coating to tools paying particular attention to heat treatment in order to optimise the properties of the substrate material while increasing the surface hardness considerably.

5. A study of baths for producing other types of carbide coatings, ie. Cr-carbide or NbC and evaluation of the coatings obtained in these baths.

6. The current problem areas should also be investigated.

9. REFERENCES

1. S. H. Avner : "Introduction to Physical Metallurgy", 2nd Ed., McGraw-Hill, 1987.

2. A. D. Sarkar : "Friction and Wear", Academic Press, London, 1980.

3. Milovic. et al. : Materials Science and Technology, Jan. 1986, Vol. 2, No. 59, pp. 59-68.

4. S. Grainger : "Engineering Coatings", Woodhead Pub., Abington, England(1989).

5. C. Davison : "Technology and Culture", Vol. 2, No. 11, 1961.

6. G. A. Saltzman : Metal Progress, Feb. 1986, pp. 25-30.

7. V. C. Venkatesh : Journal of Engineering Materials and Technology, Jan. 1984, Vol. 106, pp. 84-87.

8. K. H. Habig : Tribology International, April 1989, Vol. 22, No. 2, pp. 65-73.

9. G. V. Karpenko, et al. : "Influence of Diffusion Coatings on the Strength of Steel", Trans-Tech Pub., Switzerland, 1979.

10. A. G. von Matuschka, "Boronizing", Heyden & Son Inc., Philadelphia, 1980.

11. B. W. Mott, "Micro-Indentation Hardness Testing", Butterworths, 1956.

12. P. J. Burnett & D. S. Rickerby, "The Mechanical Properties of Wear Resistant Coatings I: Modelling of Hardness Behaviour", Thin Solid Films, 148(1987), pp. 41-50.

13. P. J. Burnett & D. S. Rickerby, "The Mechanical Properties of Wear Resistant coatings II: Experimental Studies and Interpretation of Hardness", Thin Solid Films, 148(1987), pp. 51-65.

14. L. J. Bredell & J. B. Malherbe : Thin Solid Films, 125(1985), pp. 25-28.

15. B. Jonsson & S. Hogmark : Thin Solid Films, 114(1984)257.

16. D. S. Rickerby, B. A. Bellamy & A. M. Jones : Surface Engineering, 1987, Vol. 3, No. 2, pp. 138-146. 17.

17. F. D. Richardson : "Physical Chemistry of melts in Metallurgy - Vol. 1", Academic Press, NY, 1974.

18. I. J. McColm : "Ceramic Science", Leonard Hill Pub., NY, 1983.

19. L. Dobbin & J. E. McKenzie, "Salts and Their Reactions", 7th Ed., Edinburgh Pub., 16-17 Teviot Place, 1944.

20. " Slag Atlas", Committee for Fundamental Metallurgy, Düsseldorf, 1981.

21. E. T. Turkdogan : "Physicochemical properties of Molten Slags and Glasses", The Metals Society, London, 1983.

22. Skoog & West : "Fundamentals of Analytical Chemistry", 4th Ed., Holt-Saunders International, NY, 1982.

23. R. Bock : "Handbook of decomposition methods in Analytical Chemistry", Holsted Press, NY, 1979.

24. L. Dobbin & J. E. McKenzie : "Salts and Their Reactions", 7th Ed., Edinburgh Pub., 16-17 Teviot Place, 1944.

25. T. Arai & N. Komatsu, "Development and Industrial Application of Carbide Coating Process by use of Molten Borax Bath", an article from "Research and development in Japan awarded the Okochi Memorial Prize", 1981.

26. H. C. Child, et al., "Carbide Layer Formation in Molten Borax", Heat Treatment Conference, Institute of Metals, London, 1984.

27. T. Arai, International Foundry & Heat Treatment Conference, National Exhibition Centre, Johannesburg, 30th September - 4th October 1985, SAIF.

28. T. Arai, Journal of Heat Treatment, Vol.1, No.2, 1979, pp.15-22.

29. T. Arai : Wire, 32(1981), No.3 & 5, pp. (102-104) & (208-210).

30. T. Arai & T. Iwama : 11th International Die Congress, Cleveland Convention Centre, Ohio, June 1981.

31. S. Plumb, "TD Process shows advantages", an article from Metallurgia, February 1985.

32. T. Arai, H. Fujita, Y. Sugimoto & Y. Ohta : 3rd International Congress for Surface Technology, Berlin, 1985.

33. T. Arai & Y. Tsuchiya : Advanced Technology of Plasticity, 1984, Vol. 1, pp. 225-230.

34. P.J. Burnett & D. S. Rickerby : Journal of Materials Science, 23(1988), pp. 2429-2443.

35. V. M. Weerasinghe, et. al. : Surface Engineering, 1987, Vol. 3, No. 2, pp. 147-153.

36. M. A. J. Somers & E. J. Mittemeijer : Surface Engineering, Vol.3, No.2(1987), pp. 123-137.

37. W. D. Muenz : Advanced Materials and Processes, 1987, Vol. 132, No. 8, pp. 65-68.

38. D. G. Bhat & P. F. Woerner : Journal of Metals, Vol.38, Feb.1986, No.2, pp.68-69.

39. P. Mayr & R. Chatterjee-Fischer : Metal Progress, Feb. 1986, pp. 35-43.

40. D. H. Boone : Materials Science and Technology, March 1986, Vol. 2, pp. 220-223.

41. H. Solnick-Legg & K. O. Legg : Metal Progress, May 1986, pp. 25-28.

42. P. D. Hicks & F. P. A. Robinson : The Metallurgist and Materials Technologist, June 1984, pp. 28-286.

43. A. L. Hithcox : Metal Progress, April 1986, pp. 31-33.

44. B. J. Gill & R. C. Tucker : Materials Science and Technology, March 1986, Vol. 2, pp. 207-213.

45. C. C. Brendt & R. Mcpherson : Surfacing Journal International, 1986, Vol. 1, No. 2, pp. 49-52.

46. D. M. Hulett & M. A. Taylor : Metal Progress, Aug. 1985, pp. 18-21.

47. J. K. Hirvonen : Advanced Materials and Processes, May 1986, Vol. 2, No. 5, pp.33-36.

48. J. M. Rigsbee : Journal of Metals, Aug. 1984, Vol. 36, No. 8, pp. 31-33.

49. T. B. Massalski : "Binary alloy Phase Diagrams - Vol. 1 & 2", ASM, Metals Park, Ohio, 1986.

50. G. F. Vandervoort : "Applied Metallography", Van Nostrand Reinhold Co., NY, 1986.

51. R. W. K. Honeycombe : "Steels - Microstructure and Properties", Hodder and Stoughton, Met. & Matls. Science Series, 1981.

52. R. J. Gale & D. G. Lovering : "Molten Salt Techniques - Vol. 2", Plenum Press, NY, 1984.

53. P. W. McMillan : "Glass Ceramics", Academic Press, London, 1964.

54. D. R. Stull & H. Prophet : "Janaf Thermochemical Tables", US. Dept. of Commerce, National Bureau of Standards, 1971.

55. F. D. Richardson : Journal of the Iron and Steel Institute, Sept. 1953, pp. 33-51.

56. E. M. Levin, et al. : "Phase Diagrams for Ceramists - Vol. 1 & 2", American Ceramic Society, Ohio, 1969.

57. P. A. Dearnley & K. Anderson, Journal of Materials Science, No.22, 1987, pp.679-682.

58. "Metals Handbook - Desk Edition", Ed. H. E. Gall, ASM, Metals Park, Ohio, 1985.

59. J. W. Westbrook & H. Conrad : ASM, Metals Park, Ohio, 1973, pp.453-492.

60. B. D. Cullity : "Elements of X-Ray Diffraction", Addison-Wesley Pub., USA, (1978).

61. M. Sangham & J. Nikhich : Journal of Metals, Sept. 1985, Vol. 37, No. 9.

62. A. R. Nicoll et. al. : Materials Science and Technology, March 1986, Vol. 2, pp. 214-219.

63. R. H. Van Der Jagt : Materials and Design, Feb. 1991, Vol. 12, No. 1.

64. A. Mathews : Metals and Materials, March 1991, pp. 0-153.

65. J. R. Nicholls & J. D. Stephenson : Metals and Materials, March 1991, pp. 156-162.

66. B. Garside & R. Sanderson : Metals and Materials, March 1991, pp. 165-168.

67. Green & Levy : Journal of Metals, Feb. 1986, Vol. 38, No. 2.

68. F. O. Sequeda : Journal of Metals, Feb. 1986, Vol. 38, No.2.

69. W. M. Steen : Metals and Materials, Dec. 1985, Vol.1, No. 12.

70. G. Dearnaley : Metals and Materials Technology, March 1980, pp. 129-135.

71. G. Dearnaley : Metals and Materials Technology, April 1980, pp. 178-183.

72. D. W. McCurdy : Heat Treatment of Metals, 1988, Vol. 18, No. 1, pp. 17-20.

73. M. E. O' Hern, "Discussion of Dynamic Loading - A new Microhardness Test Method", Journal of Testing and Evaluation, p 413-416, 1991.

74. M. Atkinson, "Analysis of the Size Effect in Low-Load Hardness esting of Metals", ASTM, Journal of Testing and Evaluation, Vol.19, No.5, Sept. 1991, p368-373.

75. T. S. Eyre : Metals and Materials, March 1991, pp. 143-148.

76. I-S. Lee, E. E. Stansbury & S. J. Panel, "Technical Note: Determination of Pit Susceptibility using New Sample Preparation Technique" Corrosion Science, February 1989.

77. R. Qvarfort, "CPT Measurements of Stainless Steels with an improved Electrochemical Method", Corrosion Science, Vol.29, No.8, 1989.

78. R. Wilson, Metallurgy and Heat Treatment of Toolsteels", McGraw-Hill Publishing Co., London, 1975.

79. Metals Handbook, "Corrosion - Volume 13", ASM International Pub., Metals Park, Ohio, 1987.

80. M. G. Fontana, "Corrosion Engineering", 3rd Edition, McGraw-Hill Book Co., 1987.

81. A. Van Bennekom, "The use of Surface Coatings for improving the Wear and Corrosion Resistance Properties of 304L and 316L Stainless Steels", Final Year Project, University of the Witwatersrand, Johannesburg, South Africa, 1989.

83. R. Baboian & G. S. Haynes, "Cyclic Polarization Measurements - Experimental Procedure and Evaluation of Test Data", ASTM STP 727, 1979, pp. 274-282.

84. R. Qvarfort, Corrosion Science, Vol.28, No.135, 1988.

APPENDICES

A.1. List of Typical XRD Data obtained on VC Coated Samples

UNIVERSITY OF THE WITWATERSRAND — METALLURGY DEPARTMENT

raw data file name:	VCCOAT.RD 28-oct-91 15:03
diffractometer:	PW1820
x-ray tube:	Cu LFF 40kV 30mA
wavelength(a1, a2):	1.54060 1.54438
monochromator:	YES
divergence slit:	1/2
receiving slit:	0.1
range 2theta:	5.000 - 75.000
step width, time:	0.020 2.00
peaks file name:	VCCOAT.DI 28-oct-91 15:03
range d-value:	1.2654 - 17.6596
range tip width:	0.01 - 1.00
minimum significance:	0.75

peak no.	d-value (Å)	angle (deg)	width (deg)	peak (cts)	backg. (cts)	I/Imax (%)	signif.
1	14.1189	6.255	0.080	110	123	7.72	2.13
2	9.9783	8.855	0.060	45	85	3.14	0.85
3	6.1460	14.40	0.060	44	49	3.05	1.97
4	6.0635	14.58	0.060	88	49	6.18	1.19
5	5.9888	14.78	0.080	104	48	7.28	2.49
6	5.0694	17.48	0.060	31	38	2.19	1.51
7	4.9818	17.79	0.080	44	38	3.05	1.40
8	4.7717	18.58	0.200	36	36	2.52	1.19
9	4.4569	19.90	0.080	42	32	2.96	1.46
10	4.3693	20.21	0.120	50	32	3.53	0.97
11	4.1109	21.60	0.060	76	29	5.30	1.16
12	3.8244	23.24	0.060	69	28	4.82	0.96
13	3.6101	24.64	0.060	50	18	3.53	1.04
14	3.5257	25.24	0.060	72	19	5.06	1.64
15	3.3961	26.22	0.060	202	20	14.11	2.82
16	3.0708	29.05	0.060	50	17	3.53	0.92
17	3.0376	29.38	0.060	86	17	6.05	1.64
18	3.0076	29.68	0.100	83	14	5.80	1.40
19	2.9067	30.73	0.240	37	10	2.60	1.54
20	2.4904	36.03	0.800	10	16	0.72	0.83
21	**2.4044**	**37.37**	**0.120**	**1253**	**17**	**87.70**	**6.65**
22	**2.3964**	**37.5**	**0.140**	**1340**	**17**	**93.75**	**4.74**
23	2.3039	39.06	0.060	30	14	2.12	1.53
24	2.1937	41.11	0.640	10	14	0.72	1.31

25	**2.0790**	**43.49**	**0.100**	**1429**	**16**	**100.00**	**5.45**
26	**2.0729**	**43.63**	**0.080**	**1310**	**16**	**91.71**	**1.51**
27	2.0210	44.81	0.180	180	14	12.57	3.86
28	1.9083	47.61	0.120	35	10	2.44	1.69
29	1.8976	47.90	0.060	38	9	2.69	0.77
30	1.8554	49.06	0.060	72	6	5.06	1.39
31	1.8313	49.75	0.080	67	7	4.71	3.76
32	1.7032	53.78	0.120	15	6	1.06	1.26
33	1.6743	54.78	0.060	28	5	1.97	2.44
34	1.6227	56.68	0.060	46	10	3.24	0.95
35	1.6012	57.51	0.560	16	10	1.12	2.03
36	1.5667	58.90	0.060	18	10	1.29	1.67
37	1.5533	59.46	0.240	10	10	0.72	0.95
38	1.5332	60.32	0.060	67	8	4.71	1.43
39	1.5077	61.45	0.080	27	8	1.89	1.27
40	1.4868	62.41	0.080	86	10	6.05	4.05
41	**1.4747**	**62.98**	**0.100**	**324**	**11**	**22.68**	**1.25**
42	**1.4705**	**63.18**	**0.080**	**471**	**12**	**32.96**	**0.81**
43	1.4295	65.21	0.400	27	11	1.89	2.14
44	1.3887	67.38	0.060	21	3	1.48	2.83
45	1.3552	69.28	0.120	26	3	1.82	2.86
46	1.3141	71.77	0.060	23	4	1.61	2.58
47	1.3067	72.24	0.060	29	4	2.04	0.75
48	1.2942	73.05	0.080	35	5	2.44	2.28

A.2. List of Typical XRD Data obtained from Bath Samples

UNIVERSITY OF THE WITWATERSRAND METALLURGY DEPARTMENT

raw data file name:	10V5AL.RD 1-nov-91 13:08
diffractometer:	PW1820
x-ray tube:	Cu LFF 40kV 30mA
wavelength(a1, a2):	1.54060 1.54438
monochromator:	YES
divergence slit:	1/2
receiving slit:	0.1
range 2theta:	5.000 - 75.000
step width, time:	0.020 1.00
peaks file name:	10V5AL.DF 1-nov-91 13:08
range d-value:	1.2654 - 17.6596
range tip width:	0.01 - 1.00
minimum significance:	0.75

peak no.	d-value (A°)	angle (deg)	width (deg)	peak (cts)	backg. (cts)	I/Imax (%)	signif.
1	17.3475	5.090	0.100	77	4	35.35	2.44
2	16.4897	5.359	0.480	77	4	35.35	3.26
3	10.0235	8.815	0.120	32	46	14.83	2.11
4	5.6922	15.555	0.060	32	67	14.83	0.99
5	5.1933	17.060	0.060	128	77	58.30	1.47
6	5.0365	17.595	0.060	50	86	23.01	1.47
7	4.9901	17.760	0.060	83	86	37.81	0.82
8	**3.6232**	**24.550**	**0.120**	**161**	**114**	**73.63**	**2.61**
9	2.8622	31.225	0.060	55	137	25.00	1.17
10	2.7710	32.280	0.060	56	128	25.68	1.75
11	**2.6920**	**33.255**	**0.120**	**193**	**125**	**88.21**	**2.09**
12	**2.4627**	**36.455**	**0.060**	**151**	**110**	**69.07**	**1.10**
13	**2.1755**	**41.475**	**0.200**	**59**	**104**	**27.07**	**0.91**
14	2.0142	44.970	0.120	69	107	31.45	2.05
15	**1.8429**	**49.415**	**0.060**	**49**	**110**	**22.37**	**0.86**
16	1.8232	49.985	0.080	86	104	39.49	0.90
17	**1.6930**	**54.130**	**0.080**	**219**	**74**	**100.00**	**1.46**
18	1.6649	55.120	0.060	45	67	20.49	1.59
19	1.6392	56.060	0.060	90	49	41.20	1.01
20	1.6123	57.080	0.060	71	52	32.21	0.98
21	1.5235	60.745	0.060	59	45	27.07	0.96
22	1.5079	61.440	0.120	30	46	13.81	1.42
23	1.4686	63.270	0.240	42	48	19.29	1.60
24	1.4280	65.290	0.080	135	41	61.43	2.40
25	**1.4070**	**66.390**	**0.080**	**74**	**32**	**33.77**	**2.40**
26	1.3811	67.800	0.060	104	29	47.50	1.32
27	1.3715	68.340	0.060	74	31	33.77	1.14

A.3. Microstructure of Tool Steels

A.3.1. D2 Tool Steel

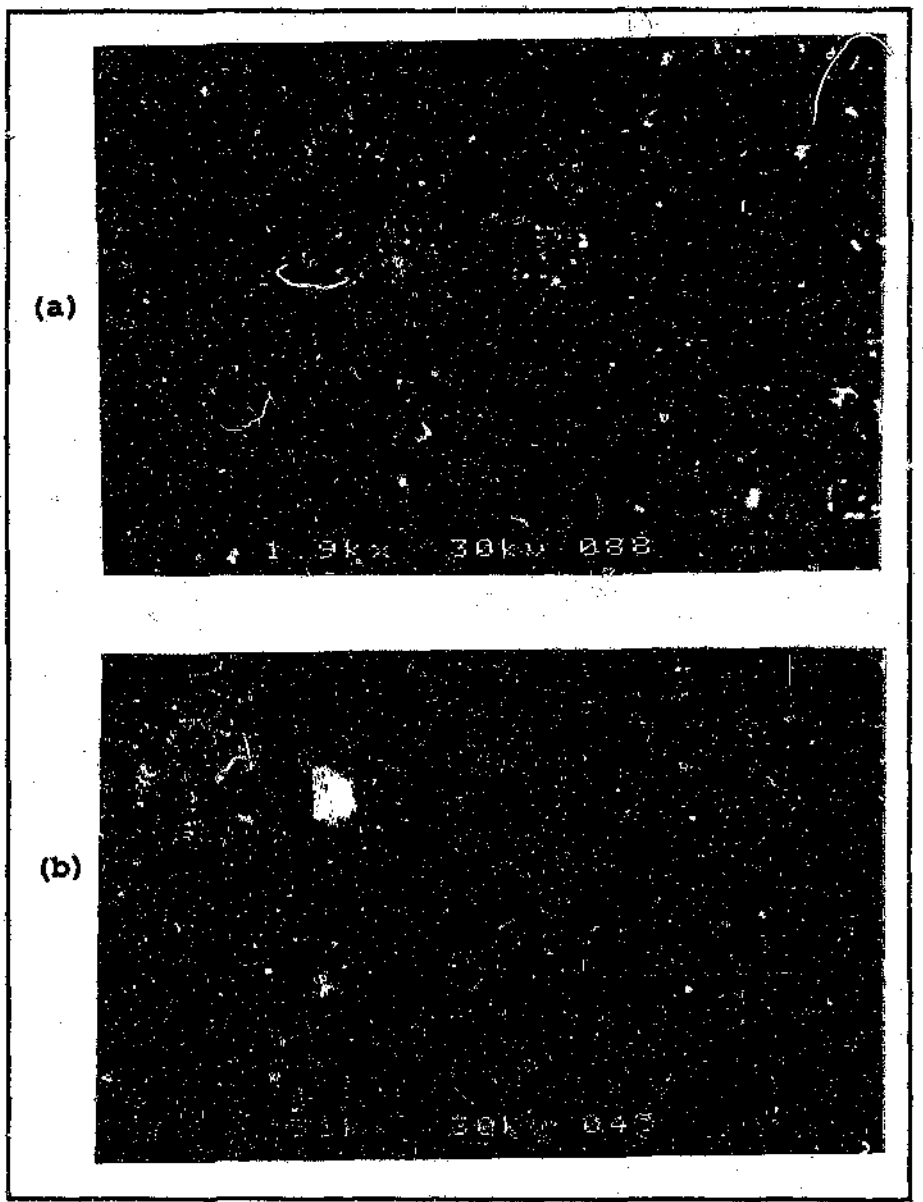


Figure.A.3.1. Microstructure of (a) as-received (b) hardened and tempered samples. Etched nital.

A.3.2. D3 Tool Steel

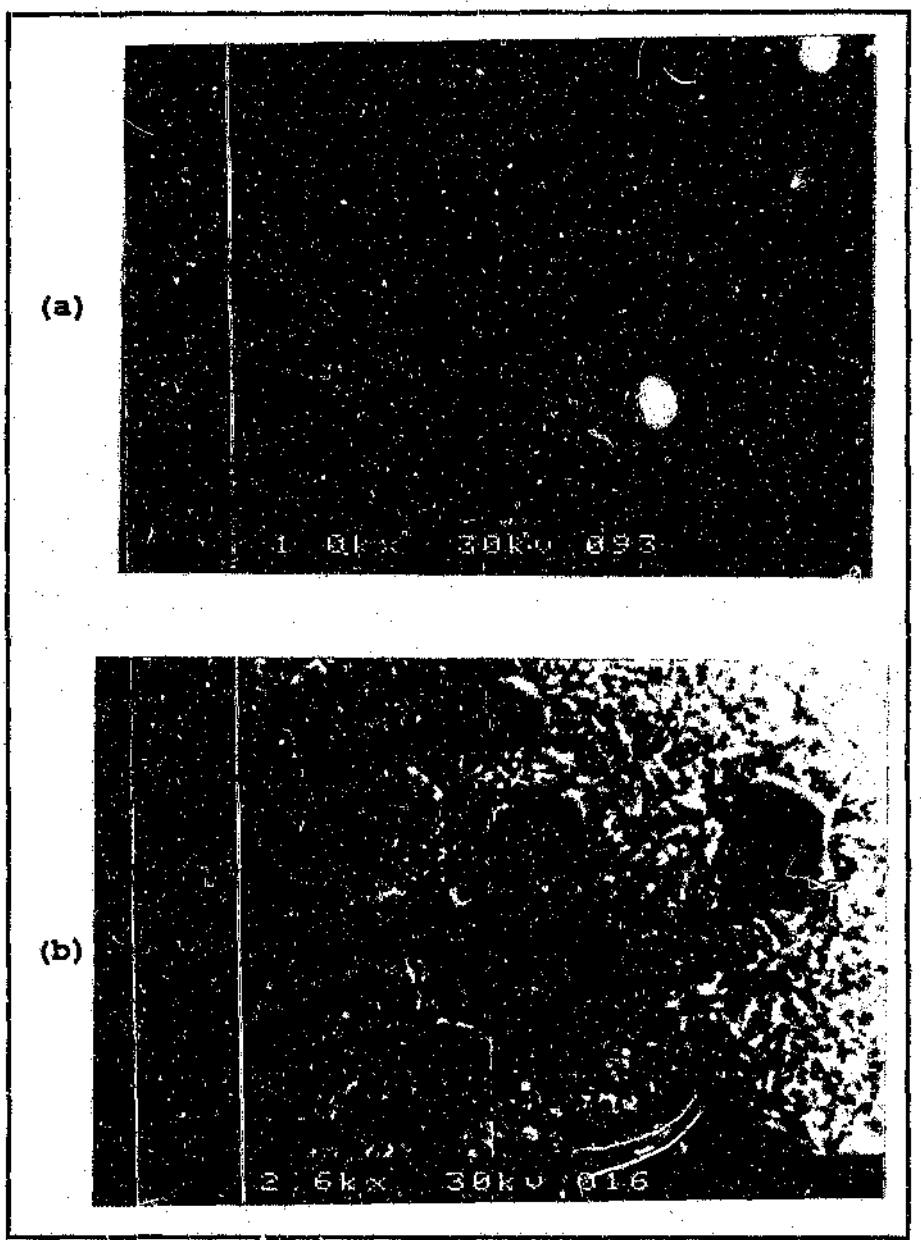


Figure.A.3.2. Microstructure of (a) as-received (b) hardened and tempered samples. Etched nital.

A.3.3. H13 Tool Steel

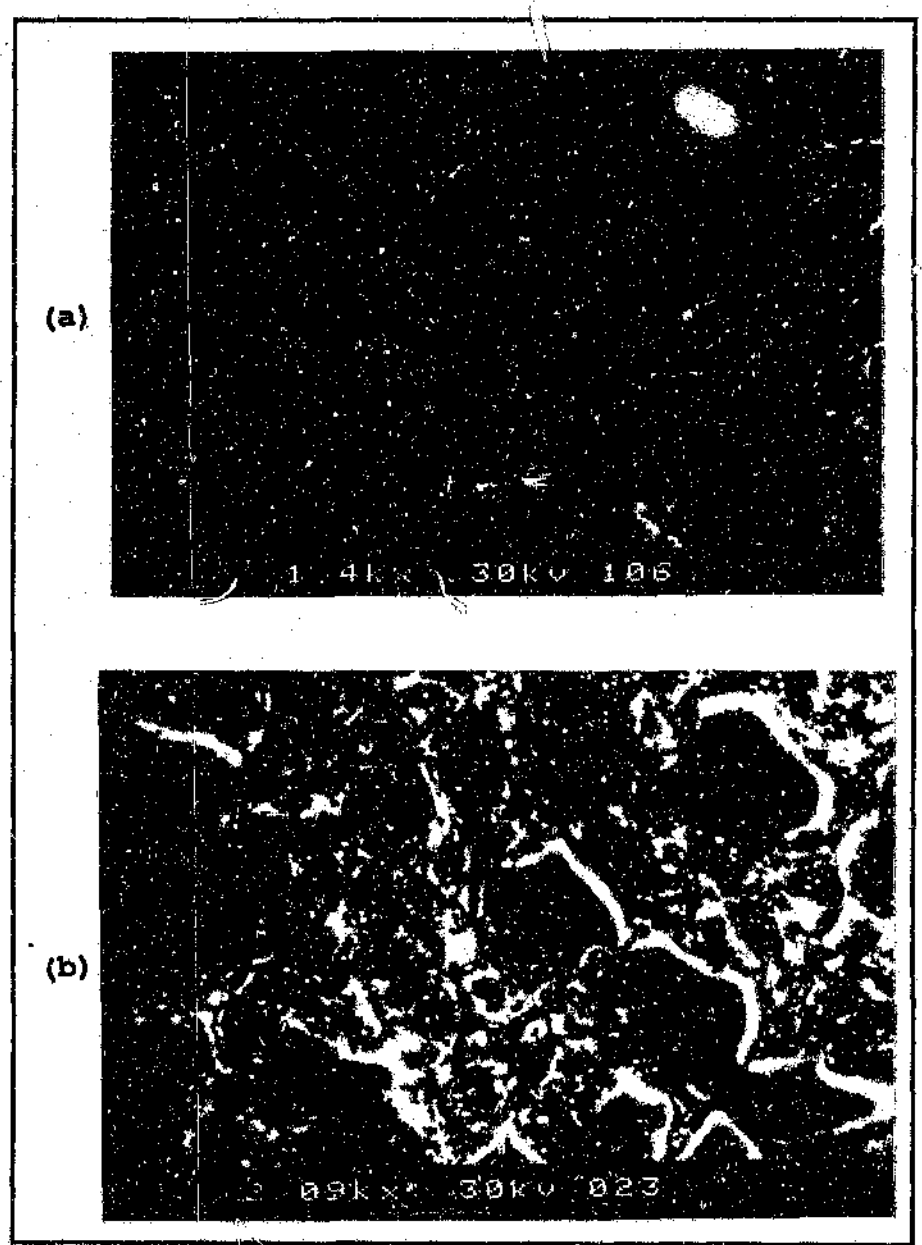


Figure.A.3.3. Microstructure of (a) as-received (b) hardened and tempered samples. Etched nital.

A.3.4. H21 Tool Steel

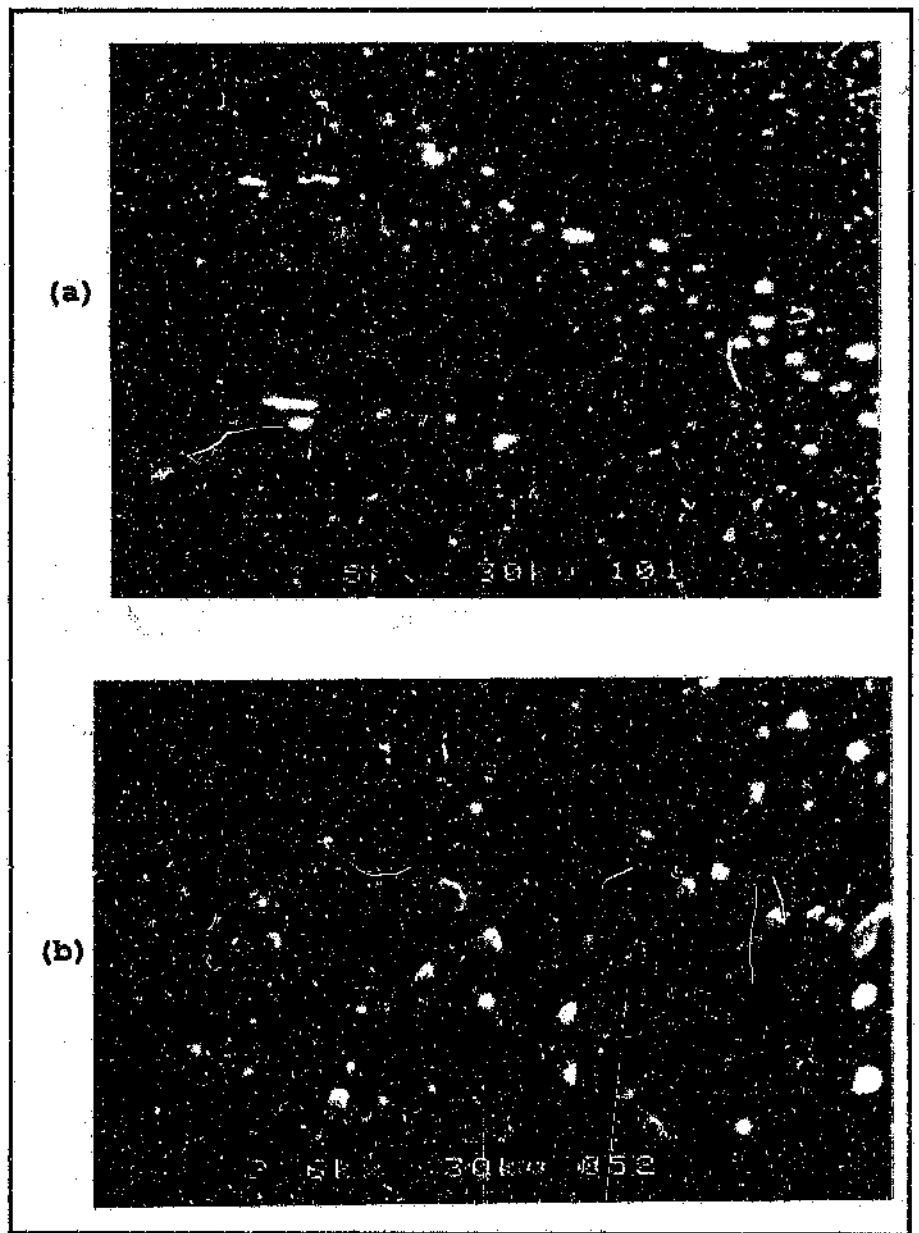


Figure.A.3.4. Microstructure of (a) as-received (b) hardened and tempered samples. Ethced nital.

A.3.5. M2 Tool Steel

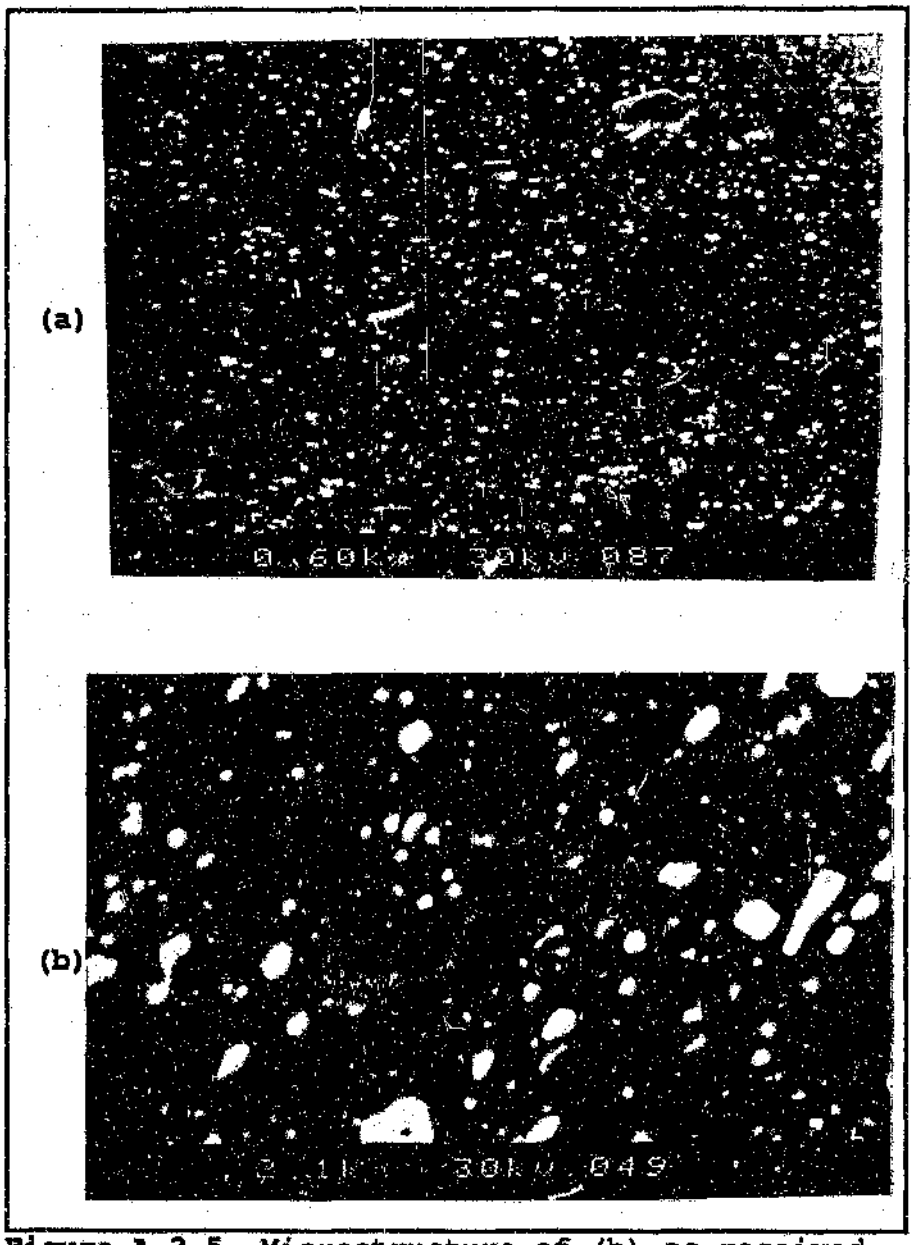


Figure.A.3.5. Microstructure of (b) as-received (c) hardened and tempered samples. Etched nital.

Author: Fazluddin Shahed Bhagga.
Name of thesis: Development of diffusion carbide coatings.

PUBLISHER:
University of the Witwatersrand, Johannesburg
©2015

LEGALNOTICES:

Copyright Notice: All materials on the University of the Witwatersrand, Johannesburg Library website are protected by South African copyright law and may not be distributed, transmitted, displayed or otherwise published in any format, without the prior written permission of the copyright owner.

Disclaimer and Terms of Use: Provided that you maintain all copyright and other notices contained therein, you may download material (one machine readable copy and one print copy per page)for your personal and/or educational non-commercial use only.

The University of the Witwatersrand, Johannesburg, is not responsible for any errors or omissions and excludes any and all liability for any errors in or omissions from the information on the Library website.